

DA-191

PROJECT RULISON FEASIBILITY STUDY

Austral Oil Company Incorporated
CER Geonuclear Corporation

CONTENTS

	<u>Page</u>
INTRODUCTION	1
TEST SITE LOCATION	3
PHYSIOGRAPHY	3
GEOLOGY	4
HYDROLOGY	6
RESERVOIR CHARACTERISTICS	7
Sand Continuity	7
Porosity	8
Permeability	9
Water Saturation	9
Average Reservoir Properties	10
SIMULATION OF EXISTING WELLS	10
Initial Reservoir Pressure	10
Completion Techniques	12
Capacities from Well Simulation Models	13
CULTURE	15
OWNERSHIP	16
EXPLOSION EFFECTS AND TEST PROGRAM	17
NUCLEAR EXPLOSION SIZE CALCULATION	17
Scaled Depth of Burial	18
Cavity Radius	19
Chimney Height	20
Radius of the Permeable Zone	20
Height of Permeable Zone	21
RADIOACTIVITY	21
SEISMIC EFFECTS	25
GENERAL SURVEY OF SURROUNDING AREA	27
Preshot Seismic Survey	29
WELL TEST AND DATA ANALYSIS PROCEDURE	29
AREAS OF RESPONSIBILITY	31
AUSTRAL OIL COMPANY INCORPORATED - CER	
GEONUCLEAR CORPORATION	31
ATOMIC ENERGY COMMISSION AND ITS CONTRACTORS	31
SCHEDULING	32
REFERENCES	33
LETTER SYMBOLS	35
APPENDIX A - PROPOSED WELL TEST PROGRAM	
APPENDIX B - ESTIMATED POST-SHOT RESERVOIR BEHAVIOR	

TABLES

Table

I	Sand Continuity Data
II	Calculated Formation Water Resistivity Values
III	Average Rock Properties
IV	Calculated Initial Bottom Hole Pressures of Rulison Wells
V	Fracture Evaluation
VI	Calculated Reservoir Capacities, Mesaverde Wells
VII	Anticipated Rulison Post Shot Geometry of Rulison Well

ILLUSTRATIONS

Figure

1	Geographic Map of Site Area
2	Topographic Map of Site Area
2A	Surface Geology Overlay
2B	Terrace Location Overlay
3	Regional Map and Structural Interpretation Map
4	Schematic Cross Section
5	Cross Section of Roan Creek Valley
6	Log Analysis of A 29-95
7	Log Cross Section of Rulison Field, Mesaverde Formation
8	Core Analysis Porosity Versus Density Plot
9	Core Analysis Porosity Versus Permeability Plot
10	Core Analysis Porosity Versus Water Saturation
11	Core Analysis Permeability Versus Water Saturation
12	Porosity Versus Water Saturation, Well 3-94
13	Porosity Versus Water Saturation, Well A 29-95
14	Lease Map Rulison Field Property
15	Anticipated Post-Shot Geometry
16	Typical Homes
17	DeBeque Canyon
18	Production from Conventional and Nuclear Stimulated Wells
19	Project Rulison Schedule of Events

INTRODUCTION

Austral Oil Company Incorporated and CER Geonuclear Corporation have undertaken a feasibility study with respect to the possible use of an underground nuclear explosive to stimulate the massive Mesaverde gas sand of the Rulison Field in Garfield County, Colorado (Piceance Basin).

This "Rulison experiment" is visualized as being commercial in nature because the reservoir formation will not produce economically using conventional techniques, but has sufficient gas in place to produce adequate quantities over its normal lifetime if properly stimulated. A market for the gas also exists.

During the latter part of 1965 Austral acquired the operating rights to approximately 36,000 acres in the Rulison Field. Austral recognized that these tremendous gas reserves could not be profitably developed using existing completion techniques and they have conducted an extensive coring, logging, and testing program to generate sufficient data to provide a basis for consideration of the Rulison Field as a site for an experiment with a nuclear explosive. We believe the successful use of such a device will lead to full-scale commercial application of nuclear explosive well-stimulation techniques and result in the development of tremendous quantities of existing non-commercial gas reserves, many of which are government owned.

It is proposed that a more sophisticated device than that planned for either Projects Gasbuggy or Dragon Trail be employed for the Rulison project. Two nuclear explosives would be used, one about 1000 feet above the other; they would be fired simultaneously.

The tandem arrangement is designed to stimulate an extremely thick zone. (The Mesaverde in the Rulison Field is 2,500 feet thick.)

This two-element device will be placed at depths considerably greater than either Projects Gasbuggy or Dragon Trail. Although the configuration of the device, the depths of each element (7,500 feet and 8,500 feet), and the thickness of the zone to be fractured, make the shot experimental, the tremendous gas reserves in place promise unusual commercial potential.

TEST SITE LOCATION

The site of the proposed underground nuclear test is in the northwest quarter of Section 36, Township 7 South, Range 95 West, Garfield County, Colorado. This site is located by red arrows on Figures 1 and 2. The site is located in the Battlement Creek Valley on the north slope of Battlement Mesa. The site elevation is approximately 8,600 feet, and the local relief is over 1,000 feet.

A dirt road parallels Battlement Creek; and nominal improvement will allow access for drilling equipment and well test and control instrumentation. There are a number of locations on the access road that could be made into control points and which would allow line of sight observation of the ground surface above the shot point.

PHYSIOGRAPHY

The site area is located in the upper reaches of Battlement Creek Valley, approximately two miles north of the Battlement reservoir. The valley walls extend to an elevation above 9,600 feet on the east, south, and west sides of the proposed site. The highest point on the valley wall is Haystack Mountain, located two miles southeast of the test site and rising to an elevation of 10,978 feet. The highest elevation on Battlement Mesa is the 11,165-foot high North Mamm Peak, which lies four and a quarter miles east of the shot area. The general site area slopes to the north toward the Colorado River, six miles away.

The region is covered with grass and cedar, Engleman spruce, and aspen forest on the uplands, which give way to sage brush and range grass in the lower elevations.

Fish are present in some of the high reservoirs of Battlement Mesa, but the streams that drain to the north are generally devoid of fish because of the intermittent nature of the runoff. Beaver dams and associated ponds are found on the south side of Battlement Mesa. These ponds could possibly contain some small fish. However, little fishing is done in this area because of the rugged terrain and the difficult access.

The area receives up to 20 inches of precipitation annually, much of it from snow. Grasses grow abundantly on the terraces and higher elevations and are used as pasture for domestic cattle. This is a national forest area, and the current regulations allow cattle to be grazed from June 16th to October 15th.

Deer, elk, and mountain sheep forage throughout the higher elevations during most of the year. The usual small ground animals also are present. The area is visited by a number of deer and elk hunters each fall.

GEOLOGY

Rulison Field is in the Piceance Creek Basin. The relative position of the field to the basin is shown on Figure 3. The field is on the southwest limb of the basin. Upper Cretaceous beds in this area dip towards the northeast at the rate of approximately 150 feet per mile. Tertiary age beds are relatively flat lying.

Rocks ranging in age from Quaternary to pre-Cambrian are present in the Rulison Field area. The sequence of rocks present and their relation to the general stratigraphy of the Piceance Creek Basin is shown in Figure 4.

Wells in the Rulison Field are productive of gas from numerous sandstone bodies in the Mesaverde formation of Upper Cretaceous age. The general character of the Mesaverde formation in Rulison Field is

illustrated by Figure 7 and by the electric log of the Austral Federal A 29-95 well which is marked Exhibit I and placed in the pocket at the back of this report. Figure 6 is an analysis of part of the Mesaverde Section from Austral's Federal A 29-95 well. This analysis shows several hundred feet of potential pay and the interbedded sand-shale stringers.

The Mesaverde formation in the Rulison Field area was deposited in a near shore environment that included marine, flood-plain and coastal swamp conditions. This depositional setting resulted in rapid lateral and vertical variations in lithology. The Mesaverde sandstone reservoirs in the Rulison Field are lenticular and for the most part have limited areal extent. The discontinuity of the Mesaverde sandstones is illustrated in Figure 7 and is further discussed in this report under the heading Reservoir Continuity. The lenticularity of the Mesaverde sandstone reservoirs is the cause of entrapment of gas in the Rulison Field.

The Mesaverde formation in Rulison Field is approximately 2,500 feet thick. It is underlain by the Mancos shale formation of approximately the same thickness. It is overlain by the Fort Union, Wasatch, and Green River formations of Tertiary age. The Tertiary age rocks are predominantly shales and nonpermeable sandstones. These rocks were disclosed in the interval from the surface to a depth of 4,544 feet in the Austral Federal A 29-95 well.

The surface geology of the Rulison Field and surrounding area is portrayed by Figures 2A and 2B, which are overlays to Figure 2. The geology shown on these figures was mapped by interpretation of aerial photographs and field reconnaissance.

The surface rocks in the Rulison Field area are the Wasatch and Green River formations of Tertiary age. There are a number of Quaternary age alluvial deposits in the valleys of the Colorado River and its tributaries and in terraces on the lower slopes of Battlement Mesa. In addition, "mud flow" type deposits are present in some of the higher valleys.

The United States Geological Survey has made detailed studies of both the surface bed-rock geology and the alluvial terraces. The results of each of these studies are being prepared for publication. Their early release in preliminary form has been requested so the data may be used in subsequent phases of this Rulison Project.

HYDROLOGY

The Colorado River and its largest tributaries in this area flow on alluvial deposits. Some limited coring by the Ground Water Branch of the United States Geological Survey shows that the sub-alluvial floors of the valleys are approximately 80 to 100 feet below the surface water table. Figure 5 is a cross section of the Roan Creek Valley just north of the Colorado River. This figure indicates the approximate thickness of the alluvial deposit.

Most of the annual precipitation in this area runs off in small streams, and flows or percolates through the alluvial fill or terraces into the Colorado River. A few springs are present where the underflow in the alluvium is deflected to the surface by the relatively impermeable bedrock.

There is a significant underflow through the alluvium of the valleys. The only water wells in this area with appreciable capacity are completed in alluvial sand and gravel lenses in the valleys. This type of deposit is only characteristic of the Colorado River and some of the larger tributaries north of the Colorado River. The smaller tributaries on the Battlement Mesa generally flow on bedrock.

There are a few shallow water wells that produce from the alluvial terraces. These provide water for ranches. However, most of the ranches obtain their water from cisterns or ponds in the intermittent creeks. Some of these ponds also supply limited irrigation water for the farming conducted on the terraces.

In general, the Wasatch formation underlying the alluvial deposits is relatively impermeable and is not used as a ground water source. There are some sandy zones near the top of the Wasatch and in the middle Wasatch. But because of the general flat-lying nature of the Wasatch beds, it is felt that little active ground water movement occurs in this formation.

All potable water supplies in the Rulison Field area are approximately 6,000 feet above the maximum anticipated extent of fracturing and there should be no problem with radioactive contamination.

The United States Bureau of Reclamation has a plan for a dam on one of the creeks on the east side of Battlement Mesa. The plans propose an associated distributory canal at approximately the 7,000 feet level around the north slope of the mesa. Unless this canal is well sealed, the bottom water loss from the canal will supply additional underflow in the terraces. Such underflow if it occurred would increase the plasticity of the beds and could result in slides even under low particle velocities. This project as yet has not been budgeted, but its development will be watched since it would become a problem in future nuclear stimulation operations at Rulison Field.

RESERVOIR CHARACTERISTICS

Sand Continuity

The Mesaverde sandstone reservoirs in the Rulison Field area are characterized by their lack of continuity. An understanding of the effect of reservoir continuity is a critical factor in the evaluation of Rulison Field. The discontinuous nature of the sandstone bodies appears to be the reason that sandstones with an average of one-half millidarcy permeability behave in aggregate as if the average reservoir permeability were much lower.

A semiquantitative approach to the definition of the degree of continuity of the Mesaverde sandstones in this area has been made by Zeito.⁽¹⁾

Part of Zeito's work was done on the Mesaverde outcrop less than 20 miles from the Rulison area. In three outcrops in this area, from 50 to 71 percent of the sand lenses pinched out within 250 feet of the arbitrary reference line. See Table I.

The results of this and additional field work have been used to construct a statistical model of the expected continuity of the lenticular sandstone reservoirs. This statistical work in the Mesaverde outcrop nearest to the Rulison Field permitted a sophisticated and realistic model of the post-shot geometry to be constructed and a better evaluation of the post-shot gas production to be expected from the Rulison Field.

The fact that the greatly enlarged "nuclear wellbore" will be directly connected to a large number of the gas-bearing sandstone reservoirs is the basic reason that nuclear stimulation is expected to greatly increase the gas production from the Mesaverde reservoirs in Rulison Field.

Porosity

Core analysis data are available from Austral Oil Company's Federal 3-95 and A 29-95 Wells. Only the gas-bearing sandstone intervals are considered in the statistical analysis of the core data.

Figure 8 is a plot of core analysis porosity versus bulk density and a cumulative porosity plot. The median porosity from the cumulative curve is 9.7 percent.

Bulk density and sonic logs are available on several of the wells in the field (3-94, 14-95, 28-95, A 29-95, and 30-95). Average porosities calculated from these logs in the productive intervals are approximately ten percent.

The core analysis median porosity value of 9.7 percent is used as being the most representative of the average porosity in the reservoir.

Permeability

A permeability versus porosity plot, is shown in Figure 9. The permeability associated with the median porosity is approximately 0.5 md. The median permeability is also approximately 0.5 md, while the mode (permeability range containing the maximum number of samples) is from 0.5 to 0.9 md.

Water Saturation

Plots were constructed for porosity versus water saturation, Figure 10, and also for permeability versus water saturation, Figure 11. Permeability and porosity are plotted as independent variables because the porosity was not measured on some of the samples that were used to determine permeability, and a number of the porosity samples were not tested for permeability. A water saturation of 45 percent is associated with a 9.7 percent median porosity and 0.5 md median permeability. These values have been used to represent the average properties of the individual sandstone lenses in the Rulison Field.

The core analysis data were used in conjunction with the induction, self-potential, and electric logs to calculate resistivity values for the Mesaverde formation water. The calculated values ranged from 0.04 to 0.065 ohm-meters. The connate waters in the upper portion of the Mesaverde had an average resistivity of 0.04 ohm-meters. The connate waters in the lower portion of the formation had resistivity averaging 0.065 ohm-meters. The water resistivity data are summarized on Table II.

Calculated porosity versus water resistivity plots were constructed from the logs of Austral Oil Company Wells Nos. 3-94 and A 29-95. It was possible to obtain reliable values from only a few sandstones, since the variation in hole diameter made it impossible to use data from many of the intervals which were "washed out." The log plots, Figures 12 and 13, show a close correspondence between values obtained from logs and the values obtained from the core analysis data.

Average Reservoir Properties

The estimated average formation properties obtained from analysis of the core and log data and the net productive interval obtained from log picks are presented in Table III. Various estimates of gas in place have ranged from 96-125 billion scf/ Section. Using the properties listed in Table III and a bottom hole pressure of 2600 psi yields gas in place of approximately 122 billion scf/ Section, in line with previous estimates.

SIMULATION OF EXISTING WELLS

The Southern Union Gas Company wells producing from the Mesaverde formation were analyzed with a computer simulation program to evaluate the apparent characteristics of the reservoir (Appendix A).

The pressure information on the Southern Union wells was rather inadequate. Therefore, the technique used to match well performance was to: (1) evaluate the original reservoir pressure, (2) evaluate completion characteristics, and (3) assume that each well had produced against a back pressure of 300 psi throughout its producing life. Additional back pressure caused by such factors as water accumulation in the wellbore and formation of hydrates was assumed not to occur in these simulations, since not enough information was available to evaluate these factors.

Tests are underway on the Austral wells in the field to evaluate more completely the pressures and productivities. The results of the testing of Federal A 29-95 are used in the more sophisticated reservoir simulation model presented in Appendix B.

Initial Reservoir Pressure

The following technique was used to obtain the original reservoir pressure. We assumed that the data on the Juhan No. 1 well were probably the most representative of a static reservoir pressure. This was because the well was drilled and allowed to stabilize for a period of approximately four years before any appreciable quantity of gas was

produced. During this four-year period, several pressure measurements were made. The bottom-hole pressure was calculated from the surface pressure and the weight of the gas column, and was found to be consistent with apparent "normal" pressure--in other words, pressure represented by water gradient of approximately 0.44 psi per foot of depth. Because of the surface relief in the area, it was felt that this technique could not be applied to the other wells. Therefore, we assumed the following:

1. The Mesaverde formation is in a condition of approximate equilibrium, and a simple piezometric surface slopes from the White Mountain region in the east toward the Book Cliff outcrops to the west.
2. The Juhan No. 1 calculated bottom-hole pressure of 2,600 psi represented a point on this piezometric surface.
3. The lenticular nature of the Mesaverde was such that the individual lenses were probably in equilibrium with the water saturated low permeability material in general contact with each lens.
4. The initial reservoir pressure of each well could be obtained by finding the initial bottom-hole pressure of the correlative layer in the Juhan No. 1 well and adding or subtracting the "normal" pressure gradient expected from their position relative to sea level, i. e. ,

$$p_1 = p_r (0.44 \Delta Z)$$

where:

p_1 = initial bottom-hole pressure of well, psi.

p_r = initial bottom-hole pressure of correlative layer in Juhan No. 1 well, psi.

ΔZ = difference in elevation (relative to sea level of layer in the subject well is below the correlative layer in Juhan No. 1, the quantity $(0.44 \Delta Z)$ is added to the Juhan No. 1 pressure to obtain p_1 in the subject well. If the layer is above (relative to sea level) the Juhan No. 1 elevation, then the quantity $(0.44 \Delta Z)$ is subtracted from the Juhan No. 1 pressure.

The initial pressures obtained using this technique are presented in Table IV. The pressures obtained by this technique seem to be reasonable, and are in agreement with that obtained in the test of Federal well A 29-95.

Completion Techniques

Early wells in the Rulison Field were fractured with multiple intervals open in each frac job. This general lack of control over fracture location, plus the use of an untreated water to fracture a low permeability formation, resulted in little effective fracture-promoted increase in productivity.

The normal completion consisted of setting casing and perforating several intervals, followed by a multistage fracture treatment. Thus, the effective wellbore radius of the treated zone should be altered considerably. However, the location and number of fractures created during a given stage of a treatment is unknown because of the long intervals treated.

To estimate the amount of fractured area created during these treatments, the treatment records of several wells were analyzed. Interest was focused on the early wells which have a relatively long production history.

In the early treatments, 40 to 60-mesh sand in water (without fluid loss additives) was used. Fluid loss to the formation was controlled by the viscosity of the fracturing fluid and the compressibility of gas in the formation. Despite a low apparent formation permeability of 0.5 md, flow loss coefficients were high. The overall effect was that a large amount of water was lost to the formation and the resulting fracture areas created were small. This large amount of water resulted in a water saturation extending outward from both faces of the fracture approximately three feet. This water block resulted in a questionable increase in productivity due to the fracture treatment.

A summary of the calculations is presented as Table V.

In calculating the theoretical productivity increases, an effective drainage area of 40 acres was assumed. This small spacing was considered adequate because of the small quantities of gas which have been produced and the discontinuities in the formation. Note that the circular horizontal fracture and an elliptical vertical fracture ($b = 1/2a$) yield an essentially identical q_f / q_o ratio. Thus, equivalent wellbore radii can be considered in these two cases. If multiple fractures were created in a given stage treatment, the total created fracture area would remain constant but fracture penetration would decrease. The expected productivity increase would also be less in this case. For example, if each stage treatment in Federal 28-95 created two separate fractures, the productivity ratio would be reduced to 3.8. However, more net pay would be tied to the wellbore. Logs show that the gas-bearing zones generally wash out and conventional perforating devices may not be able to penetrate the thick cement sheath. Thus, perforation breakdown may be necessary to open up any given pay interval.

The most significant column in Table V is the average depth of penetration by the fracture fluid into the formation. Fluid penetration ranges from two to four feet. Generally, fresh water was used as a fracturing fluid. Since the formation has a low permeability, water blocking creates a large skin effect around the fracture face. This essentially negates the effects of fracturing except that some perforations were broken down and those zones were tied into the wellbore. This was not the case for the Austral well. Evaluation of Austral's well is discussed in Appendix B and summarized on the second page of Table V.

Capacities from Well Simulation Models

The well performance from the Southern Union Mesaverde producers could be simulated by using a radial, non-steady state, two-dimensional, compressible fluid flow model developed by O. G. Kiel^(2, 3). The program runs on the IBM 7094 computer.

The well performance was simulated by using (1) porosity and saturation data from Table II, (2) reservoir pressures from Table IV, (3) a wellbore radius of 1/2 foot (the fractures were assumed to be noneffective in increasing the wellbore radius, and their only effect was to tie in the formation) and a drainage radius of 2980 feet, (4) a surface line pressure of 300 pounds, (5) a series of net pays (total net pay, h , perforated, $1/2 h$, $1/4 h$, $1/8 h$, etc.) and (6) a series of permeabilities (total or average permeability, k , from core analysis, $1/2 k$, $1/4 k$, $1/8 k$, etc.)

The series of net pay, h , and average permeability, k , that successfully match Southern Union's well performance are presented in Table VI. It is interesting to note that the net pays and permeabilities were quite low except for the case of Federal A 29-95. This well was air-drilled and completed open-hole and produced a small total volume of gas so that only a relatively small area around the wellbore was affected. In this case the radial flow model seemed to yield a reasonable set of formation properties and seemed to be a reasonable model.

In the case of the other wells where a longer producing history is present and where the reservoir is affected out to a greater distance, the radial model, with its constant h values, does not seem to be adequate. The net pay calculated seems to be too low.

A non-radial three-dimensional model was used to evaluate the performance of Austral's A 29-95 well, Appendix B. This model and the concept of a reservoir that has poor sand continuity and a resulting decreasing effective net pay away from the wellbore proves to be a much better simulation than the simpler radial model used to evaluate the Southern Union wells (with their minimum amount of information).

The gas well testing and the two-dimensional radial model are discussed in Appendix A, and the sand continuity plus the three-dimensional grid model are discussed in Appendix B.

CULTURE

The small towns of Grand Valley (population 245 - 1960 census) and Rulison (population 25 - 1960 census) are located approximately 6-3/4 miles northwest and north of the proposed site. The town of Rifle (population 2,135 - 1960 census) is located approximately 12-3/4 miles northeast of the site. The town of Colbran (population 310 - 1960 census) is located approximately 12 miles due south of the area. Grand Junction (population 18,694 - 1960 census) is located 40 airline miles to the west and is serviced by commercial air lines.

A small line cabin, corral, and barn are located one mile north in the immediate area of the site. This cabin is of frame construction and has been only periodically occupied. The nearest houses and ranches are located in an arc at distances greater than four miles north of the area and extend outward across the Colorado River valley. On the south side of Battlement Mesa, only a few summer cattle camps are present and are located approximately seven miles from the site.

The area is serviced by a county-maintained road up to 4-1/2 miles from the proposed site. The closest approach of U.S. highways 6 and 24 to the shot area is at Grand Valley. County-maintained roads run along the lower mesa roughly parallel to the Colorado River. Lease roads connect the individual gas wells to this road network. Lease roads, although maintained to service the wells in the area, are unimproved dirt. They are capable, however, of handling trucks which haul heavy oil field rigs, pipes, and other machinery. The jeep trail to the site can easily be improved to withstand this type of traffic.

The closest gas wells to the site are Federal 28-95 (three miles), and Federal 14-95 (3-1/2 miles). The next closest wells are Federal A 29-95 at four miles, Goss Hahnewald No. 1 at 4-1/2 miles, and Federal 30-95 located five miles away.

All the wells in the area are interconnected by the gas gathering lines of the Western Slope Pipeline Company, which gathers and purchases the gas from the area. This line generally follows around the foothills and above the lower mesa road and comes within 3-1/2 miles of the site to the north.

Adequate services are available in the general area to support the logistic requirements of the proposed project, such as well logging, cementing, supplies, and storage. For a minimum operation, the town of Rifle would suffice for housing of the personnel involved, since it has four motels and adequate office and warehouse space. This could be headquarters for both the drilling and the construction personnel.

OWNERSHIP .

Austral Oil Company Incorporated has the operating rights to approximately 36,000 acres in the area containing the proposed site. A map outlining Austral's holdings is presented as Figure 14.

EXPLOSION EFFECTS AND TEST PROGRAM

NUCLEAR EXPLOSION SIZE CALCULATION

A preliminary review of the possible surface effects of various size devices indicates that approximately 100 kiloton is a reasonable compromise between favorable reservoir stimulation and unfavorable surface damage. The post-shot geometries produced by two 50-kiloton devices are displayed as Figure 15; and the calculations are summarized in Table VII. As shown in Figure 15, the proposed Rulison shot depth would be approximately 7,500 feet to 8,500 feet subsurface.

The cross-section of the general sand development through the Rulison Field (Figure 5) shows that none of the devices permissible from a surface seismic standpoint would yield permeable zones tall enough to connect the entire Mesaverde sand interval with the chimney and fractured formation surrounding the wellbore. Thus, it is proposed that two 50-kiloton devices, one set about 1000 feet below the other, be fired simultaneously to stimulate the reservoir. Based upon the surface ditching experience with the simultaneous detonation of cratering shots, ⁽⁴⁾ it is probable that there would be some reinforcement of waves between the two devices and that the resultant fracture zone around each explosive element would extend further than the fracture zone predicted for a single device of the same total force. This effect would result in a chimney-permeable zone height of from 1.25 to 1.5 times that from a single shot. It is also felt that probably the general surface seismic effect would be somewhat less than for a single 100-kiloton device.

If the 1.5 factor is appropriate, then the two 50-kiloton devices would cover approximately 1,600 feet of the vertical section, i. e., :

Upper 50-kiloton device, approximately	600-foot coverage
20 percent safety factor above upper device	120-foot coverage
Lower 50 kiloton device plus simultaneous shot factor	900-foot coverage
Total	1,620-foot coverage

A much more decisive evaluation of the postshot geometry should be possible prior to the actual detonation of the Rulison shot because the information from the Projects Gasbuggy and Dragon Trail detonations in gas reservoirs should be available at this time. The actual depth of burial of devices will depend on the information obtained in drilling, coring, and logging the preshot test well at the proposed site.

The explosive yield calculations were based upon the following considerations.

Scaled Depth of Burial

The scaled depth of burial is a convenient expression to allow a correlation of results from explosions having different yields and depths of burial. It relates those results on the basis of an equivalent one-kiloton yield, through:

$$\text{SDB}/(1 \text{ kt})^{1/3} = D_b / W^{1/3}$$

where:

SDB = scaled depth of burial, feet.

D_b = actual depth of burial, feet.

W = device size, kilotons.

Empirical data from a number of reported underground explosions in competent rock material such as tuff, salt, and granite indicate that a SDB greater than 500 is sufficient for containment. (5, 6, 7)

The scaled depth of burial for the two 50-kiloton devices should be less than the scaled depth of burial for a single 100-kiloton device buried at an intermediate depth. However, for a conservative estimate of seismic effects we are using a 100-kiloton device buried in intermediate depth of 8,000 feet. Therefore, the scaled depth of burial can be calculated from the relation:

$$\text{SDB} = D_b / W^{1/3} = 8,000 \text{ feet} / 100^{1/3} = 1,720 \text{ feet}$$

The scaled depth of burial is much greater than that required for containment. However, other criteria should be considered in selection of the maximum device size. Among these factors are:

1. Sufficient non-waterbearing or impermeable formation above the maximum projected vertical fracture zone to insure that the cavity and chimney are not drowned out and that the overlying waterbearing zones do not act as thief zones for the gas from the reservoir nor will they become radioactively contaminated.
2. Sufficient overburden must remain above the fractured matrix to contain the pressure of the hydrocarbon fluid. (No breakout of gas to other permeable formations or the surface can be tolerated.)
3. From explosion efficiency standpoints, only the producing formation need be fractured, although the larger the permeable radius the better the deliverability (within the other criteria).

Cavity Radius

The predicted radius of the cavity is based upon that calculated from the effects of a single 50-kiloton explosion and was based upon the empirical relations obtained from analysis of a number of contained shots. (5, 8, 8)

$$r_c = CW^{1/3} / (\rho D_b)^{1/4} = 270 \times 50^{1/3} / (2.35 \times 7,500)^{1/4} = 86 \text{ feet}$$

where:

r_c = cavity radius, feet.

C = constant for the material, assumed to be 270 for this formation.

W = size of device in kilotons (50).

ρ = bulk density of the media, estimated from density log measurements to be 2.35 gms/cm³.

D_b = true depth of burial, 7,500 and 8,500 feet.

The equation is most sensitive to the constant C. This constant is apparently a function of the water content of the rock and the lithologic composition. The constant varies from 252 to 231 for alluvium shots, from 321 to 361 for tuff, from 258 to 336 for a combination of tuff and alluvium, and from 262 to 275 for granite. ⁽⁶⁾ The factor 270 seemed to be reasonable for this formation because of its limited water and gas saturation, and the fracture characteristics are thought to be somewhat similar to that of granite.

Chimney Height

The chimney dimensions resulting from contained nuclear explosions have been studied in four media, and the radius of the chimney has been found approximately equal to that of the initial cavity. On the basis of strictly empirical correlation of the height of chimney versus the radius of the chimney for the tuff and granite shots, the following relationship was obtained:

$$h_c = C_h r_c = 5 \times 86 \text{ feet} = 430 \text{ feet}$$

where:

h_c = height of chimney, feet.

C_h = height factor, 5.

r_c = radius of cavity, feet.

Radius of the Permeable Zone

In addition to the chimney cavity features created by the explosion, of equal importance to the production of natural gas from the post-shot environment is the increased permeability created by the zone of fractures surrounding the chimney area. Observations of increased permeability have been made specifically at Project Gnome in salt, Project Hardhat in granite, and Project Rainier in tuff. ^(9, 10, 11) Zones of increased permeability, as indicated by the loss of drilling fluid, have been observed at other events.

The equation describing the average permeable zone radius based upon an empirical correlation of data from brittle rock is as follows:

$$r_p = C_r r_c = 4 \times 86 \text{ feet} = 344 \text{ feet}$$

where

r_p = radius of the permeable zone in feet.

C_r = fracture zone radius factor, 4.

r_c = radius of the cavity in feet.

Height of Permeable Zone

Similarly the height of the permeable zone can be calculated from the available data. The relationship is as follows:

$$h_p = C_h r_c = 7 \times 86 \text{ feet} = 602 \text{ feet}$$

where:

h_p = height of the permeable zone in feet.

C_h = fracture zone height factor, 7.

r_c = cavity radius in feet.

The largest fracture zone height factor is 7.7 noted at the Hardhat event. Because it is important that the vertical fractures do not communicate with other permeable zones above the formation of interest and because the maximum noted height of permeable zone is 10 percent greater than the factor used in these equations, it is suggested that at least a 20 percent safety factor be used in the calculations to provide a buffer zone between the calculated height of the permeable zone and the overlying formation which should be unaffected by the event.

RADIOACTIVITY

The amounts and kinds of radioactivities produced by the detonation of a practical nuclear explosive are dependent upon the design of the device and will vary between the theoretical extremes of a pure fission or pure

fusion reaction. Unclassified information in this area is quite sketchy and can only be used as a guide to the magnitude of the problem.

A substantial portion of the radioactivity created is associated with solid radioactive elements which will be contained within the explosion melt and fused rock material associated with cavity and subsequent rubble formation. (7, 12, 13, 14, 15, 16) The Mesaverde does contain a wet hydrocarbon gas; however, little liquid dropout should occur in the chimney during the early phases of gas production. In addition, the small amount of liquid that does condense from the gas in the formation should not flow to the wellbore and will remain in the matrix and chimney rubble. Thus, solid isotopes should not create hazards in the gas produced.

A certain amount of the fission products are gaseous and these will permeate the cavity and rubble void space. A number of these gaseous elements have short half-lives and rapidly decay to solid "daughter" elements which will deposit on the solid rubble surface. The deposited solid isotopes, although radioactive, should create no contamination problem to the hydrocarbon gas present in the formation and during subsequent production.

Some of the gaseous radioactive isotopes which will be present in the natural gas at an appreciable time after the explosion are iodine-131, xenon-133, and krypton-85. Both iodine-131 and xenon-133 are formed in considerable yield. The fact that both have relatively short half-life periods (I-131, 8.1 days, and Xe-133, 5.3 days) will allow their concentration to decay fairly rapidly after the explosion. For example, as a result of the time required to drill, core, complete, and test a production well into the explosion cavity-chimney zone, the original concentrations would decay several orders of magnitude. In addition, iodine-131 is extremely reactive and may be readily removed

from a gaseous stream with a number of basic chemicals (such as caustic) or by absorption on activated charcoal. Thus, iodine and xenon are not considered to constitute a radiation problem in the gas stream.

Another problem radioactive isotope is krypton-85, which is produced in quantity and has a long half-life, 10.3 years. Calculations show that it will occur in the initial cavity-chimney volume in concentrations greater than the "maximum permissible concentration" (MPC) for biological tolerance standards set by the federal government. The actual magnitude of the problem will be further defined as a result of the data from the Gasbuggy explosion in a similar gas-bearing formation. If it is found from Gasbuggy that a serious problem may in fact exist, there are several possible techniques to alleviate the problem. These are:

1. Dilution of the chimney gas with uncontaminated gas from other wells and fields in the area to below the MPC. The resultant diluted gas could be sold. In practice, only the initial volume of gas contained in the cavity-chimney zone needs to be diluted, since the gas flowing into the chimney from the surrounding formation will not be contaminated and will itself be a diluent.
2. Flaring an initial volume of gas until the radioactive contamination is below MPC. This is wasteful of gas, but may prove easiest to accomplish, since a portion of the gas may be flared during the post-shot production well evaluation tests.
3. Removal of the krypton-85 and subsequent sale of the decontaminated gas. Physical removal schemes such as absorption appear to have some merit for purifying the gas and research into the area is being conducted at a number of laboratories.

Tritium, an isotope with a long half-life (12.3 years), may well be a problem if introduced into the gas system. Tritium, since it is an isotope of hydrogen may enter into exchange reactions with the hydrocarbons and water present in the cavity-chimney zone.

In addition to venting and flaring the cavity-chimney to the atmosphere and diluting the gas, it may also be possible to stem the device in the emplacement hole with a reactive material to retain the tritium in a solid or least easily removable form. If the tritium occurs mainly as water in the vapor phase, the dehydration procedures using molecular sieves, etc., well known to the petroleum industry will remove a portion of the contamination. A number of other possibilities exist as described by Bonner, et al, ⁽¹⁸⁾ but the true magnitude of the problem cannot be evaluated until an actual test is made to evaluate the reactions occurring at the explosion conditions and the resulting concentrations. A portion of the Gasbuggy project will be to evaluate the magnitude and possible removal scheme for tritium contamination in the natural gas.

In addition to the radioactivity produced in the fission products and tritium, consideration must be given to the problem of induced radioactivity in the reservoir rock and gaseous material (hydrocarbon plus connate water which may be vaporized) as a result of neutron capture during the explosion. Based on the assumption that 1×10^{23} neutrons are emitted from an explosion per kiloton of yield, ^(12, 15, 16) it is possible to calculate the amount captured in the surrounding media. Those captured by the elements comprising the solid rock material will again present no hazard to subsequent production of the gas stream. An extremely small fraction of the neutrons, however, will be captured by the hydrogen present in both the hydrocarbon gas and the water in the formation. Calculations of the amounts of tritium or isotopes of carbon formed show that no additional contamination problem will result from induced radioactivity. As a result of the extremely fast explosion time, inconsequential amounts of both of these radioactive elements are formed.

SEISMIC EFFECTS

Seismic effects from an underground nuclear explosion are functions of both the yield of the device and the geology of the area. The surface location of the Rulison emplacement hole is tentatively placed in the northwest corner of Section 36 at an elevation of 8,600 feet. The control point would be tentatively located in the center of the northwest quarter of Section 23 at an elevation of 7,000 feet and approximately 2-1/4 miles from the shot point. It is estimated that the control point will receive less than 30 centimeters per second maximum particle velocity, which is a safe limit of ground movement for both personnel and equipment.

Mickey⁽¹⁹⁾ has summarized the various investigations and arrives at the conclusion that the threshold particle velocity for minor damage to residential structures could be as low as 8 centimeters per second. The available data for underground explosions indicates that this threshold for minor damage zone--in other words, plaster cracking, etc.--for the 100-kiloton Rulison explosion would occur at 2.9 miles if the rock were tuff, and at 5.9 miles if the rock were granite.

Bonner, et al,⁽¹⁸⁾ state that this radius for plaster cracking would be approximately four miles for a 100-kiloton explosion in the San Juan Basin. The seismic effects could be felt at distances greater than this, but the possibility of damage to residential structures is remote.

Cauthen has analyzed similar data^(20, 21) and indicates that threshold particle velocity for plaster cracking damage is more like 11 centimeters per second. This results in an even more favorable situation.

Using the surface shot point as the center, a 4-1/2-mile radius circle was scribed on the USGS map of the area. This circle defines the area in which some damage to dwellings and structures may occur

(conservatively based on a calculation for granite, see Figure 2, and using an intermediate critical velocity of 10 centimeters per second). Beyond the 4-1/2-mile circle, little if any plaster cracking or chimney breakage should occur, and then only if the building is very old or standing on very poor soil. Inside this line, minor plaster cracking will be expected as well as some chimney damage.

The closest gas well installation, three miles from the shot point, should experience no damage. Criteria developed at the Nevada Test Site by the AEC show that cased holes at distances greater than $600 W^{1/3}$ feet are not damaged by the ground explosions in alluvium. No such rule of thumb exists for other media; but according to Cauthen, ⁽²¹⁾ it is generally felt that this figure represents a conservative safe range for other media.

A recent experiment at the Nevada Test Site reported by Rabb ⁽²²⁾ indicates that the buried line wellhead and other surface equipment should not experience any damage. In this experiment, a simple Christmas tree and a short run of line pipe was laid out in a "T" conforming to standard oil field practice. The system was partially buried and partially above the ground. The pipe run was pressurized with Freon during and after a 10-kiloton shot which was detonated 950 feet away. The equipment took a 5.6 g vertical and 1 g radial shock with no physical damage or loss of pressure. No leaks were detected in this closed system.

The closest surface gas facility in the Rulison Field test area should experience only 1/2 g, based upon the granite data. Therefore, no damage to gas well surface equipment or pipelines is anticipated.

GENERAL SURVEY OF SURROUNDING AREA

There are approximately 100 homes within a four to five mile radius from the ground zero, predominantly of frame construction but with a few masonry dwellings. Every home has a brick chimney, many of which are considered to be marginal to poor structurally.

It is felt that these homes and the following areas should be checked and documented preshot.

On the south side of the river near Grand Valley is an old abandoned school house built of fieldstone in 1909. Some of the ceiling has already fallen in, and the walls are in bad shape. The school house may incur some additional damage.

A cemetery approximately a quarter of a mile from the school house may also have some of the headstones overturned due to the poor cement.

Rulison (6.8 miles from ground zero) - There are a 10-ton capacity bridge, a concrete block house, and a barn in this area which should be documented. It is felt that no shock effect damage will occur here.

Grand Valley (6.9 miles from ground zero) - There is a 10-ton capacity bridge in this area. The high school is constructed of brick. There are also approximately 15 concrete block and 13 plaster structures. An estimated 20,000-gallon water tank is located on a hill. If the water level was lowered in the tank for the shot, we would not anticipate any damage in this community.

Anvil Points Oil Shale Facility (8.2 miles from ground zero) - Twenty-five percent of the houses in this area have metal siding. Seventy-five percent of the houses are frame with asbestos shingles.

There are approximately ten 20,000-gallon capacity water tanks and five 20,000-gallon capacity oil tanks in this area. These tanks should have their liquid level lowered. One large concrete block warehouse, 40 feet by 100 feet by 20 feet high, is located in this area. All the smoke stacks and refining equipment are well guyed and secured to concrete blocks. If the liquid levels in the tanks are lowered, no damage is anticipated in this area. No one should be allowed in the shale mine above the plant during shot time in case of unstable ceiling slabs.

Rifle (12-3/4 miles from ground zero) - Of the approximately 1,000 structures in this community, 850 are frame, 100 masonry and 50 plaster. Many of these buildings are quite old, showing age cracks and settlement. The area lies on gravel fill approximately 75 feet thick. All the power lines in the area are in good condition. There are a mausoleum and a fairly well-kept cemetery in the area, as well as a large new brick school and a 50-bed brick hospital.

East of the town are a 75-foot microwave tower and a 20,000-gallon capacity water tank, which should have its liquid level lowered at test time. Northwest of the town of Rifle is a 30 x 100 foot reservoir; its dikes are 20 feet high and it is in good condition except for the flume supplying the reservoir which appears to leak badly at the center span. Further northwest of Rifle is a trail road leading up the steep slopes to the Naval oil shale reserve. This road should be blocked for safety, and all personnel evacuated from the mine as previously noted. There is a 10-ton capacity bridge with a long span at Rifle.

The Union Carbide Yellow Cake plant which upgrades uranium ores is located south of Rifle on the north side of the Colorado River and contains six concrete block buildings. Two 40-foot high silos appear to be made of steel, and there is also one 25,000 to 50,000-gallon steel elevated water tank which should have its liquid level lowered at shot time.

Little damage is anticipated in the Rifle area.

DeBeque Canyon (18.4 miles from ground zero) - The DeBeque Canyon is located southwest of the town DeBeque on the main highway, U. S. 6 and 40. We anticipate no effect this far from the shot point, but this canyon should be blocked to traffic for a 15-minute period during the test in case of rock falls at places where the highway runs close to the steep cliffs.

Figures 16 and 17 display some typical houses in the four to five-mile radius from the shot point, the church at Rifle, and the canyon in the DeBeque narrows.

Preshot Seismic Survey

Currently, a preshot seismic survey is being considered, to more closely define the thickness of the alluvium and to evaluate the difference between the maximum velocity experienced by structures located on bedrock and structures located on the terrace deposits or in the valley alluvial fill.

The result of this survey should allow a much closer estimate of the maximum velocities to be experienced by structures located within ten miles of the proposed shot point. However, a good deal of additional instrumentation will probably be required during the time of the shot to gain some idea of local characteristics of focusing and addition of shock effects which could result in local velocities that are much higher than anticipated.

WELL TEST AND DATA ANALYSIS PROCEDURE

Austral's Federal A 29-95 well near the proposed shot location has been comprehensively logged, and extensively cored. In addition, a detailed testing and data analysis program has been carried out on this to more adequately define the reservoir conditions in the southwestern portion of the field. This test data is discussed in detail in Appendix B.

It is anticipated that a comprehensive coring, logging, and well-test program will be carried out on the emplacement hole and/or instrumentation hole prior to the shot. This program will be necessary to evaluate the optimum placement of the shots in the formation, as well as to aid in determining the amount of stimulation achieved by the nuclear explosion.

A similar coring, logging, and well-test program will be conducted on the reentry well into the explosion environment to determine the size and characteristics of the post-shot geometry.

The currently estimated potential for a conventional well at the proposed test site is 150,000 scf/ d with surface pressure of 300 pounds. The estimated potential due to the increased wellbore radius effect, as well as to the effect of connecting an increased amount of the pay to the wellbore, will be in the order of 12-fold. The maximum anticipated pipeline allowable will be 5 million scf/ d during the early production from the well and the well should stabilize at approximately 1.5 million scf/ d. A rate-versus-time plot of the anticipated post-shot production which results from the computer analysis of the anticipated post-shot geometry is presented as Figure.18. This figure considers three cases as well as the conventional well performance: (1) a two-dimensional radial flow model with a shot effectively draining a 100 billion scf per section reservoir, (2) a two-dimensional radial flow model with a shot effectively draining a 50 billion scf per section reservoir, and (3) a three-dimensional flow model with a shot effectively connecting only 34 billion scf of a 100 billion scf per section reservoir.

A rigorous three dimensional mathematical isothermal flow model for gas in porous media will be used to analyze the data from the test program. An IBM 7094 and/ or an IBM 360 computer system will be used to fit the pre- and post-shot dynamic flow data together with the knowledge of the post-shot formation environments.

The detailed well test procedure is presented as Appendix A.

AREAS OF RESPONSIBILITY

AUSTRAL - CER

In addition to the preliminary technical studies which are reported in this proposal and which are currently underway, Austral Oil Company Incorporated and CER Geonuclear Corporation will be responsible for:

1. Providing adequate emplacement hole for the nuclear device and providing expert supervision on drilling, casing, and completing this hole.
2. Drilling, coring, logging and testing the proposed emplacement hole and the post-shot producing well.
3. Providing the preshot feasibility studies and pre- and post-shot production evaluation.
4. Providing additional computer simulation runs on the calculations of post-shot geometry.
5. Providing logistical and technical support for its own personnel.
6. Furnishing at AEC direction and expense, any services the AEC deems to be necessary to its part of the experiment.

ATOMIC ENERGY COMMISSION AND ITS CONTRACTORS

The Atomic Energy Commission will provide project management in the fielding and firing of the nuclear device. Thus, they will be responsible for:

1. Public safety from pre- and post-shot nuclear effects.
2. Furnishing and protection of device.
3. Device emplacement and detonation.
4. Instrumentation as needed to support their tasks.

We have purposely listed the areas of responsibility between the AEC and Austral-CER in general terms. One of the first tasks should be discussions between the AEC and Austral-CER to work up cost estimates for the project.

SCHEDULING

The Austral shot could be fired approximately 10 months after the Gasbuggy and Dragon Trail shots. This would allow time for analysis of the effect of nuclear stimulation and drilling and testing of the emplacement holes. A 12-month post-shot test period is anticipated. A tentative AEC, Austral-CER time schedule is presented in Figure 19.

REFERENCES

1. Zeito, G. A., "Interbedding of Shale Breaks and Reservoir Heterogeneities," SPE Paper 1128, Denver 1965 Meeting.
2. Kiel, O. G., and Campbell, J. M., "Analysis of Gas Well Behavior Using a Two-Dimensional Unsteady-State Model," AIME Paper 562, April 29-30, 1963.
3. Kiel, O. G., PhD Dissertation, University of Oklahoma, Norman, Oklahoma (1963).
4. Nordyke, M. D., "Cratering Experience with Chemical and Nuclear Explosives, USAEC TID 7695 (Engineering with Nuclear Explosives) pp 51-63 (1964).
5. Boardman, C. R., Rabb, D. D., and McArthur, R. D., "Characteristic Effects of Contained Nuclear Explosions for Evaluation of Mining Applications," Lawrence Radiation Laboratory, Livermore, California, UCRL 7350 (May 1963).
6. Boardman, C. R., Rabb, D. D., and McArthur, R. D., "Contained Nuclear Detonations in Four Media--Geologic Factors in Cavity and Chimney Formation," USAEC TID 7695 (Engineering with Nuclear Explosives) pp 109-126 (1964).
7. Johnson, G. W., and Violet, C. E., "Phenomenology of Contained Nuclear Explosions," UCRL 5124, Rev. I; Univ. of Calif.; Lawrence Radiation Laboratory, Livermore (Dec. 1958).
8. Coffey, H. F., Bray, B. G., Knutson, C. F., and Rawson, D. E., "Some Effects of Nuclear Explosions on Oil Reservoir Stimulation," J. Pet. Tech., v 16, No. 5, pp 473-480 (May 1964). (Appendix)
9. Rawson, D. E., "Review and Summary of Some Project Gnome Results," UCRL 7166 (Dec. 1962).
10. Atkinson, C. H., "Subsurface Fracturing from Shoal Nuclear Detonation," Report PNE 3001, USAEC - U. S. Bu. Mines (Nov. 1964).
11. Boardman, C. R., "Changes in the Fracture Permeability of a Granite Rock Mass Resulting from a Contained Nuclear Explosion," SPE Paper No. 1358, Denver 1965 Meeting.
12. Miskel, J. A., "Characteristics of Radioactivity Produced by Nuclear Explosives," USAEC TID 7695 (Engineering with Nuclear Explosives) pp 153-159 (1964).
13. Bennett, W. P., Anderson, A. L., and Smith, B. L., "Cavity Definition, Radiation, and Temperature Distributions from the Logan Event," UCRL 6240 (Dec. 1960).

14. Peterson, J. D., and Bennett, W. P., "Radiation and Temperature Measurements of the Neptune Event," UCRL 6251 (Jan. 1961).
15. Batzel, R. E., "Radioactivity Associated with Underground Nuclear Explosions," UCRL 5623 (June 1959).
16. Batzel, R. E., "Distribution of Radioactivity from a Nuclear Explosion," UCRL 6249-T (Oct. 1960).
17. Higgins, G. H., Rodean, H. C., "Some Calculations for Affecting an Oil Field Stimulation by Nuclear Means." AIME-SPE Paper No. 1301, presented at annual SPE meeting, Denver, October 3-6, 1965.
18. Bonner, N., Holzer, F., James, R., Lombard, D., and Rawson, D., "Plowshare Technical Information Related to Gas Reservoir Stimulation," Lawrence Radiation Laboratory, Livermore (July 28, 1964).
19. Mickey, W. V., "Seismic Wave Propagation," USAEC TID 7695 (Engineering with Nuclear Explosives) pp 181-194 (1964).
20. Cauthen, L. M., "The Effects of Seismic Waves on Structures and Other Facilities," USAEC TID 7695 (Engineering with Nuclear Explosives) pp 207-227 (1964).
21. Cauthen, L. J., "Survey of Shock Damage to Surface Facilities and Drilled Holes Resulting from Underground Nuclear Detonation," UCRL 7694 (July 1964).
22. Rabb, D. D., "Test Field Equipment Survives Nuclear Blast," Oil and Gas J., p 71 (Jan. 3, 1966).

LETTER SYMBOLS

a	=	minor semi-axis of an ellipse
a'	=	constant = $9.03 \times 10^4 kh (p_i^2 - p_w^2) / T_f \ln (.606 r_e / r_w)$
A	=	constant = $1.39 \times 10^{-2} k p_w / (r_w^2)$
b	=	minor semi-axis of an ellipse
B	=	constant = $19.7 \times 10^{-6} kh T_{sc} / T$
BPM	=	barrels per minute
BH	=	bottom hole
BHF	=	bottom hole flowing
c	=	$\ln a' - t_b$
cc	=	cubic centimeter
C	=	lithology factor for cavity radius calculations
C _h	=	factor for chimney height calculation
C _p	=	factor for permeable zone height calculation
C _r	=	factor for permeability zone radius calculation
d	=	day
D	=	constant = $2.715 \times 10^{-15} k p_{sc} MB / (h T_{sc} T_w)$
D _b	=	depth of burial of nuclear device
f	=	equal probability factor
g	=	gravity
gal	=	gallon
gm	=	gram

h	=	net pay thickness
h_c	=	height of nuclear chimney
h_p	=	height of permeable zone
h_t	=	height of sand lenses
k	=	permeability
k_r	=	radial permeability
kt	=	kiloton
k_z	=	vertical permeability
ln	=	natural log
\log_{10}	=	log to base 10
L	=	length of sandstone lense
m	=	slope of build-up curve
md	=	millidarcy
Mg	=	molecular weight of gas
$M_{(p)}$	=	constant = $2 \frac{P}{P_m} \left(\frac{d}{(p)} \right)^z (p) d_p$
MPC	=	maximum permissible concentration
p	=	pressure
P_d	=	pressure at well's drainage radius
P_e	=	pressure at well's maximum effective drainage radius
P_i	=	initial pressure
P_r	=	initial pressure of corralative layer
P_{sc}	=	standard reference base pressure
psi	=	pounds per square inch

psia	=	pounds per square inch absolute
p_w	=	pressure at well bore
q	=	flow rate
q_f	=	flow rate after fracture
q_o	=	flow rate before fracture
r	=	radius
r_c	=	radius of cavity
r_d	=	radius of drainage
r_e	=	radius of maximum effective drainage
r_{ef}	=	radius to zone of effective minimum net pay
r_p	=	radius of permeable zone
r_w	=	radius of well bore
S	=	skin factor
scf	=	standard cubic feet
SDB	=	scaled depth of burial
t	=	time
t_b	=	time constant
T	=	absolute temperature
TD	=	total depth
T_f	=	subsurface flowing temperature
T_{sc}	=	temperature at standard conditions
T_w	=	temperature at well datum plane
V	=	volume

W	=	yield of nuclear device, kilotons
x	=	horizontal distance
X	=	horizontal distance in east-west direction
y	=	horizontal distance perpendicular to x
Y	=	horizontal distance in north-south direction
z	=	gas deviation factor
Z	=	vertical distance
α	=	constant = $1.25 \times 10^{-2} k_{p_i} / [\mu \phi r_e^2 \ln (.472 r_e / r_w)]$
μ	=	viscosity
π	=	3.1416
ρ	=	density
ϕ	=	effective porosity
ϕ_{HC}	=	effective porosity filled with hydrocarbons
r_m	=	ohm-meters

TABLE I
SAND CONTINUITY DATA (After Zeito⁽¹⁾)

PERCENT OF SAND PINCHING OUT
WITHIN INDICATED DISTANCE FROM REFERENCE

<u>Zeito's Outcrop Nos.</u>	<u>250 feet</u>	<u>500 feet</u>	<u>1,000 feet</u>
5	67%	67%	67%
6	50%	*	*
24	71%	71%	*

*Outcrop was not wide enough to determine.

TABLE II
CALCULATED FORMATION WATER RESISTIVITY VALUES

<u>Well No.</u>	<u>Formation or Member</u>	<u>Depth, in feet</u>	
3-94	Paleocene Ft. Union	4,000 -5,000	0.075 Ω_m
3-94	Cretaceous Farrer	5,000 -6,000	0.04 Ω_m
3-94	Cretaceous Neslen	6,000 -TD	0.065 Ω_m
A 29-95	Cretaceous Neslen	5,200 -5,800	0.065 Ω_m

TABLE III
AVERAGE ROCK PROPERTIES

<u>Sandstone Lens Rock Property</u>	<u>Average Value</u>
Porosity	9.7%
Permeability	0.5 md.
Water Saturation	45%
Average Possible Gas Bearing Sandstone	500 net feet
Estimated Gas in Place	90-125 billion scf/ Section

TABLE IV
CALCULATED INITIAL BOTTOM HOLE PRESSURES
OF RULISON WELLS

<u>Well No.</u>	<u>Datum Plane Elevation (feet from Sea Level)</u>	<u>Initial Datum Plane Pressure (psi)</u>
Juhan No. 1	- 500	2600
Gross Hahnewald No. 1	- 500	2600
Federal 28-95	+1000	1950
Federal A 29-95	+2500	1280
Federal 30-95	+1000	1950

TABLE V
EVALUATION OF CONVENTIONAL FRACTURING ON EARLY RULISON WELLS

Interval (feet)	Horizontal				Vertical Orientation						
	Slurry Volume (gal)	Pounds of Sand	Avg. Pump Rate BPM	Fluid Loss Coef. ft/(min) ^{1/2} x10 ⁻³	Created Area (feet)	Eqiv. Circular Radius (feet)	Produc- tivity Increase q _r / q _o	Elliptical Pene- tration (feet)	Produc- tivity Increase q _r / q _o	Eqiv. Wellbore Radius (feet)	Avg. Fluid Loss Penetration (inches)
<u>No. 1 Juhan</u>											
5066-5092	40,000	20,000	14.3	11.8	17,200	74	3.3	105	3.4	65	35
5600-5624	31,080	20,000	7.3	12.4	10,300	57	3.2	81	3.2	52	46
5966-6008	22,600	17,500	7.8	12.8	8,700	53	3.1	75	3.1	49	40
6227-6255											
6283-6302	31,080	25,000	7.1	13.0	9,700	56	3.2	79	3.2	52	49
6417-6440	27,300	20,000	8.2	13.1	9,800	56	3.2	79	3.2	52	43
<u>No. 1 Juhan Federal</u>											
5354-5404	39,300	20,000	29.6	12.2	23,000	86	3.7	121	3.7	77	25
6150-6198	44,900	19,500	22.0	13.0	20,300	81	3.6	114	3.6	71	33
6570-6596	46,000	21,500	17.1	13.4	17,100	74	3.5	105	3.6	71	41
6762-6796											
6830-6856	51,000	24,100	21.5	13.6	20,400	81	3.6	114	3.7	77	38
8020-8090*											
8136-8186*	40,900	20,000	20.0	9.7	24,100	87	3.7	124	3.8	81	25
8344-8424*	18,700	16,000	5.2	9.9	8,400	52	3.1	73	3.1	49	34
<u>Federal No. 3-94</u>											
6333-6353	55,100	50,000	71.0	13.1	38,800	111	4.3	157	4.4	105	21
<u>Federal No. 28-95</u>											
5084-6140	79,300	96,000	48	12.4	41,100	114	4.6	161	4.8	124	28
6243-7204	100,000	96,000	39	13.5	38,800	111	4.6	157	4.8	124	39

*Cozette Formation ($\phi = 0.10$; $k = .2$ md)

TABLE V (Cont.)

Interval (feet)	Slurry Volume (gal)	Pounds of Sand	Avg. Pump Rate BPM	Fluid Loss Coef. $\text{ft}/(\text{min})^{1/2} \times 10^{-3}$	Propped**Circular Area (feet ²)	Horizontal		Vertical Orientation			
						Eqiv. Circular Radius (feet)	Productivity Increase q_t / q_o	Elliptical Penetration (feet)	Productivity Increase q_t / q_o	Wellbore Radius (feet)	Avg. Fluid Loss Penetration (inches)
<u>Summary - Federal 3-94</u>											
6333-53	91,100	60,000	71	0.5	88,700	168	5.6	238	6.2	180	Low
6198-6210	75,100	42,000	41	0.5	60,700	139	5.0	197	5.4	150	Low
5474-5630	110,700	83,500	76	0.5	117,000	193	5.8	273	7.0	210	Low
5170-5434	66,600	46,200	44	0.5	63,400	142	4.7	201	5.5	155	Low
*5484-5630	115,600	105,420	67	0.5	225,000	268	7.2	378	9.10	275	Low
<u>Summary - Federal A 29-95</u>											
5264-5394	115,200	73,500	72	0.5	107,400	185	5.3	262	6.8	210	Low
Unknown	107,000	73,500	55	0.5	97,300	176	5.2	249	6.7	205	Low
5967-6427	124,200	95,300	68	0.5	121,800	197	4.7	278	7.1	218	Low
6668-6924	153,100	105,400	65	0.5	138,500	210	5.3	297	7.4	225	Low

*Includes the 110,000 gallon treatment performed earlier in this interval.

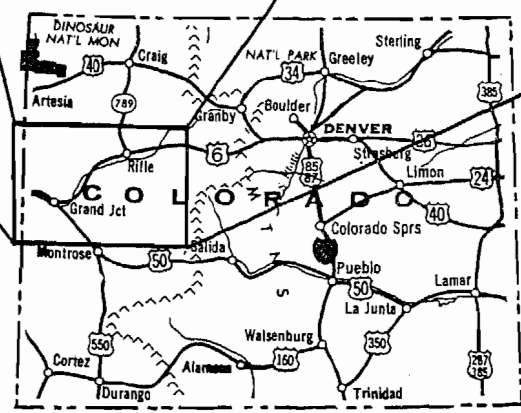
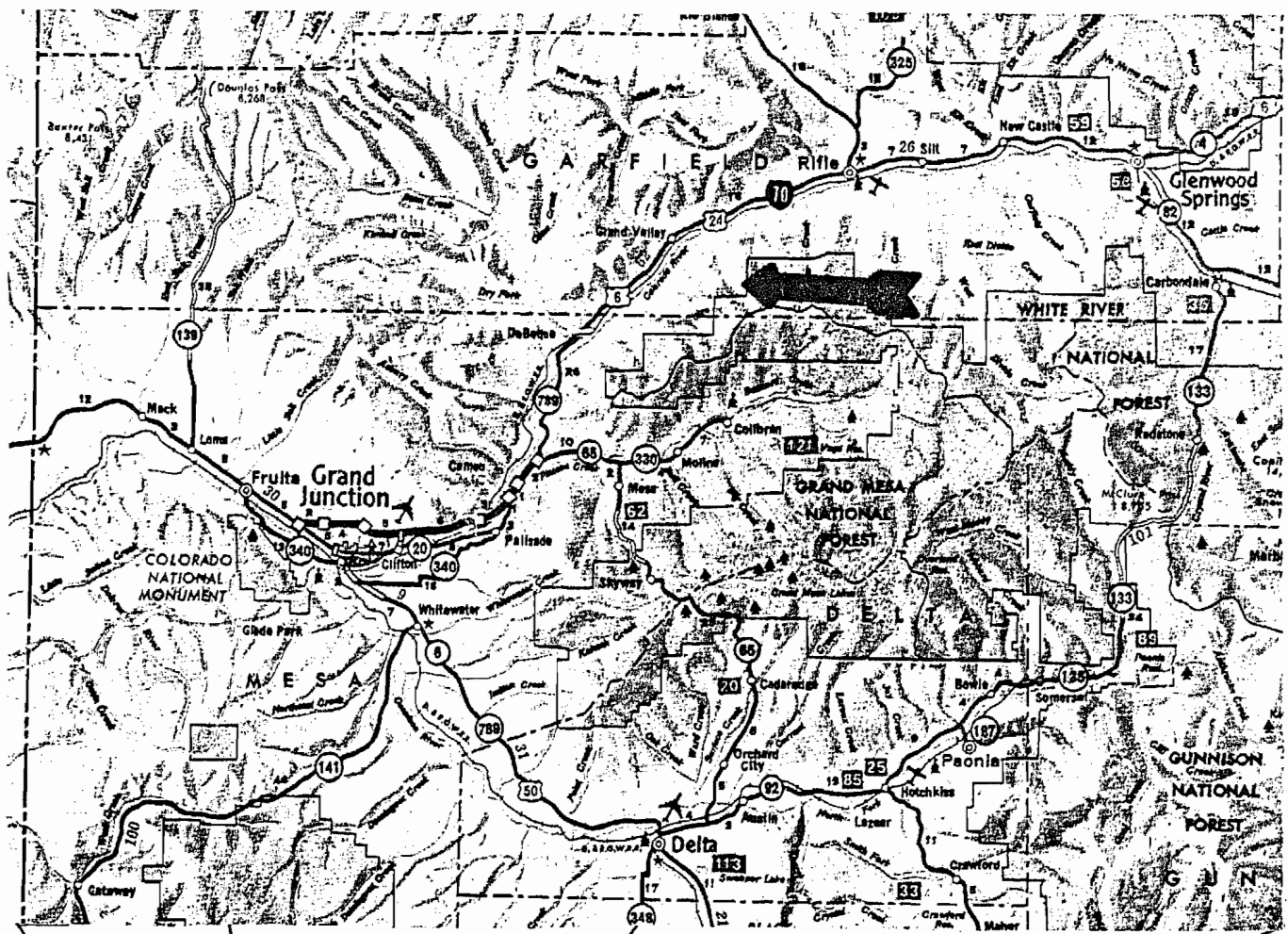
**For Federal 3-94 and Federal A 29-95, calculations are based on the propped (effective) fracture area. The excellent fluid loss control achieved by the guar gum-water frac fluids result in extremely large created fracture areas. For example, the treatment in the 6333-53 foot interval in Federal 3-94 creates a total area of 429,000 square feet; while only 88,700 square feet is propped and remains open after the treatment ends. When fluid loss to the formation is high, as in the earlier treatments, the created area and propped areas are essentially equal.

TABLE VI
 CALCULATED RESERVOIR CAPACITIES,
 MESAVERDE WELLS

<u>Well No.</u>	<u>Contributing Net Pay (feet)</u>	<u>Average Calculated Permeability (md)</u>
Juhan No. 1	50	0.06
Federal 28-95	64	0.04
Federal 29-95	25	0.5
Federal 30-95	35	0.03

TABLE VII
ANTICIPATED POST SHOT GEOMETRY OF RULISON FIELD

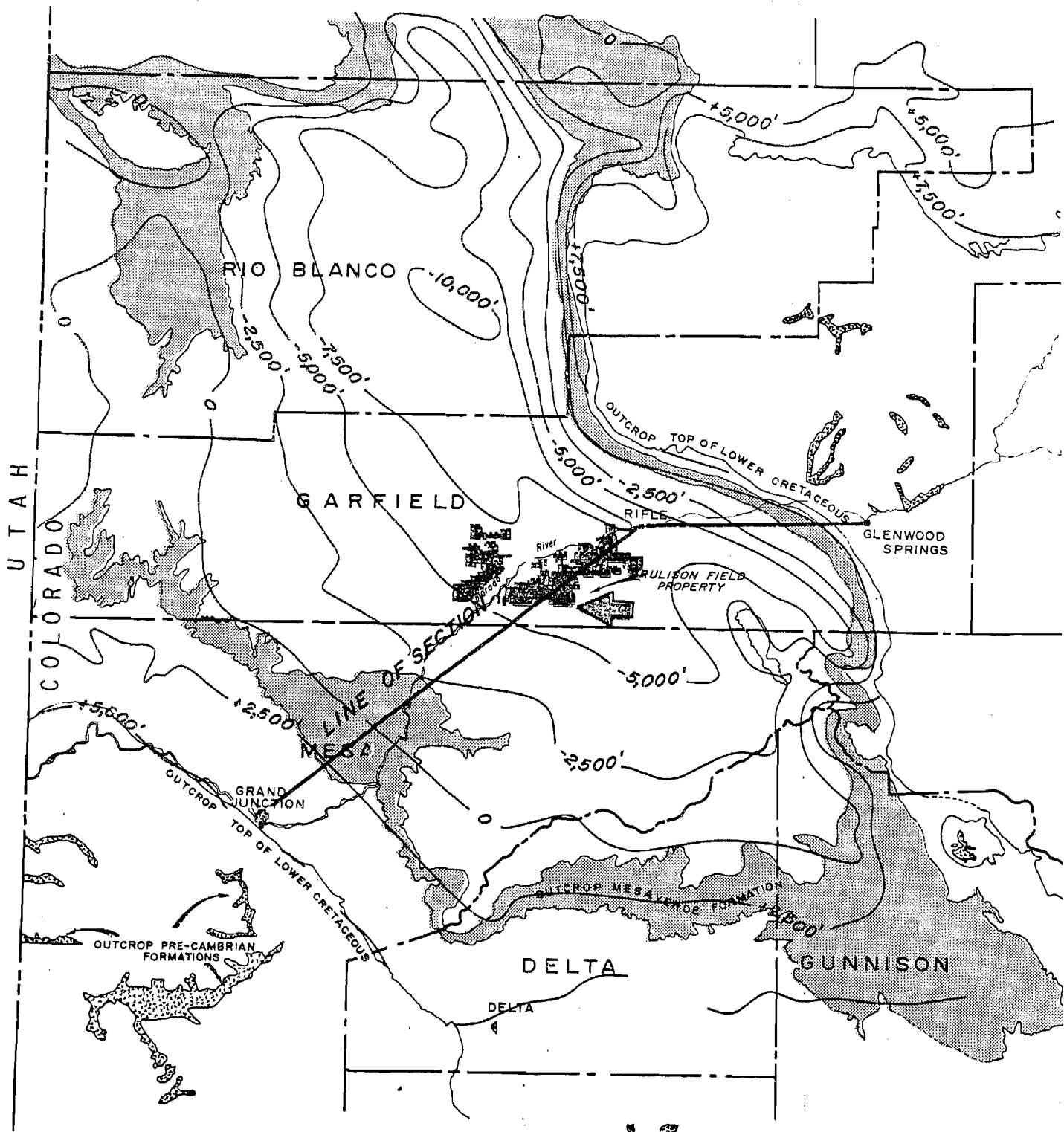
Cavity Radius	
50-kiloton at 7500 feet	88 feet
50-kiloton at 8500 feet	86 feet
Chimney Height	
50-kiloton at 7500 feet	440 feet
50-kiloton at 8500 feet	
With addition factor of 1	430 feet
With addition factor of 1.25	538 feet
With addition factor of 1.5	645 feet
Height of Permeable Zone	
50-kiloton at 7500 feet	616 feet
50-kiloton at 8500 feet	
With addition factor of 1	602 feet
With addition factor of 1.25	754 feet
With addition factor of 1.5	904 feet
Radius of Permeable Zone	
50-kiloton at 7500 feet	352 feet
50-kiloton at 8500 feet	344 feet
Lithology Factor "C" (in $r_c = \frac{CW^{1/3}}{(ph)^{1/4}}$)	270
Volume occupied by gas in Chimney	
50-kiloton at 7500 feet	3.29 x 10 ⁶ cubic feet
50-kiloton at 8500 feet	
Multiplier of 1	3.01 x 10 ⁶ cubic feet
Multiplier of 1.25	3.76 x 10 ⁶ cubic feet
Multiplier of 1.5	4.51 x 10 ⁶ cubic feet
Volume occupied by gas in Fractured Zone	
50-kiloton at 7500 feet	14.9 x 10 ⁶ cubic feet
50-kiloton at 8500 feet	
Multiplier of 1	13.6 x 10 ⁶ cubic feet
Multiplier of 1.25	17.0 x 10 ⁶ cubic feet
Multiplier of 1.5	20.4 x 10 ⁶ cubic feet



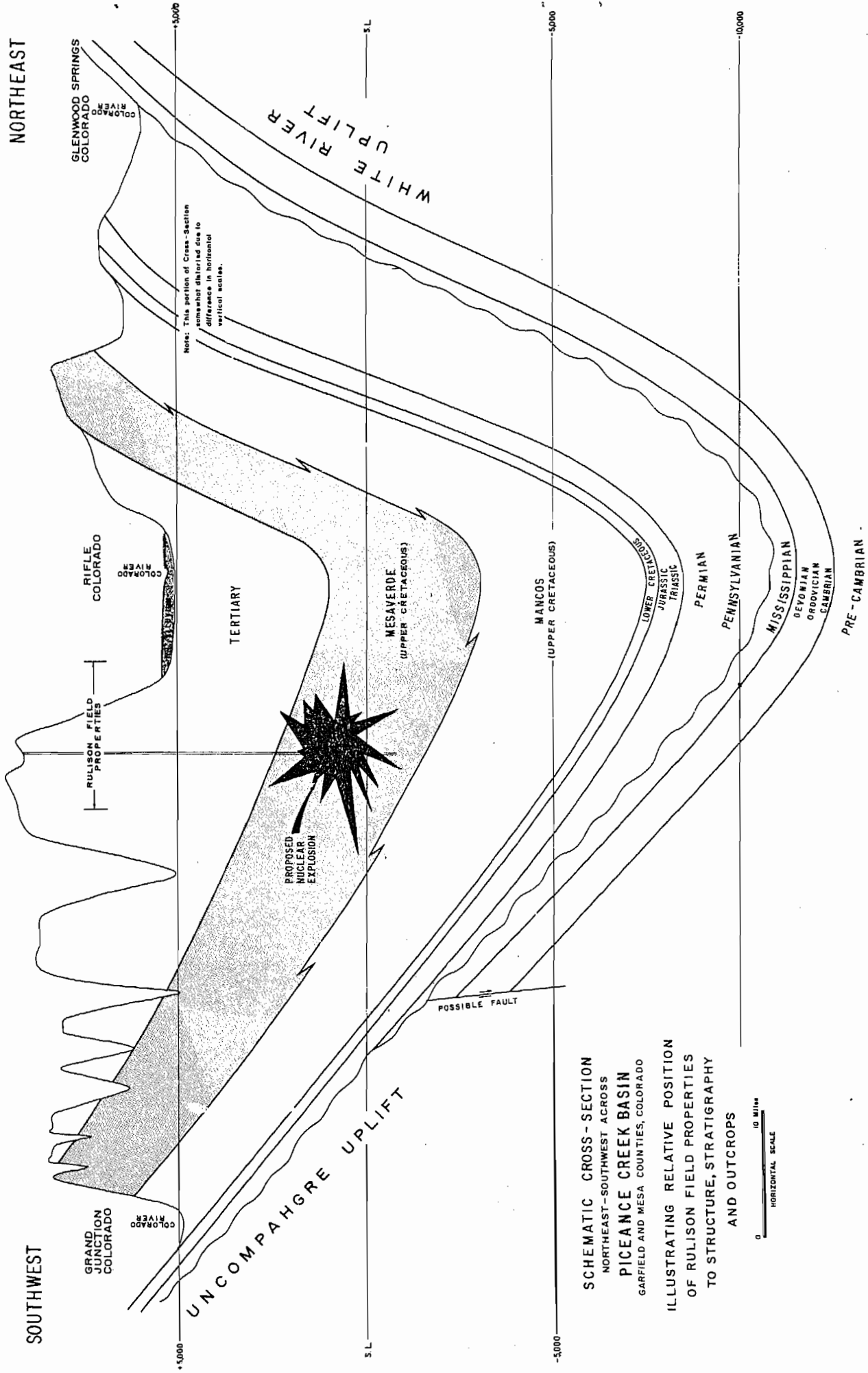
ROAD MAP OF NORTHWEST COLORADO



FIGURE 1



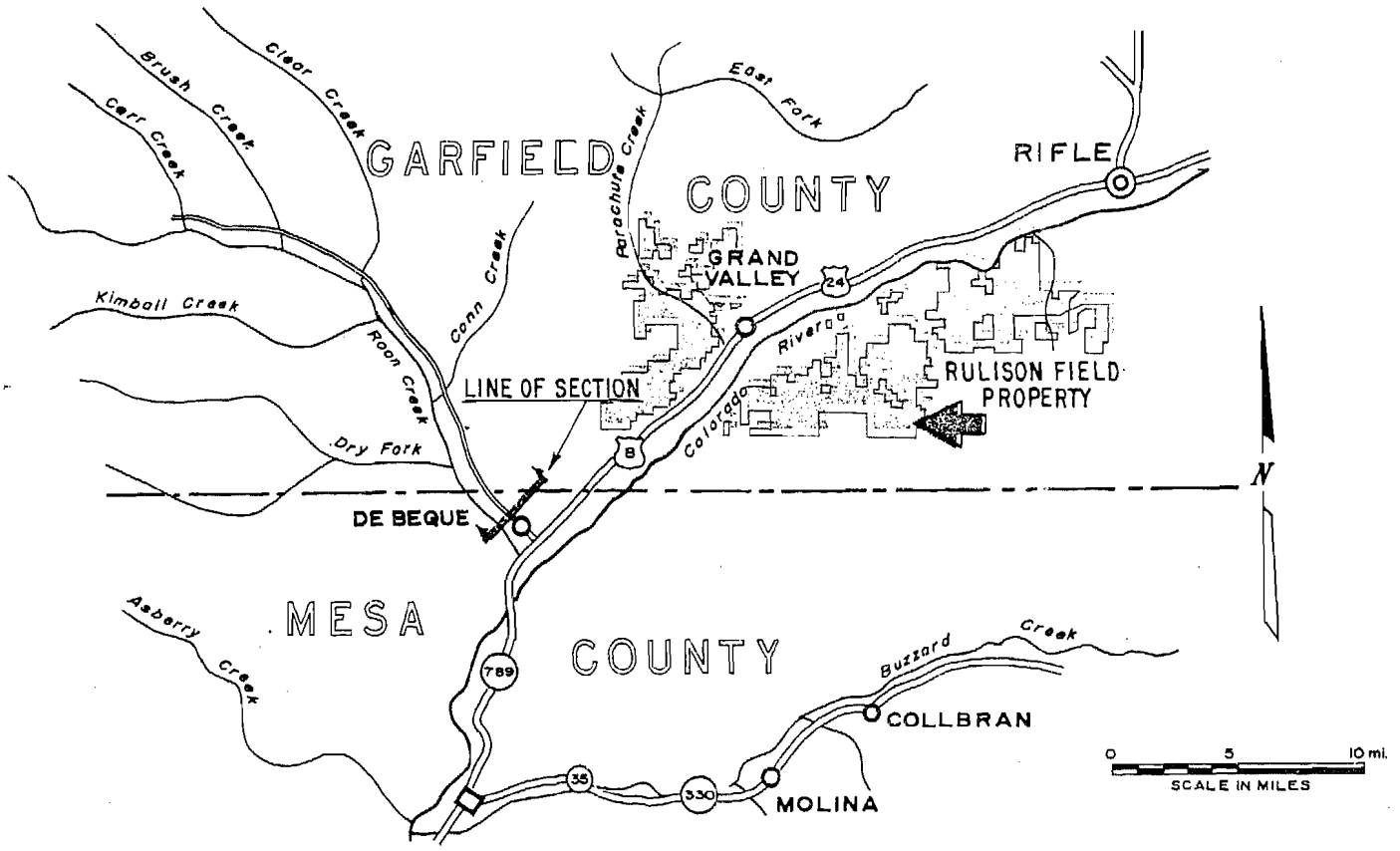
REGIONAL MAP AND STRUCTURAL INTERPRETATION
 CONTOURED ON TOP OF LOWER CRETACEOUS
 AND
 SHOWING THE POSITION OF RULISON FIELD PROPERTIES
 RELATIVE TO SURFACE EXPOSURES OF MESAVERDE AND
 PRE-CAMBRIAN FORMATIONS.



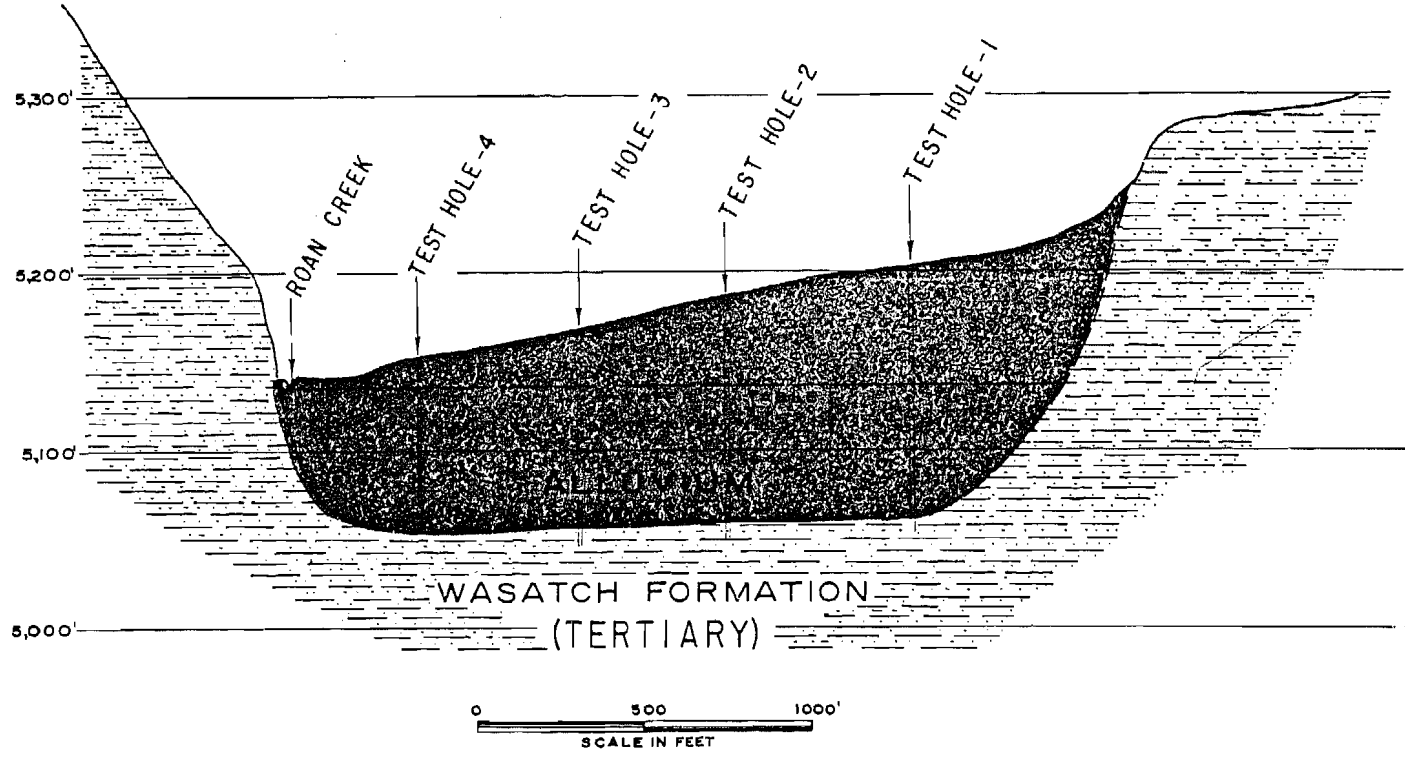
SCHEMATIC CROSS-SECTION
 NORTHWEST-SOUTHWEST ACROSS
PICEANCE CREEK BASIN
 GARFIELD AND MESA COUNTIES, COLORADO

ILLUSTRATING RELATIVE POSITION
 OF RULISON FIELD PROPERTIES
 TO STRUCTURE, STRATIGRAPHY
 AND OUTCROPS

0 10 MILES
 HORIZONTAL SCALE

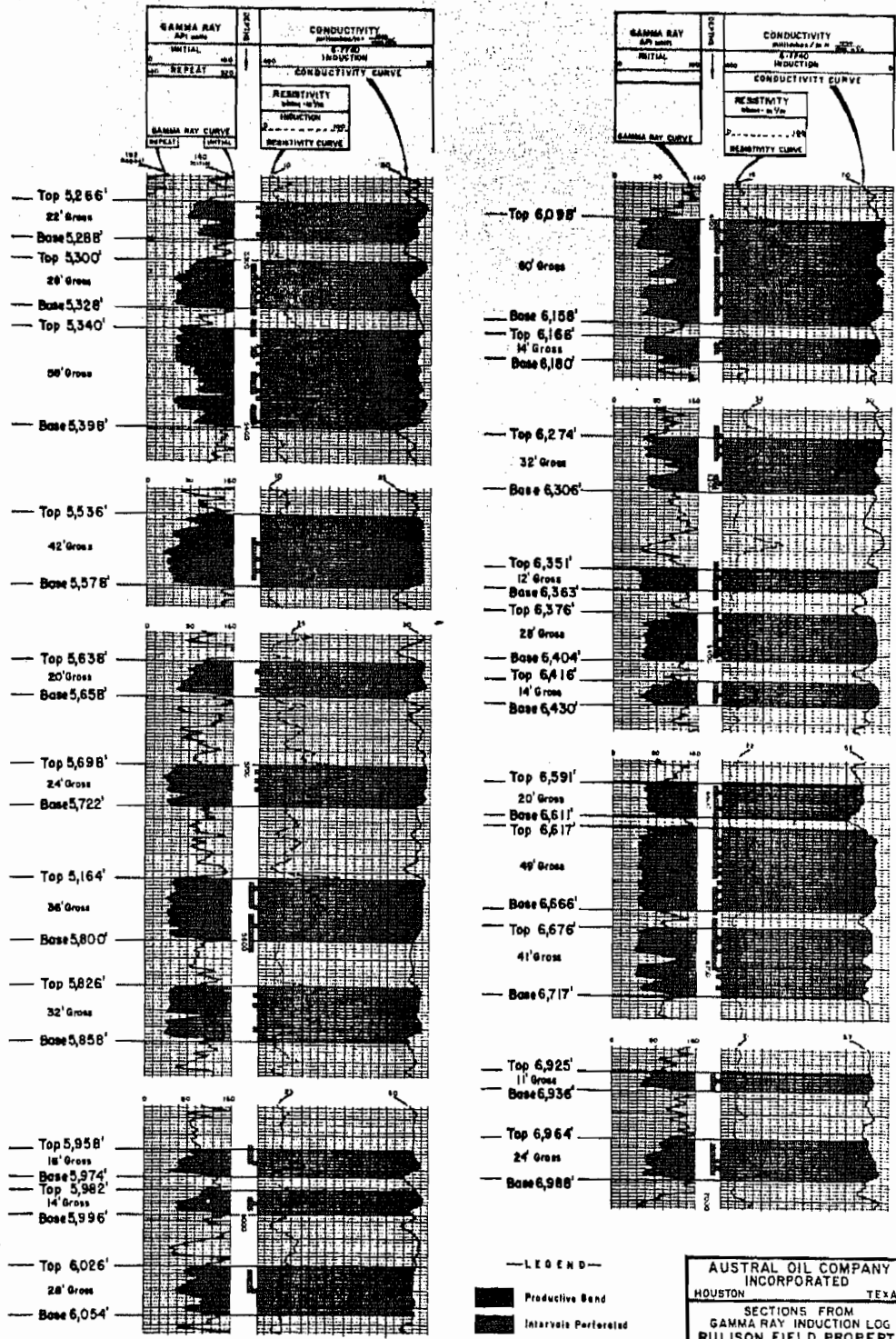


WEST ——— LOCATION MAP ——— EAST



CROSS-SECTION OF ROAN CREEK VALLEY
 ILLUSTRATING THE PROFILE OF THE VALLEY FLOOR AND
 THE THICKNESS OF THE ALLUVIAL FILL

SECTIONS FROM GAMMA RAY INDUCTION LOG
FEDERAL(654.1) A #29-95



—LEGEND—
 Productive Sand
 Intervals Perforated
 Intervals Effectively Fractured

AUSTRAL OIL COMPANY
INCORPORATED
HOUSTON TEXAS
 SECTIONS FROM
GAMMA RAY INDUCTION LOG
RULISON FIELD PROPERTY
GARFIELD COUNTY, COLORADO
DRILLING BLOCK 65-41
33,960 GROSS ACRES
DATE: FEBRUARY 4, 1966

Fig. 6



GRAPH SHOWING RELATIVE POSITION
 MESAVERDE SANDS IN PRODUCTIVE WELLS
RULISON FIELD PROPERTY
 GARFIELD COUNTY, COLORADO

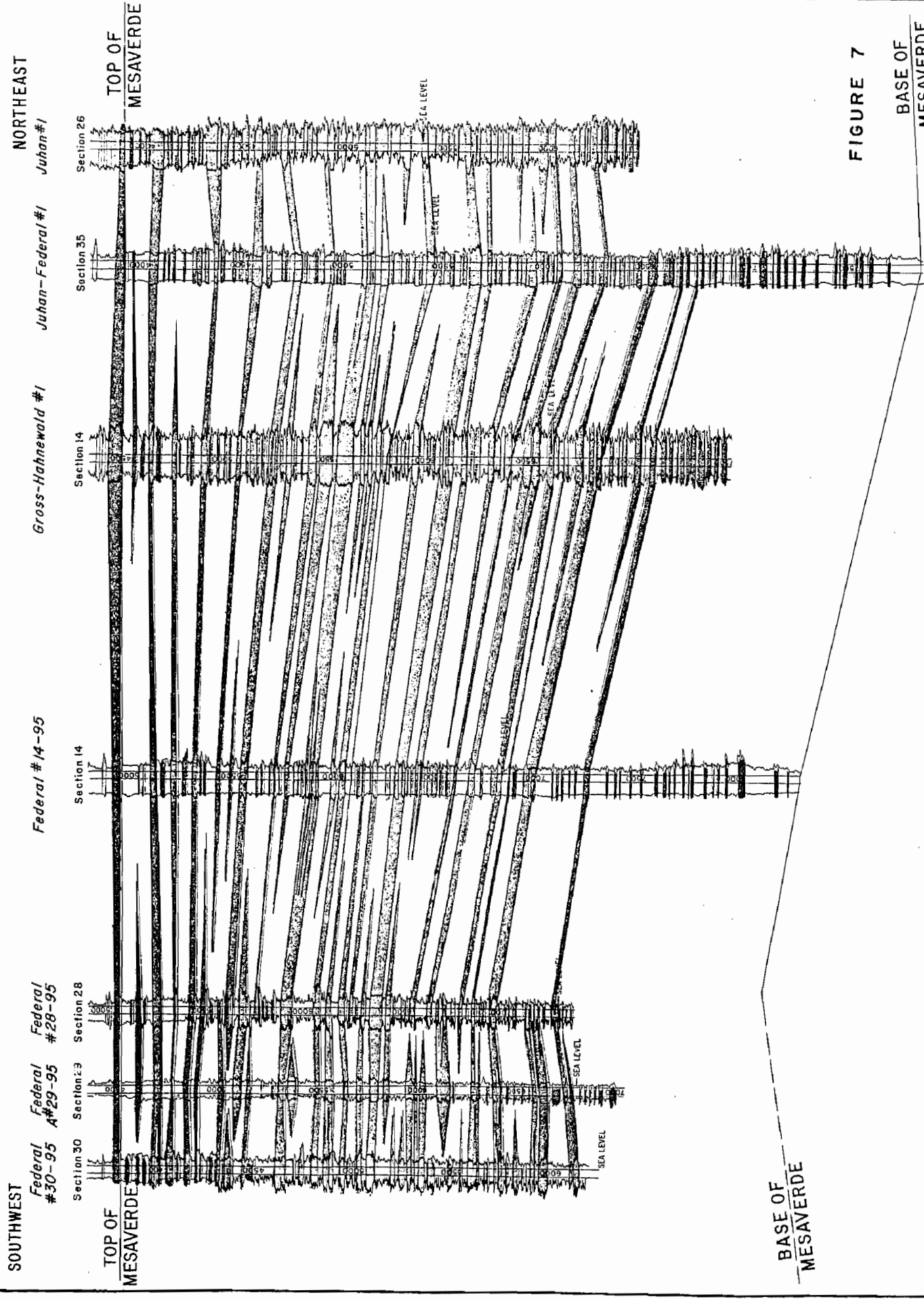
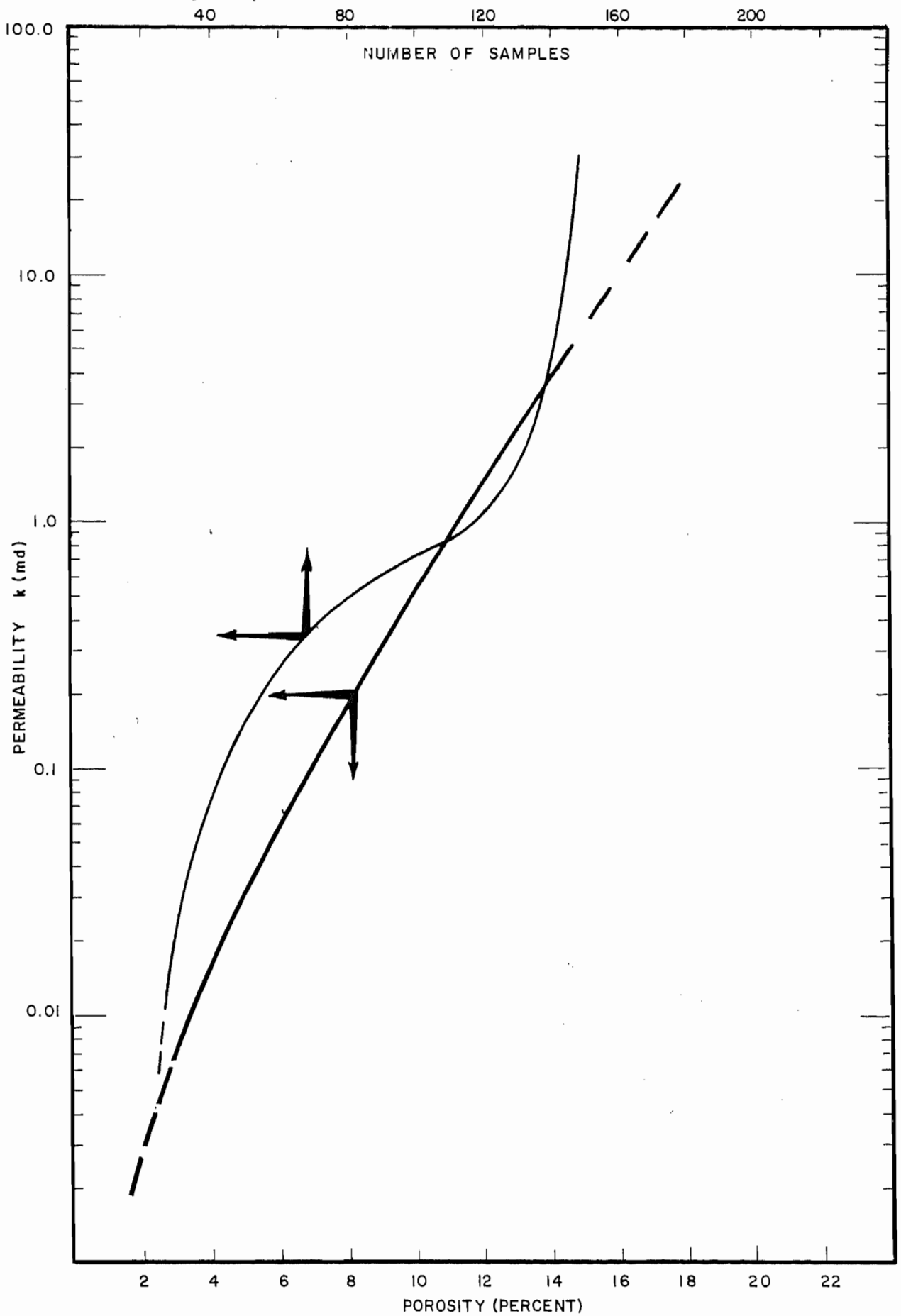


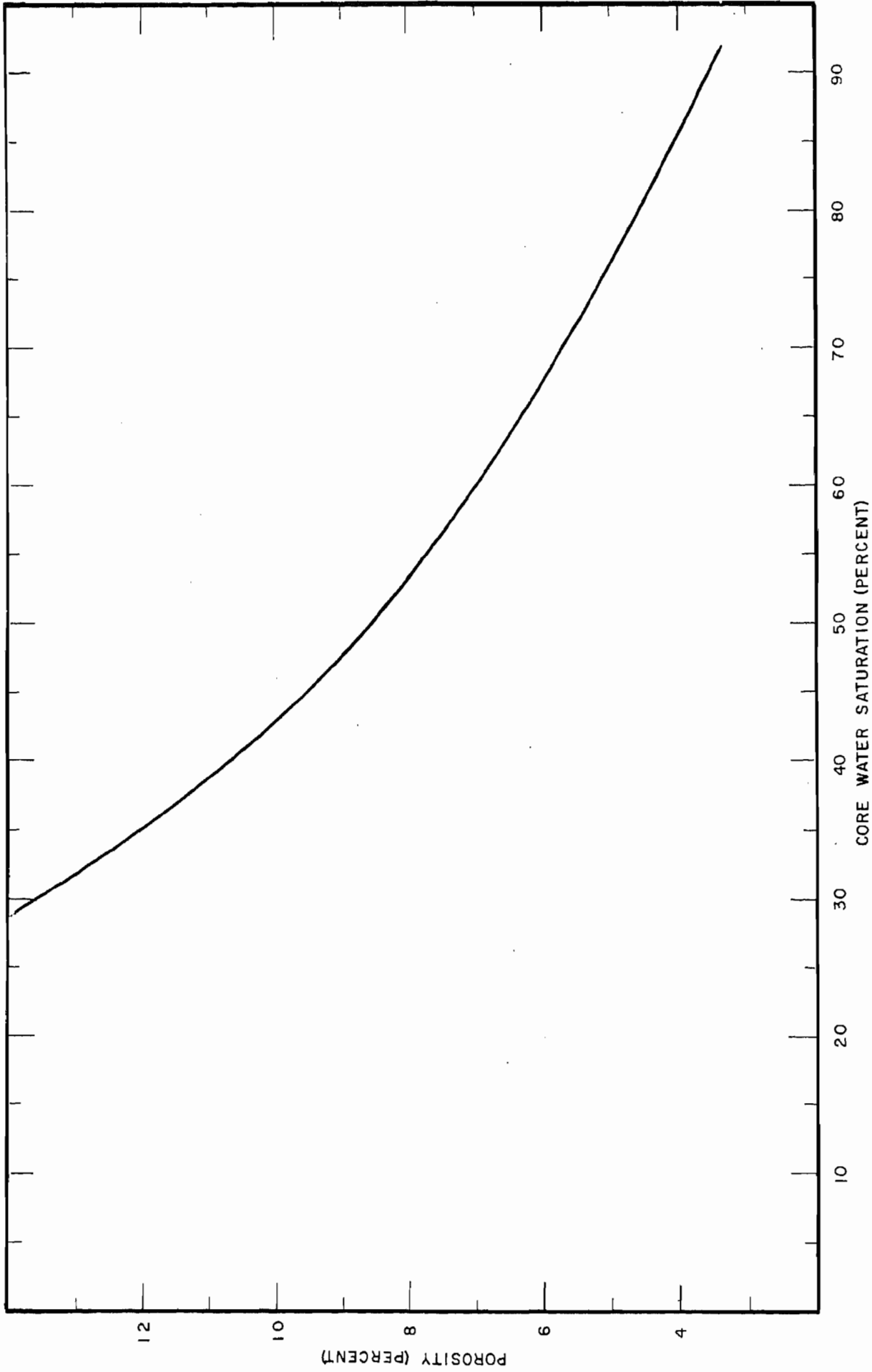
FIGURE 7

BASE OF
 MESAVERDE

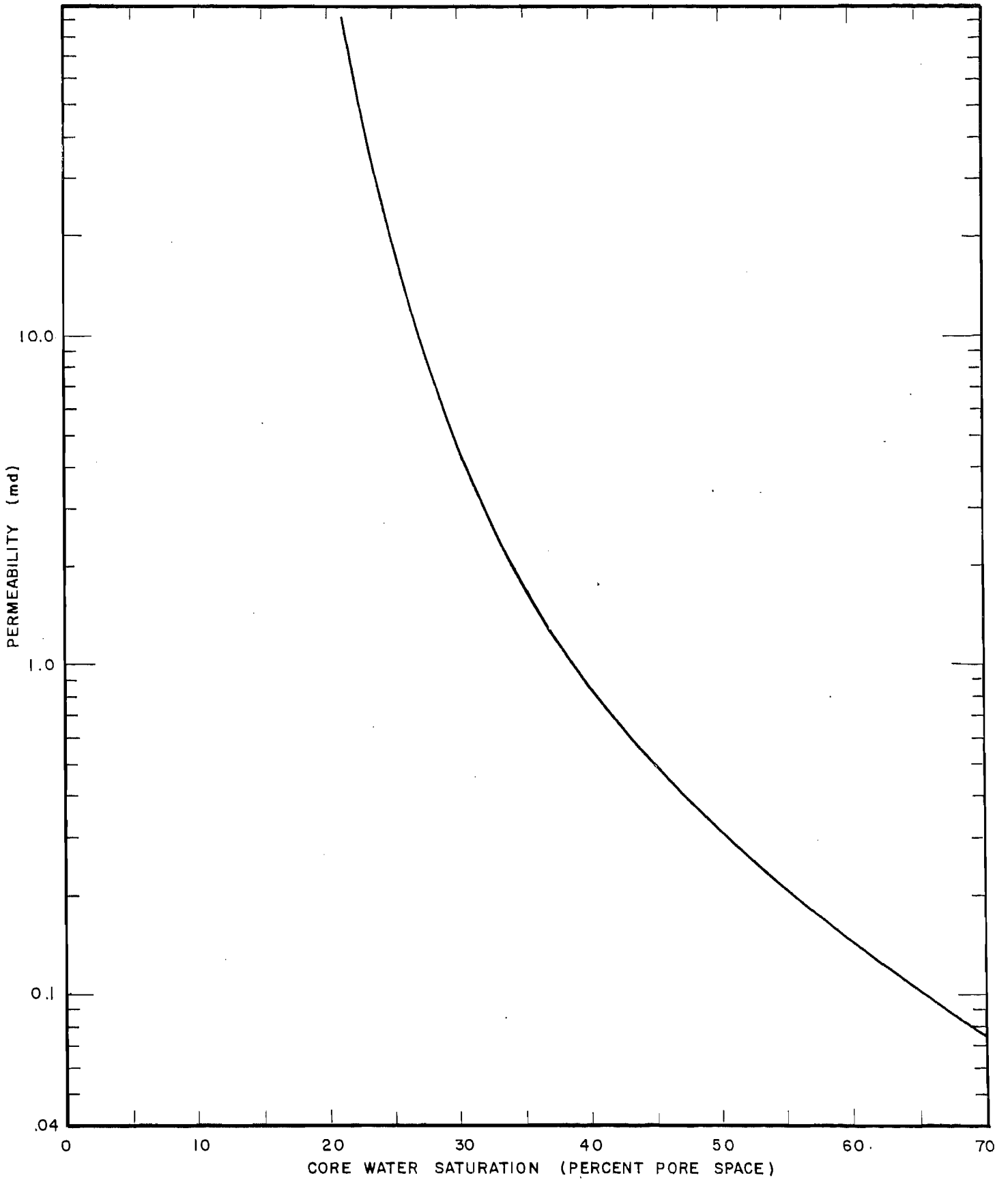


PERMEABILITY VS POROSITY
RULISON FIELD, COLO.

FIGURE 9



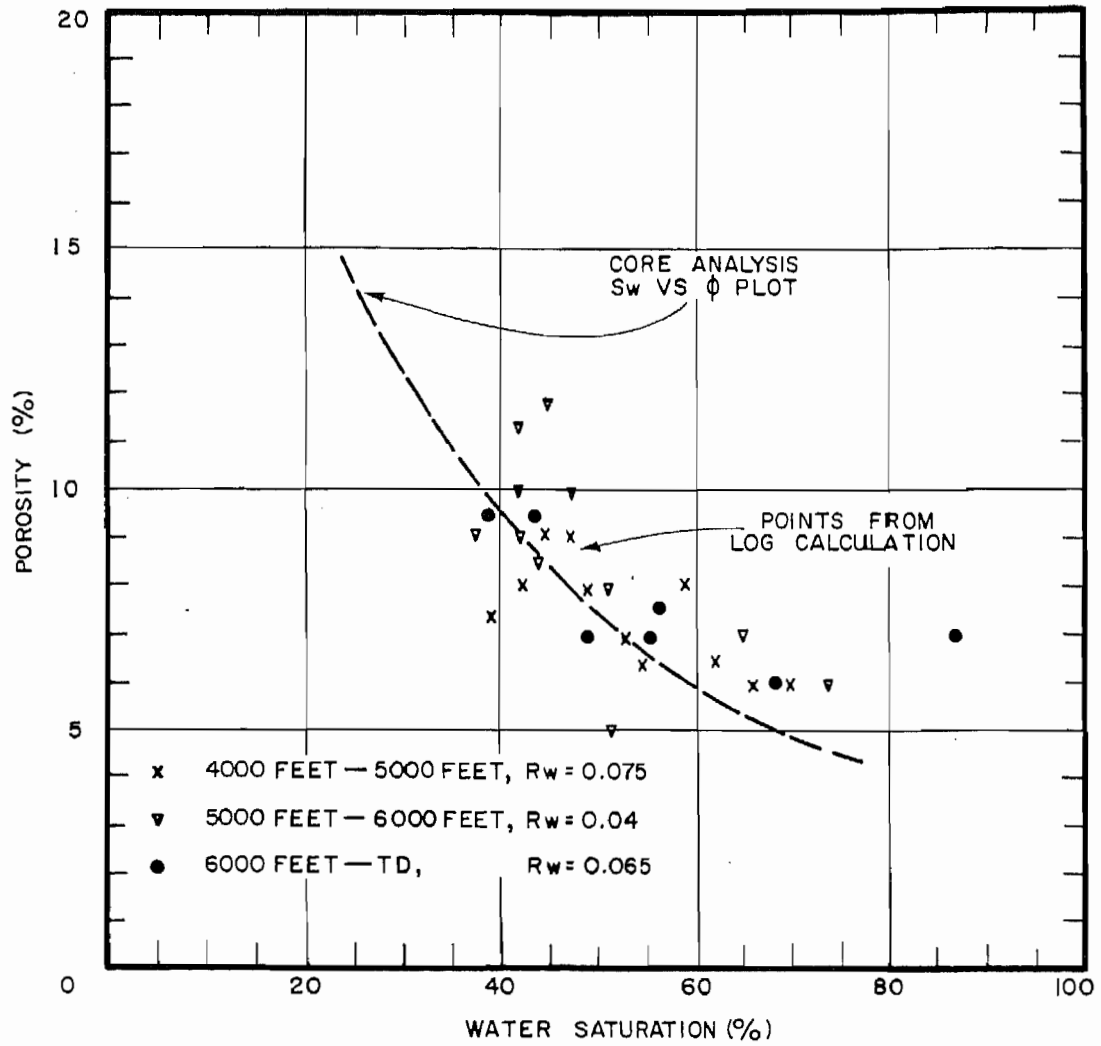
POROSITY VS WATER SATURATION
(CORE ANALYSIS DATA)
RULISON FIELD, COLO.



PERMEABILITY VS CORE WATER SATURATION

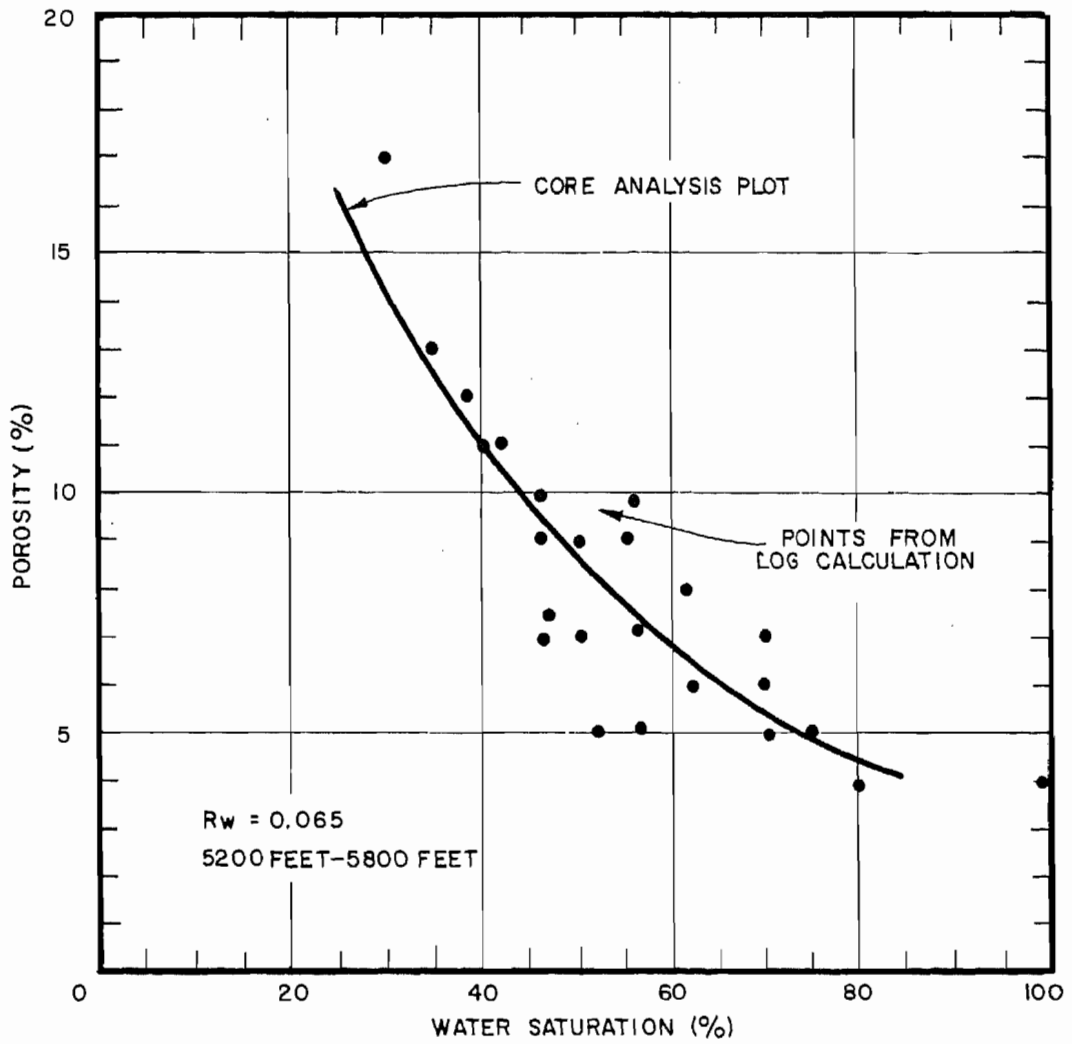
RULISON FIELD, COL.
MESAVERDE FORMATION

FIGURE 11



CALCULATED (LOGS) WATER SATURATION

VS POROSITY WELL 3-94



CALCULATED (LOGS) WATER SATURATION

VS POROSITY WELL A 29-95

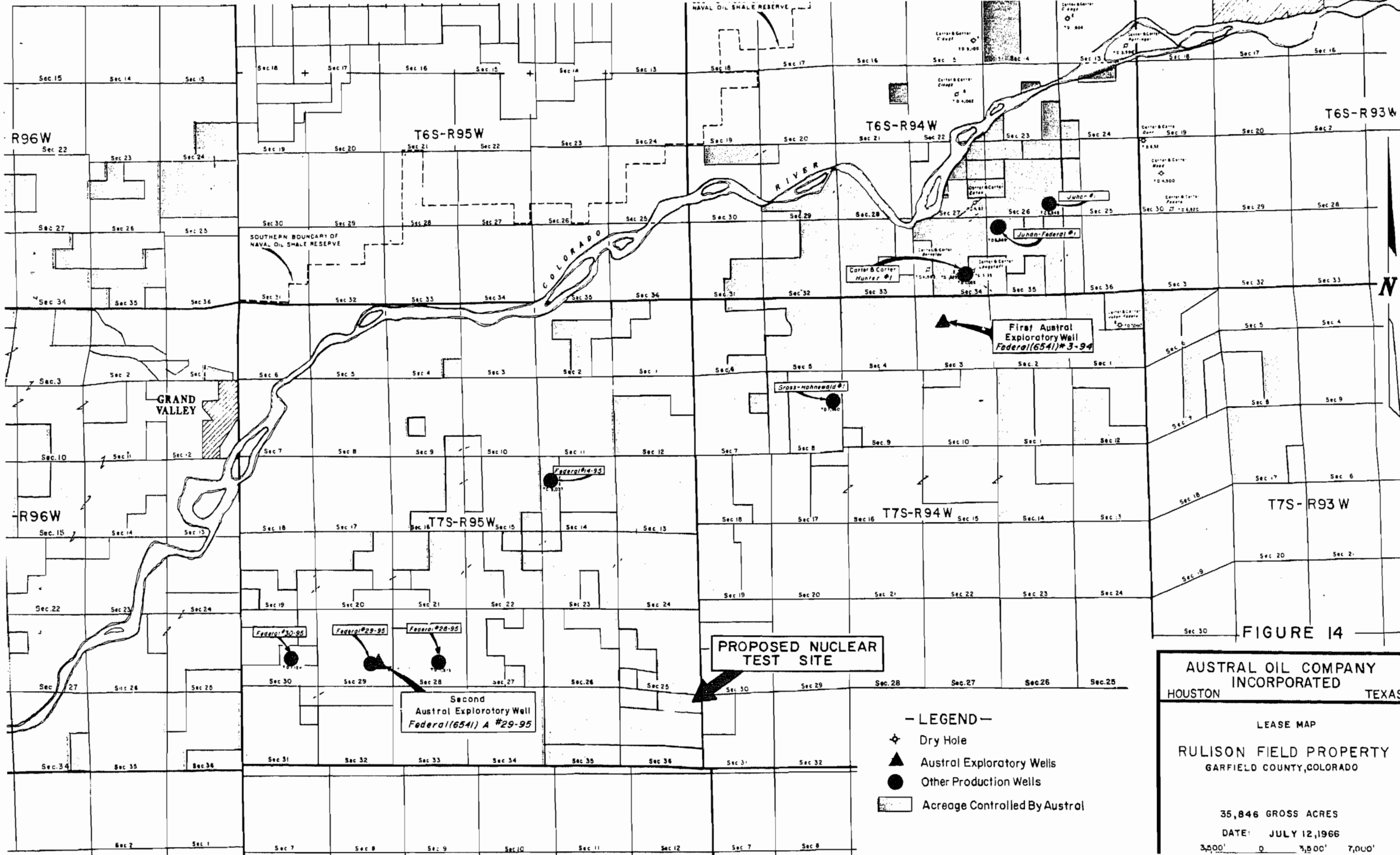


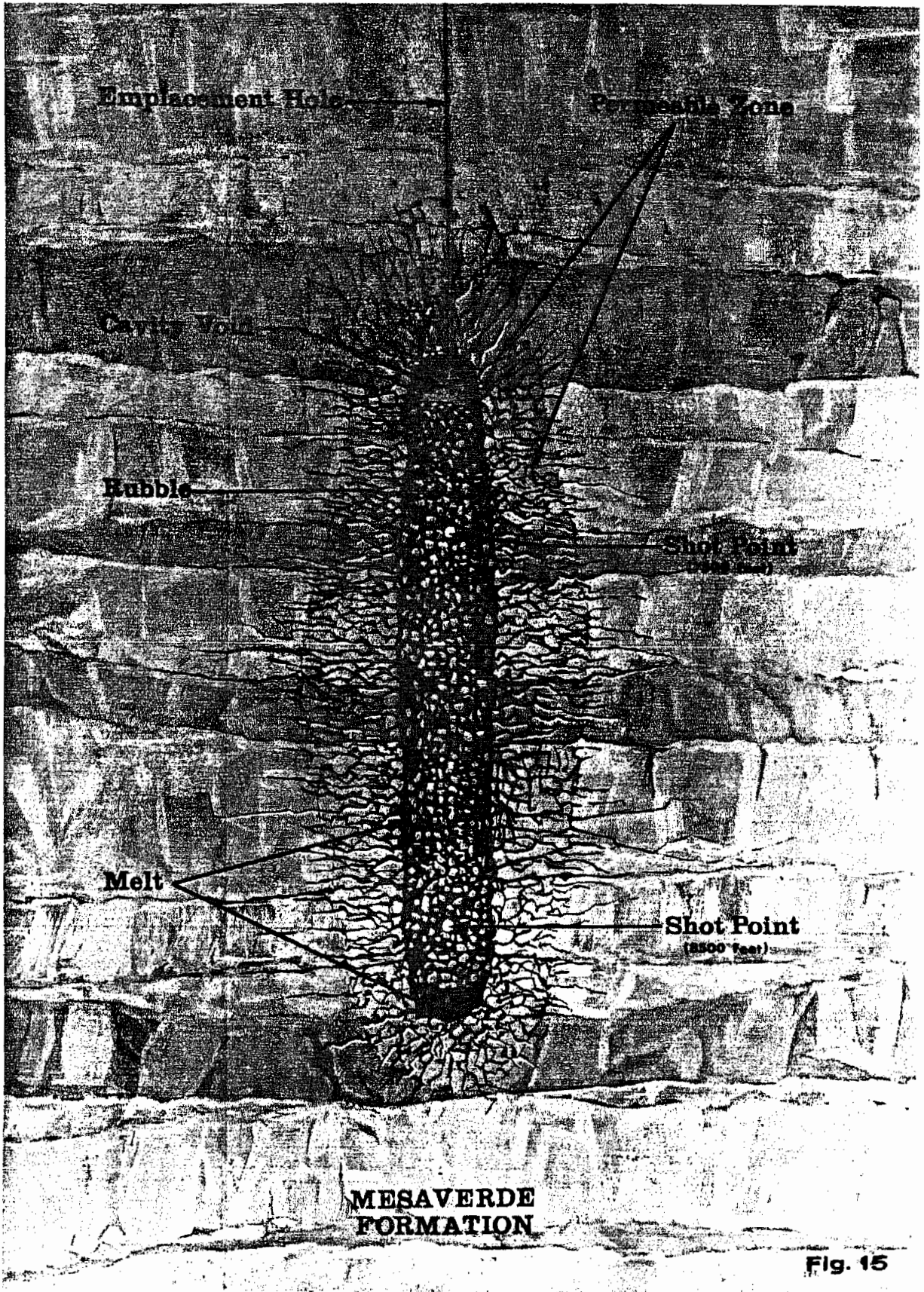
FIGURE 14

AUSTRAL OIL COMPANY
INCORPORATED
HOUSTON TEXAS

LEASE MAP
RULISON FIELD PROPERTY
GARFIELD COUNTY, COLORADO

35,846 GROSS ACRES
DATE: JULY 12, 1966
3,000' 0 3,000' 7,000'

- LEGEND —
- ⊕ Dry Hole
 - ▲ Austral Exploratory Wells
 - Other Production Wells
 - ▭ Acreage Controlled By Austral



Emplacement Hole

Permeable Zone

Cavity Zone

Bubble

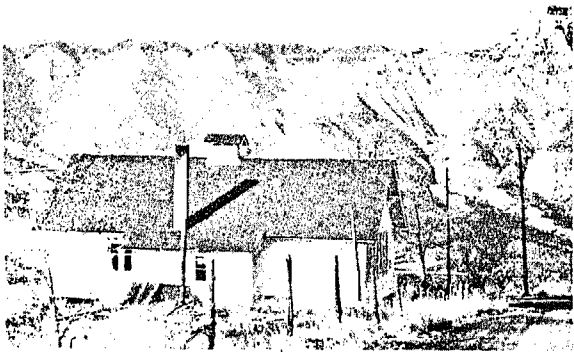
Shot Point
(2500 feet)

Melt

Shot Point
(2500 feet)

MESAVERDE
FORMATION

Fig. 15



MORRISCANA COMMUNITY HOUSE
BATTLEMENT CREEK
SECT. 10 T7S, R95W.

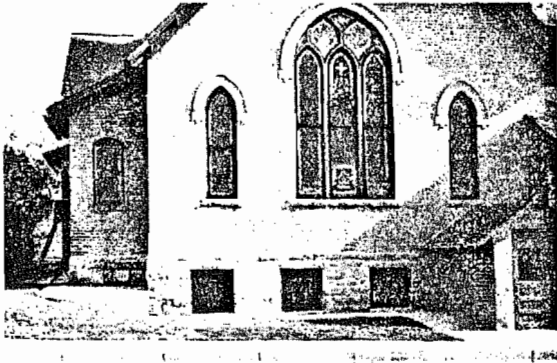
HOUSE CLOSE IN
LOCATION: SECT. 10
T7S, R95W.



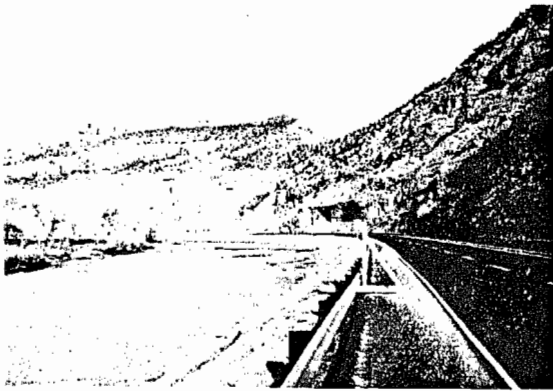
CHIMNEY TYPE ALL HOUSES
SECT. 10 T7S, R95W.

CLOSEST HOUSE
SECT. 10
T7S, R95W.

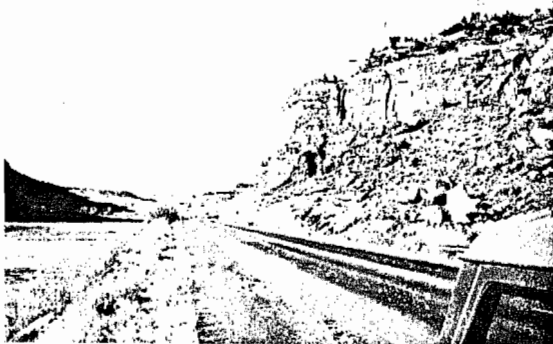




CHURCH IN RIFLE.
CRACKS IN THE LOWER
FOUNDATION.



DE BEQUE, NARROWS
POSSIBLE ROCK SLIDE.



DE BEQUE, NARROWS
POSSIBLE ROCK SLIDE.

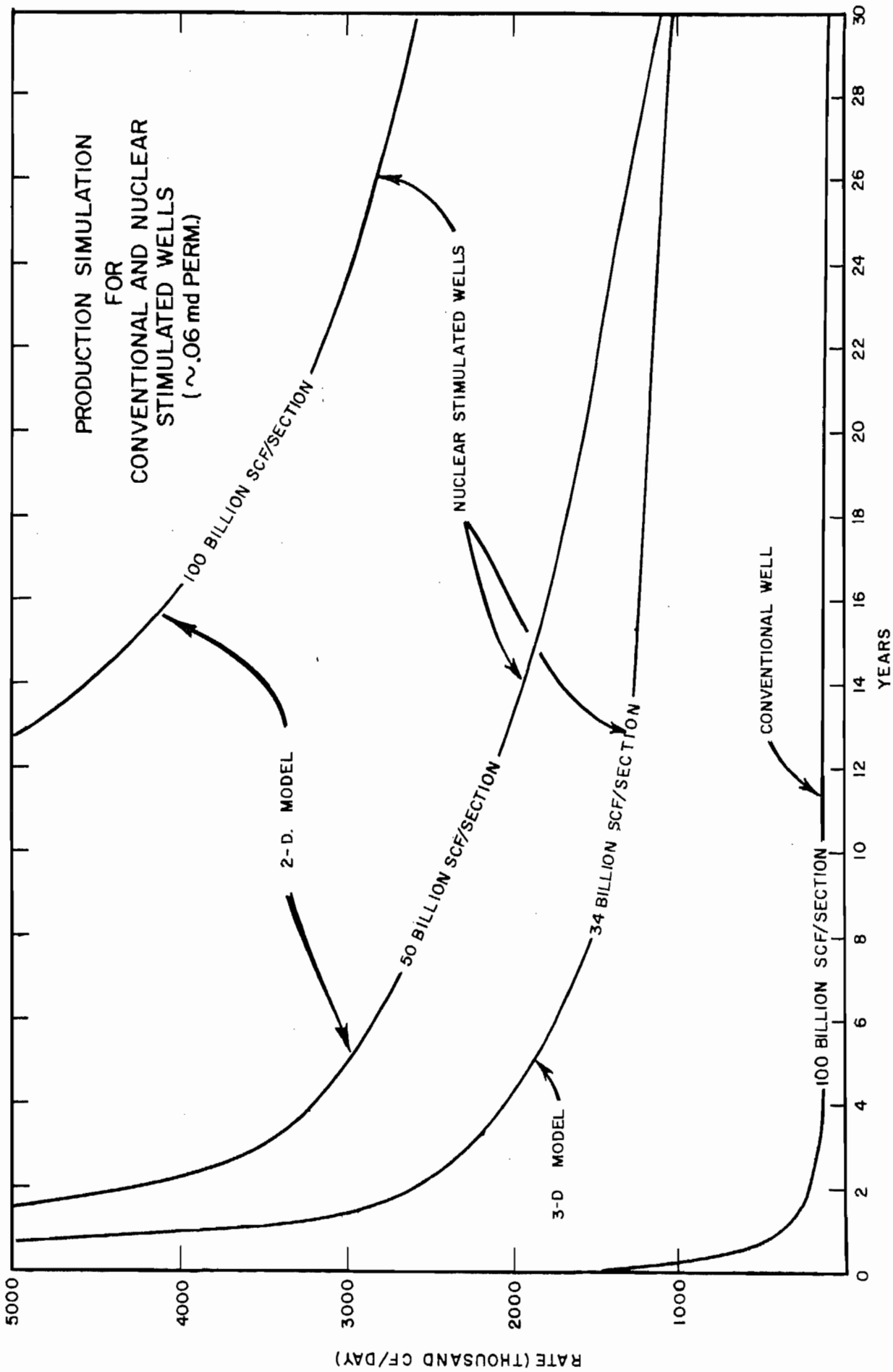


FIGURE 18

**PROJECT RULISON
Schedule of Events**

MONTHS

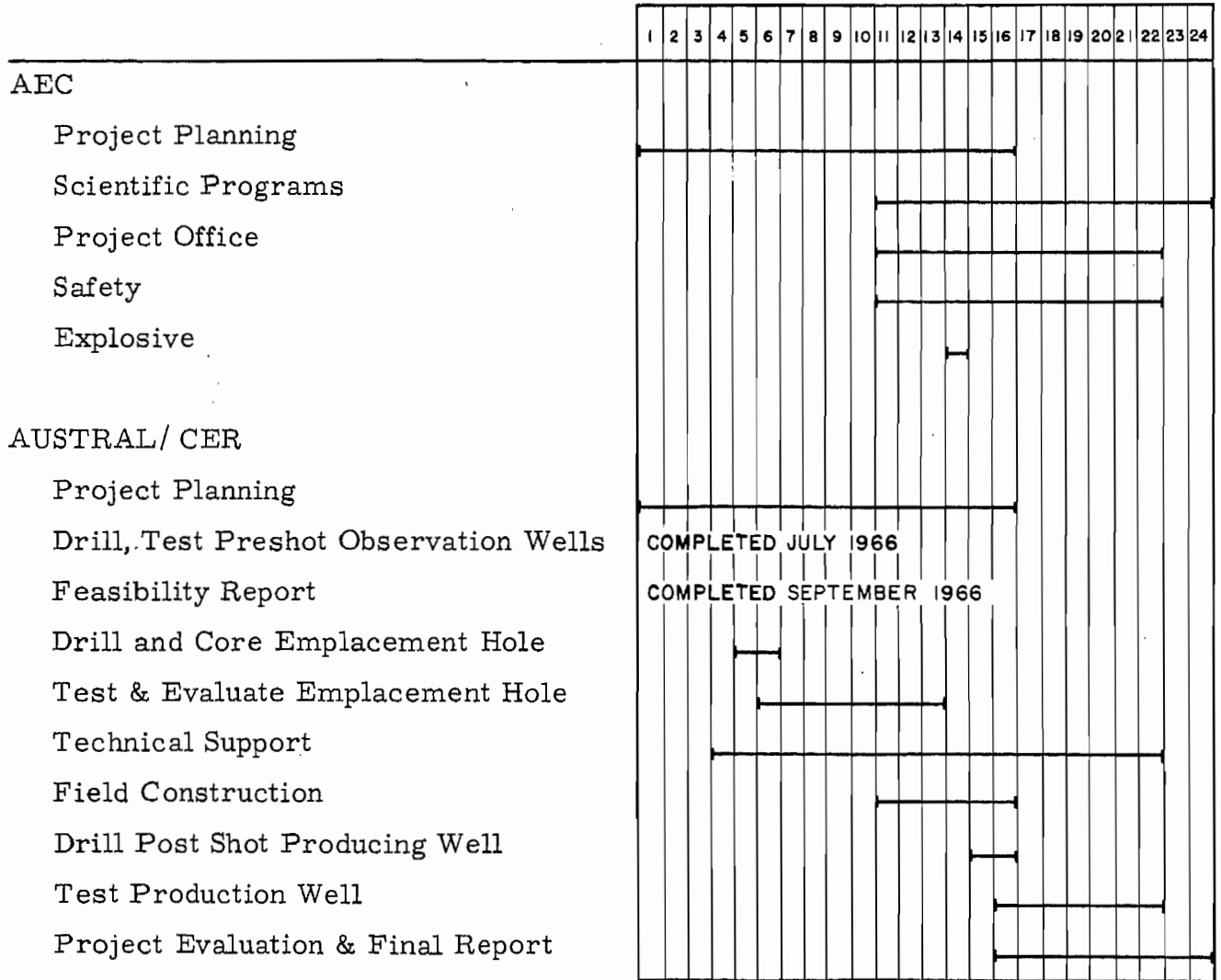


FIGURE 19

APPENDIX A

APPENDIX A
PROPOSED WELL TEST PROGRAM
TABLE OF CONTENTS

	<u>Page</u>
INTRODUCTION	A-1
GENERAL	A-1
THEORY	A-1
CALCULATED WELL DELIVERABILITY	A-3
PRE-SHOT TESTING TECHNIQUE	A-4
REFERENCES	
FIGURE A-1	
FIGURE A-2	

APPENDIX A

PROPOSED WELL TEST PROGRAM

INTRODUCTION

The following well test program is suggested for the preshot testing of the emplacement well. An appropriate program will have to be developed for post shot well testing of the producing well. Adequate well testing will be required in both instances to evaluate the results of the nuclear shot. Any well test program must depend on at least two things-- (1) accurate and well-instrumented tests performed by capable and experienced personnel, and (2) evaluation of the test data using suitable techniques.

GENERAL

The practice of well testing in the petroleum and natural gas industry has been followed for many years. The experience has resulted in the development of a number of experimental testing techniques, data analysis procedures, and fluid flow models to determine flow capacity of the formation and wellbore.

Although the rigorous model of isothermal flow of a homogeneous fluid in porous media has been available for a number of years, ⁽¹⁾ the well test and data analysis techniques have been based on many simplifying assumptions until only recently.

THEORY

The production of natural gas from a wellbore is dependent upon the transient behavior of flow within the reservoir. For production from a finite reservoir, the transient flow behavior can be subdivided into two parts. At first, the transient caused by the movement of the pressure "wave" into the reservoir is of importance. Later in the production history, the pressure-wave movement ceases, and the second transient

stage of material depletion becomes controlling. For reservoirs of relatively high permeability it can be shown that the pressure wave moves into the reservoir and "stabilizes" quite rapidly. In the case of relatively impermeable reservoirs, quite the opposite is true, as is the case with the Rulison or, in fact, most nuclear stimulation candidates.

Although it is theoretically possible to compute the production capability of a well from the properties of the reservoir as determined by static tests and core analyses, much more reliable information is obtained by conducting flow tests on the well.

Unsteady-state gas flow in a single well, symmetric, radial system of varying radial and vertical permeability can be described by the equation:^(2, 3)

$$2\phi\mu \frac{\partial p}{\partial t} = \frac{1}{r} \frac{\partial}{\partial r} k_r r \frac{\partial p^2}{\partial r} + \frac{\partial}{\partial Z} k_z \frac{\partial p^2}{\partial Z}$$

where:

- ϕ = effective porosity
- μ = viscosity
- p = pressure
- t = time
- r = radius
- Z = vertical distance
- k_r = radial permeability
- k_z = vertical permeability

In essence, the equation represents the basic principles of conservation of mass (continuity equation) and of momentum (Darcy's law in the radial case) applied to flow in porous media. It assumes an ideal gas at constant temperature with viscosity independent of pressure and neglects gravitational effects. The assumptions of ideal gas and pressure independent viscosity are not necessary if compressibility factor and viscosity can be suitably expressed as functions of pressure.

Because of the nonlinear properties of the equation, analytic solutions are only available for certain special cases. However, numerical solutions may be effected by the use of high speed computers employing finite difference techniques.

As such then, solution of the equation with appropriate boundary conditions gives a detailed accounting of flow for any drainage geometry from the vicinity of the wellbore out to a distance where the flow can be successfully approximated by a radial system. The radial extent of a fracture system created by an explosion in a gas-bearing formation and the radial permeability distribution of the immediate adjacent system can be studied. In addition, the flow capacity, including the effect of "wellbore storage unloading," of the post-shot chimney and fracture system can be compared with preshot formation deliverability. Model fit of the experimental data will allow long time prediction of the behavior of the pre-and post-shot system in a simple reservoir, as well as the evaluation of the "close in" portion of the post-shot environment of the Rulison case.

A more complete description of the model, its development, capabilities, and use has been by Keil, et al. (2, 3, 4)

CALCULATED WELL DELIVERABILITY

To demonstrate one use of this radial model, predictions have been made of the increased productivity from the nuclear stimulated well at the Rulison site. The post-shot geometry of the complex chimney and increased permeability zone were based on the dimensions calculated for two 50-kiloton devices.

The finite difference solution of the model involved subdividing the total drainage area into a number of cells, in this case 50 concentric, annular, cylindrical cells, of specified permeability, and calculating the well production-pressure-time history for a large number of time increments. Flow capacity of the existing reservoir matrix was determined

from a computer fit of well test data from existing wells in the formation. This value was also used in the unaffected area in the explosion-stimulated calculations. Permeability (or flow capacity) in the cavity-chimney area near the wellbore in the explosion-stimulated cases was arbitrarily assumed to be 2,000 md. This value was logarithmically decreased to .06 md at the unaffected formation boundary. In effect, this variation implies that a large wellbore was created, but it allows material balance accounting of the gas present in the blocks of rubble and in the matrix rock between fractures. An example of the permeability function characteristic for an explosion-stimulated well is given in Figure A-1. In addition, the production schedule was controlled at the onset by the gas pipeline allowable which was assumed to be 5,000 thousand scf/d. After the well could no longer produce this rate against a back pressure at the surface of 450 psi, the rate was allowed to decline. The well was assumed to produce its maximum capability flowing against the 450 psi surface pressure.

The mathematical model was used to predict the production-pressure-time history for two cases where various reservoir parameters were considered. Specifically, these cases correspond to:

1. One well per 640 acres, nuclear fractured to connect with pay containing a total in-place gas of 50 billion scf and having average equivalent permeability of 0.06 md.
2. Same as 1 except 100 billion scf/section.

The resultant numerical data for each of the cases include the pressures in each incremental cell for each time period. Two such pressure-radius relationships are shown in Figure A-1. The gas deliverability as predicted by the radial flow model for the two cases is shown in Figure 18.

PRE-SHOT TESTING TECHNIQUE

As a result of the extremely low permeability of the Mesaverde reservoir matrix rock in the Rulison Field area, it has been shown (2)

that the more conventional "Long-Time Flow Test Method" or the "Flow-After-Flow Test Method"⁽⁵⁾ is not particularly feasible in the area.

The reasons are:

1. Excessively long times are required before "stabilized" flow is attained.
2. Excessive gas is wasted during the test procedure.
3. Valid results are not obtained with the flow-after-flow tests in the low permeability reservoir as pressure transients are superimposed on one another.

The previous testing in the area has also shown that constant rate, isochronal testing procedure provides accurate data for the solution of the nonlinear partial differential equations describing the transient isothermal flow of gas in porous media. It has also been shown⁽²⁾ that the "succession of steady states" solutions proposed by Muskat⁽¹⁾ to the equations and verified by the approximations of Aronofsky and Jenkins⁽⁶⁾ and independently by Cullender's isochronal testing technique⁽⁷⁾ are equally satisfactory for deliverability prediction with either Darcy or non-Darcy flow, if such meaningful test data are obtained.

It is proposed to use this constant rate, isochronal testing technique to obtain reservoir flow characteristics and to evaluate and/or compare the reservoir condition before and after the proposed underground nuclear explosion. The optimum experimental program prior to the explosion would consist of:

1. Drilling a 15-inch hole to 5,000 feet, logging, then cementing a 13-3/8-inch combination H40 buttress and soft casing string in place. Continuing to drill with a 12-inch hole to 8,500 feet with representative intervals cored, logged, and tested open hole. Air or gas will be used as circulating fluid for the drilling.
2. Any wet intervals in "Paleocene" or Ohio Creek conglomerate will be tested prior to setting pipe at approximately 5,000 feet.

3. Formation data, including cores and logs of the complete interval, will be obtained during the drilling and completion phases of the well. Complete core analyses will be run on the formation. Electric, gamma ray, caliper, etc., logs will be taken by commercial companies for formation evaluation purposes.
4. Initial static formation pressure and temperature will be determined with subsurface recording instruments.
5. Constant flow rate tests will be made of the complete open hole interval using the experimental wellhead equipment shown in Figure B-3. Flowing sand face pressures and temperatures, as well as surface conditions, will be determined for at least 4 constant rates of flow. The motor control valve in the flow wing will be used to control the pressure upstream from the critical flow prover at a constant value, thereby fixing the rate of flow through the prover.

Between flow periods, the well will be shut in to allow complete pressure build up in the wellbore and in the formation around the wellbore to within at least 50 psi of the original static pressure. Thus, the pressure transient created by flow will be removed from the formation, allowing more rigorous mathematical analysis.

The post-shot evaluation program will be somewhat determined by the conditions encountered following the explosion. However, the currently anticipated program is:

1. Re-drill the emplacement well below 5,000 feet and equip as a production well through the center of the device emplacement (working) points to anticipate a symmetrical increased permeability chimney or rubble zone for ease in subsequent data analysis. The well would also be used initially by the AEC for samples of gas and device debris for radiochemical yield determinations.

Drilling logs and returns will give some indication of the height of the permeable zone and/or cavity produced by the explosion. The surface casing and intermediate casing to the base of the Ohio Creek conglomerate should be intact, and only clean-out operations should be necessary. The remainder of the well will be gas-drilled in order not to contaminate the permeable rubble and/or cavity zone with water or drilling fluid.

2. A core drill will be used from the base of the Ohio Creek conglomerate in order to obtain samples of the shot-affected rock. These will be obtained in the attempt to locate and identify the shock-altered height of increased permeability. Logs of the complete interval will also be obtained to provide similar information and also to monitor any zones of increased radioactivity.
3. Pressures, temperatures, radiation levels, and gas compositions will be monitored both during drilling operations and on entry into the rubble zone or standing cavity created by the explosion.
4. Flowing tests will be made on the well in order to provide data for comparison with the preshot formation characteristics. Because of the "wellbore storage" or "unloading" effects of the extremely large, high permeability zone created, the initial flow tests must necessarily be at higher rates and for longer time periods than those of the preshot tests. A similar well-head equipment scheme to that used on preshot testing should be satisfactory except that the well should be connected into a gas gathering line to the Western Slopes pipeline when radiation levels are satisfactory in order to conserve the large volumes of gas which will be produced during the testing periods. Gas rates will probably be measured with either a conventional orifice run or turbine mass flow meter. Such devices are currently available with high reliability and accuracy.

APPENDIX A REFERENCES

1. Muskat, Morris, The Flow of Homogeneous Fluids Through Porous Media, McGraw Hill Book Company, Inc., New York (1937). Also, J. W. Edwards, Inc., Ann Arbor, Michigan (1946).
2. Swift, G. W., and Kiel, O. G., "The Prediction of Gas-Well Performance Including the Effect of Non-Darcy Flow," Trans AIME; 255:1 791-798 (1962). Also, J Pet Tech, 14, No. 7, 791-798 (July 1962).
3. Kiel, O. G., and Campbell, J. M., "Analysis of Gas Well Behavior Using a Two-Dimensional, Unsteady-State Model," AIME-SPE Paper No. 562, presented at Oklahoma University-SPE Production Research Symposium, April 29-30, 1963, Norman, Oklahoma.
4. Kiel, O. G., PhD Dissertation, University of Oklahoma, Norman, Oklahoma (1963).
5. Rawlins, E. L., and Schellhardt, M. A., "Back-Pressure Data on Natural-Gas Wells and Their Application to Production Practices," Monograph 7 U.S. Dept of the Interior, Bu of Mines (1936).
6. Aronofsky, J. S., and Jenkins, R., "A Simplified Analysis of Unsteady Radial Gas Flow," Trans AIME, 201, 149 (1954).
7. Cullender, M. D., "The Isochronal Performance Method of Determining the Flow Characteristics of Gas Wells," Trans. AIME, 204: 137 (1955).

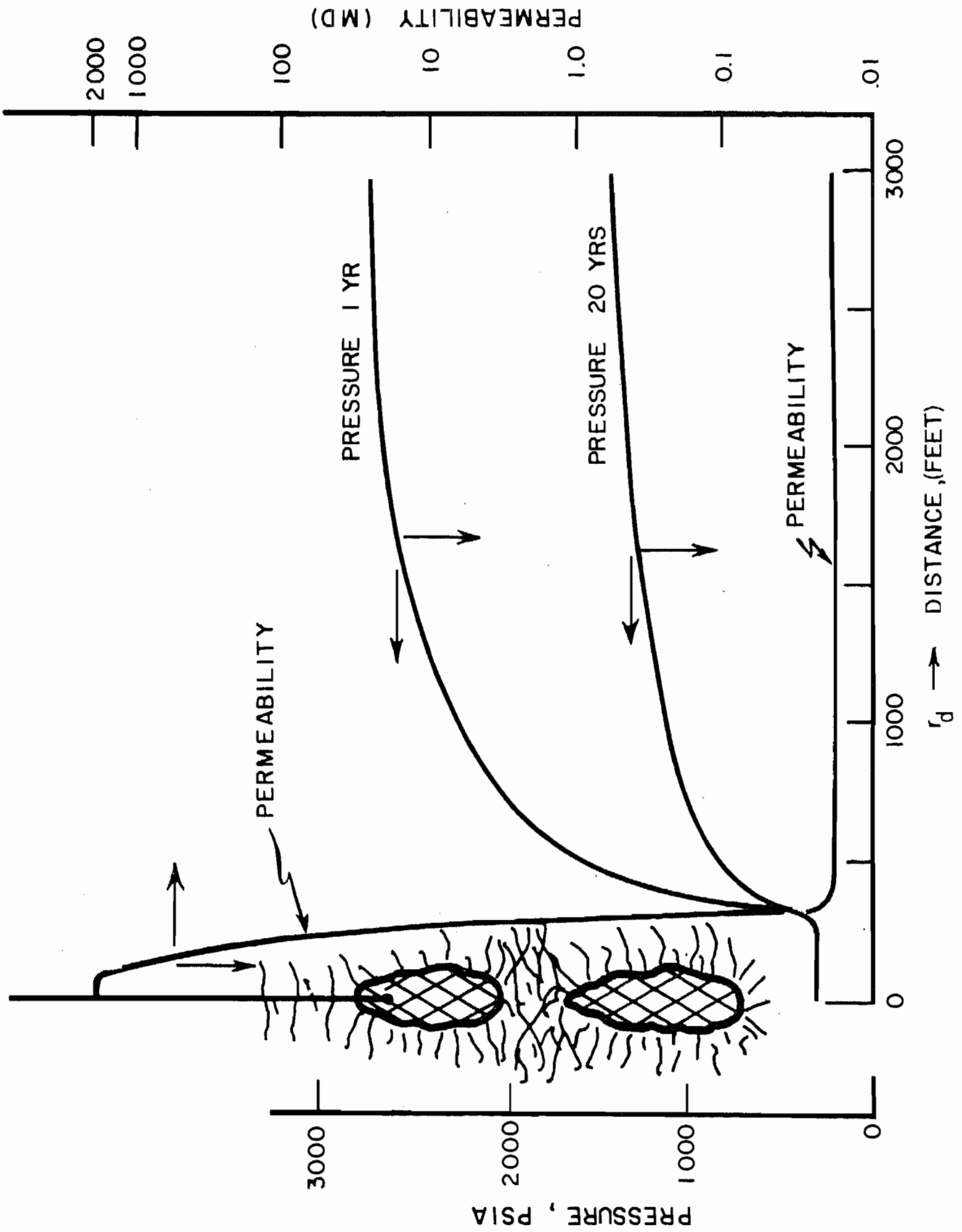


FIGURE A1 CALCULATED CHARACTERISTICS FOR NUCLEAR STIMULATED RULISON WELL

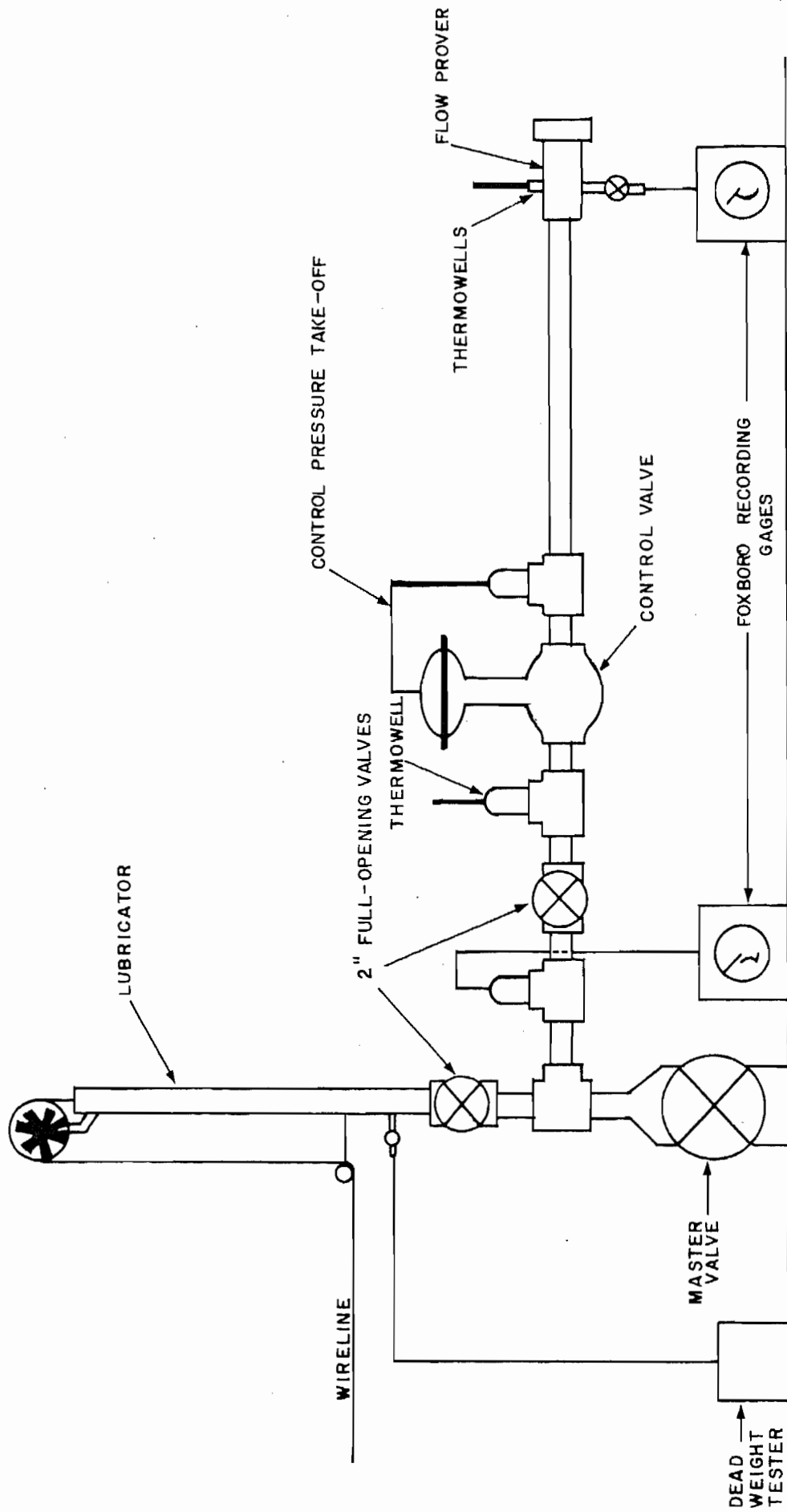


FIGURE A-2
 SCHEMATIC OF WELL-HEAD RIGGING FOR GAS WELL TESTS

APPENDIX B

ESTIMATED POST-SHOT RESERVOIR BEHAVIOR

(APPENDIX B)

TABLE OF CONTENTS

	<u>Page</u>
SUMMARY OF THE WELL TESTS PERFORMED ON FEDERAL A-29-95	B- 1
ANALYSIS OF FEDERAL A-29-95 AND OTHER MESAVERDE WELLS IN THE RULISON FIELD.	B- 2
SAND CONTINUITY STUDY	B-12
MATHEMATICAL MODEL CONSTRUCTIONS FOR THE NUCLEAR STIMULATED MESAVERDE GAS RESERVOIR (RULISON AREA)	B-16
REFERENCES	B-19

LIST OF TABLES

(APPENDIX B)

Table

B-I	Pressure Build-Up Data
B-II	Pressure Drawdown Data
B-III	Table of Well, Reservoir, and Fluid Properties for Federal A-29-95
B-IV	Real Gas Flow Theory Integral
B-V	List of Symbols Used in Equations
B-VIA	Rulison Project Sand Continuity Study Evaluation of Location Effects
B-VIB	Rulison Project Sand Continuity Study Evaluation of Outcrop Orientation Effects
B-VII	Geometric Factors Used in Reservoir Model
B-VIII	Table of Nuclear Stimulated Reservoir Properties
B-IX	Table of Flow Rate Schedules for Deliverability Predictions - Nuclear Stimulation Study - Case 1
B-X	Table of Flow Rate Schedules for Deliverability Predictions - Nuclear Stimulation Study - Case 2

LIST OF ILLUSTRATIONS
(APPENDIX B)

Figure

- B- 1 Austral Well A-29-95 Decline Curve
- B- 2 Austral Well A-29-95 Pressure Build-Up Plots
- B- 3 Flow Diagram of Surface Well Test Hook-Up for Federal A-29-95
- B- 4 Flow Rate Versus Time for the Drawdown Test on Federal A
- B- 5 Austral Well A-29-95 Drawdown Test Plot
- B- 6 Decline Curves for the Rulison Field Wells Producing from the Mesaverde Formation
- B- 7 Range of Extrapolations of Kh Versus Distance for Federal A - 29-95
- B- 8 Closeup Mesaverde Outcrop
- B- 9 Mesaverde Outcrop
- B-10 Plan View of Reservoir Model
- B-11 Permeability Function Calculated From A-29-95
- B-12 Isopach Map Mesaverde Reservoir Nuclear Stimulation Model
- B-13 Case No. 1 Chimney and Reservoir Bulk Pressure Decline With Time
- B-14 Case No. 1 Isobaric Map After 20 Years of Production Nuclear Stimulated Well
- B-15 Case No. 2 Chimney and Reservoir Bulk Pressure Decline With Time
- B-16 Case No. 2 Isobaric Map After 20 Years of Production Nuclear Stimulated Well
- B-17 Conventional Versus Nuclear Stimulated Flow Rates
- B-18 Conventional Versus Nuclear Stimulated Predicted Production

APPENDIX B

ESTIMATED POST-SHOT RESERVOIR BEHAVIOR

This appendix contains a best estimate of the reservoir behavior following nuclear simulation. These evaluations were based upon the testing of Federal A 29-95 and the analysis of test results, as well as an insight into the reservoir geometry based upon an outcrop study of sand continuity.

Since the reservoir model is based upon the well test and outcrop study results, these phases will be discussed before the section on reservoir simulation.

SUMMARY OF THE WELL TESTS PERFORMED ON FEDERAL A 29-95

A well testing program was designed to evaluate the flow capacity of the Mesaverde Reservoir in the Rulison area. This program consisted of letting a well build up for a period of time, and then conducting a constant rate drawdown test.

The well selected for these tests was Federal A 29-95. This well was completed by Austral Oil Company Incorporated on February 2, 1966. The completion consisted of perforating four main intervals in stages, and then fracturing each stage separately. After each stage, the well was cleaned up and tested. Federal A 29-95 was then placed on production. Figure B-1 is a plot of the flow rate decline prior to testing. Before the buildup was started this well had produced for approximately 90 days. Because of this short period of production and the optimum completion performed on this well, Federal A 29-95 appeared to be the logical choice for this testing program. Also, higher flow rates could be maintained for a longer period of time from Federal A 29-95 than the other Rulison wells.

Federal A 29-95 was shut in May 12, 1966, at 3:10 P.M. A series of five 72-hour bottom hole pressure surveys were conducted during this 519-hour buildup. Table B-1 is a summary of the pressure buildup data. Figure B-2 (in pocket) is a plot of the buildup data.

After 519 hours of buildup, Federal A 29-95 was prepared for a constant rate pressure drawdown test. The testing arrangement was designed so that a constant flow rate was maintained by a differential pressure controller and a back pressure valve. Figure B-3 is a diagram of the surface hook-up. Initially, the heaters were not used and the back-pressure valve froze off after nine hours of flow. After letting the well build up for another day the drawdown test was restarted using both line heaters. With these heaters the temperature of the gas was raised high enough to prevent further hydrate formation. The constant rate drawdown test proceeded for 48 hours and then the rate started to decline. This was because of liquid accumulation in the well. With the size diameter of the tubing and the flow rate of 500 thousand scf/ d this liquid could not be lifted to the surface, thus causing the tubing pressure to drop rapidly. Figure B-4 is a plot of the flow rate data for the 48-hour constant rate test. The average flow rate was determined to be 514.7 thousand scf/ d at base conditions of 15.025 psia and 60° F. Table B-II is a summary of the drawdown test data, Table B-III contains the gas analysis and other pertinent reservoir and well information.

ANALYSIS OF FEDERAL A 29-95 AND OTHER MESAVERDE WELLS IN THE RULISON FIELD

The following is the drawdown test analysis for Federal A 29-95.

Figure B-5 is a plot of $(p_d^2 - p_w^2)/q$ versus $\ln t$ for the drawdown test conducted on this well. The changing slope at the beginning of the test is attributed to the fractures near the wellbore. As time progresses

the relative influence of the fracture disappears and the matrix permeability is reflected. Since the average bulk pressure of the reservoir at the time of testing was unknown, a pressure of 2400 psia was chosen, which was the calculated initial static reservoir pressure.

The relationship that approximates unsteady state radial gas flow is given by the equation

$$(p_d^2 - p_w^2)/q = \frac{1}{2B} \ln t + \frac{1}{2B} \ln A + \frac{D}{B} q^* \quad (1)$$

(Note: Constants A, B, and D are defined on the next page.)

If $p_d^2 - p_w^2/q$ is plotted versus $\ln t$ the slope of the curve is $\frac{1}{2B}$. In the case of the drawdown test performed on Federal A 29-95, the slope of the latter portion of the curve is seen to be linear over a period of one day. Therefore, it is assumed that this slope is the best representation of the lense flow capacity. This drawdown can be analyzed as:

$$\frac{1}{2B} = \text{SLOPE} = 340 \text{ psi/cycle}$$

$$kh = \frac{\bar{\mu} z p_{sc}}{(19.87 \times 10^{-6})} \frac{T}{T_{sc}} B = \frac{(.015)(.903)(15.025)}{(19.87 \times 10^{-6})} \left(\frac{644}{520} \right)$$

$$kh = 6352 \frac{B}{2} = \frac{6352}{340} = 18.65 \text{ md ft}$$

Because flowing temperature surveys were not run on Federal A 29-95, logs had to be used to estimate net pays. Approximately 350 feet of sand was perforated and fractured. Furthermore, radioactive material was used in the sand to check to see if all the perms had been treated. In checking the tracer survey there are only a few perforations that do not

*Symbols used in this and subsequent equations are defined in Table B-V.

exhibit fracturing. Also, individual testing of each interval after fracturing indicates the perforated 350 feet is productive to some extent. Therefore, it is assumed that the best net pay to use is 350 feet. This yields an effective permeability of

$$k = \frac{18.65}{350.0} = .0535 \text{ md}$$

Before testing, this well had been producing for 90 days. Knowing the effective permeability, an estimate can be made of how far the drainage radius has traveled in this period of time. Using Equation (2)

$$r_d = \sqrt{\frac{1.39 \times 10^{-2} p_i kt}{\bar{\mu} \phi_{HC}}} \quad (2)$$

and assuming an initial pressure of 2400 psi and a hydrocarbon porosity of 5.0%

$$r_d = \sqrt{\frac{1.39 \times 10^{-2} (2.4 \times 10^3)(5.35 \times 10^{-2})(90)}{(1.5 \times 10^{-2})(5.0 \times 10^{-2})}}$$

$$r_d = 460 \text{ feet.}$$

To check the validity of this test analysis, a calculation can be made to estimate the bottom hole flowing pressure after some period of production.

$$p_d^2 - p_w^2 = \frac{q}{2B} \ln At + \frac{D}{B} q^2 \quad (1)$$

where

$$A = \frac{1.39 \times 10^{-2} k P_w}{\mu \phi r_w^2} \quad (3)$$

$$B = \frac{(19.7 \times 10^{-6}) kh}{\mu z} \frac{Tsc}{T} \quad (4)$$

$$D = \frac{2.715 \times 10^{-15} kPscMgB}{h\mu Tsc r_w} \quad (5)$$

$$p_d = p_i \left(1 - \frac{qt}{V_{t=0}} \right)^2 \quad (6)$$

(when t is small and $V_{t=0}$ is large, $p_d \cong p_i$)

Since the multiple rate tests were not conducted, the effective wellbore radius and turbulence factor could not be obtained. From Katz's⁽¹⁾ correlation of permeability versus turbulence factors for various porosities, the estimated value of the turbulence factor for the Mesaverde is 5.0×10^{13} /foot. For the type of fracture performance exhibited by Federal A 25-95 an effective wellbore radius of 5.0 feet is not unreasonable.

The constants A and D are obtained from Equations (3) and (5).

$$A = \frac{(1.39 \times 10^{-2})(.0535)(2400)}{(.015)(.05)(25)} = 95.2$$

$$A = 95.2$$

$$D = \frac{(2.715 \times 10^{-16})(.0535)(15.025)(12.5)(5.0 \times 10^{13})}{(350)(.015)(520)(5)}$$

$$D = 1.4 \times 10^{-4}$$

$$B = \frac{1}{680} \frac{D}{B} = .095$$

Using Equation (1) and the calculated constants, plus B as determined from the test, the BHF pressures can be calculated at various times:

$$p_w^2 = 5.75 \times 10^6 - 340 q \ln(92.5 t) = q^2 (.095)$$

For an initial rate of 1.8 million scf/d

$$p_w^2 = 5.75 \times 10^6 - 6.12 \times 10^5 (\ln 92.5 t) - .308 \times 10^6$$

t (days)	p_w^2 (psia ²)	p_w (psia)
1	2.65×10^6	1630 psig
10	1.25×10^6	1115 psig
20	$.82 \times 10^6$	910 psig

The calculated pressures are in approximate agreement with the BHF pressures of Federal A 29-95 and other Rulison Mesaverde wells when they are initially put on production. Also these calculations have some important qualitative information. First, even using a large turbulence coefficient, the total term D/B turns out to be insignificant because of the large net pay section. Therefore, not knowing the turbulent coefficient exactly will not change the results by an appreciable amount. The guess of the effective wellbore radius was approximately correct since the value of the constant (A) forces a rapid pressure decline on these wells. The buildup on Federal A 29-95 tests also indicate a negative skin is justified, i. e. , effective wellbore radius $r_w > r_{wa}$.

Therefore, it appears that the best value for the matrix permeability is .0535 md.

To make a further check of the analysis, the unsteady-state radial gas flow model was used to simulate the production of Federal A 29-95. Input data for this calculation is cited on the last page of the output. Results from the calculation show an initial rapid pressure decline, causing the well to go on rate decline in less than 120 days. What the results also show is a flow rate that stabilizes at approximately 1200 thousand scf and has a small rate of decline. This does not even come close to matching the flow rate decline performance of the Mesaverde wells which stabilize at close to 100 to 150 thousand scf/d.

To try to reconcile this discrepancy, the decline curves, Figure B-6, were analyzed for the Rulison wells. An equation that approximates changing flow rate as a function of time was presented by Rowan and Clegg. (2)

$$q = \frac{9.03 \times 10^4 kh (p_i^2 - p_w^2)}{zT_f \ln (.606 r_e / r_w)} e^{-\alpha(t-t_b)} \quad (7)$$

where

$$\alpha = \frac{1.264 \times 10^{-2} kp_i}{\mu \phi r_e^2 \ln (.472 r_e / r_w)} \quad (8)$$

This equation is for a gas well producing at a constant pressure from a bounded reservoir. Rewriting this equation in a simpler form

$$q = (a')e^{-\alpha(t-t_b)} \quad (9)$$

or a simpler version by multiplying through by \ln is

$$\ln q = c - \alpha t \quad (10)$$

where c is a constant. By plotting $\log q$ versus time, a straight linear curve should be obtained with a slope of $-\alpha$. Knowing everything but r_e , constant α can be solved by trial and error for an effective drainage radius r_e . From the five wells analyzed, the following slopes ($\partial q / \partial t$) were obtained.

<u>Well</u>	<u>Slope Cycle/day</u>
Federal A 29-95	23.80×10^{-4}
Federal 28-95	2.85×10^{-4}
Juhan No. 1	$.91 \times 10^{-4}$
Federal 30-95	3.14×10^{-4}
Gross Hahnewald No. 1	1.43×10^{-4}

Solving for the boundary radius r_e , using a permeability of .0535 md, the following values were obtained.

Federal A 29-95	$r_e = 340$ feet
Federal 28-95	$r_e = 880$ feet
Juhan No. 1	$r_e = 1,850$ feet
Federal 30-95	$r_e = 950$ feet
Gross Hahnewald No. 1	$r_e = 1,400$ feet

It is interesting to note that the drainage radius for Federal A 29-95 (340 feet) approximately agrees with the previous calculated value of 450 feet. This analysis brings out some other important points. Juhan No. 1, which is the best well, is apparently only draining 246 acres with the other wells draining less. Also notice it takes approximately two years to achieve a relatively constant drainage boundary since dq/dt is changing until this time. Another point is that all the wells but Federal A 29-95 and Federal 30-95 have approximately the same intercept. Federal A 29-95 will probably achieve this intercept after a sufficient amount of production time.

Remembering that the intercept is a constant, $c = (\ln a' - \alpha t_0)$, which is defined by Equation (10), notice that kh enters this constant whereas only permeability enters the slope constant, α . The term t_0 is a time constant. This means that when the well appears to reach a constant rate decline, a certain value of (kh) is achieved that is less than when the well first goes on decline. Assuming the permeability is relatively constant, the effective net pay is decreasing to a certain minimum value.

To check this concept of decreasing effective net pay with distance, the three-week buildup test was analyzed. The buildup is typical of exponential pressure behavior at first glance, but upon closer inspection the buildup is made up of a series of straight line segments that change slope. This is more obvious from the plot of $M(p)$ versus $\Delta t/(t + \Delta t)$ (see Figure B-2).

The concept of Real Gas Flow Theory was presented by Al Hussainy.⁽³⁾ In gas reservoirs the physical properties of the gas, viscosity and gas deviation factor varies with pressure, and in analyzing some gas well tests these variances must be taken into account. Al Hussainy did this by redefining the pressure term as

$$\frac{1}{r} \frac{\partial}{\partial r} \left[r \frac{\partial p^2}{\partial r} \right] = \frac{\phi}{k} \frac{\partial p}{\partial t} \quad (11)$$

or

$$M(p) = 2 \int_{p_m}^p \frac{p}{\mu(p) z(p)} dp \quad (12)$$

which takes care of the non-linear functions of viscosity and the gas deviation factor. By evaluating Equation (8) for different pressures, a plot of $M(p)$ versus pressure is obtained. Table B-IV is the data needed for such a plot. In the case of the pressure drawdown test the Real Gas Theory was not needed since the pressure difference was small enough over the testing period of two days (1107 to 1009 psia).

The pressure buildup covered a pressure range of 300 psia to 1100 psia, therefore the Real Gas Theory was used. Figure B-2 presents the conventional buildup and the buildup of $M(p)$ versus $\Delta t/t + \Delta t$. The $M(p)$ data were calculated by the computer rather than picking the values off a curve. This residual curve should not be influenced by the variable gas properties.

From this analysis the following calculation was made to determine the changing flow capacity kh with distance.

$$kh = 5.792 \frac{(10^4) q P_{sc} T}{m T_{sc}}$$

$$kh = \frac{773 \times 10^6}{m}$$

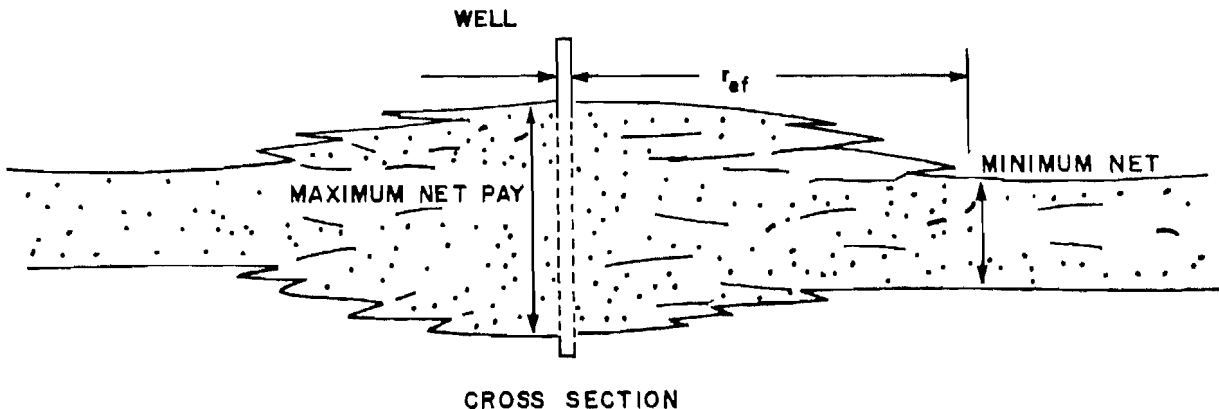
Where m is the slope from the buildup plot of $M(p)$ versus $\Delta t/t + \Delta t$.

<u>m Slope</u>	<u>Time of Slope Change</u>	<u>kh (md feet)</u>	<u>r_d^* (feet)</u>
11 x 10 ⁶	.65 day	70.2	24.3
16	.63 day	48.2	38.7
22	1.30 days	35.0	55.5
38	2.78 days	20.4	81.0
53	4.70 days	14.6	106.0
77	20.95 days	10.0	224.0
155	--	5.0	--

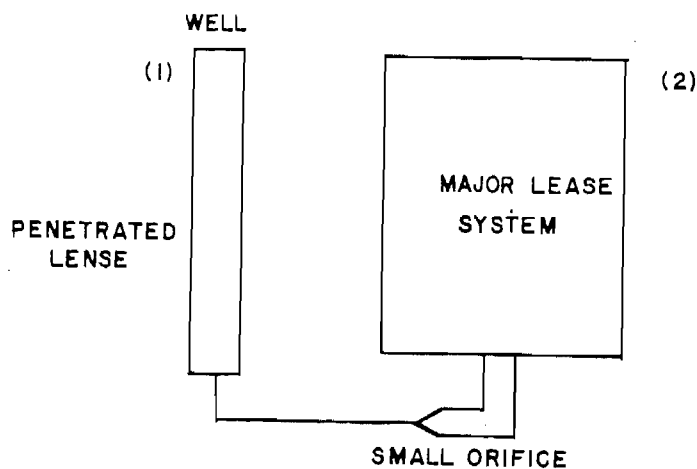
*Calculated using Equation (2)

Figure B-7 is a plot of effect kh versus drainage radius. Notice that the first few values indicate the fracture capacity, but after 2.5 days the kh is approximately the same as from the drawdown test. This capacity term, kh, does not change appreciably until 20.95 days when kh is now 10 md feet. Assuming a constant permeability this would mean the effective net pay is decreasing with distance and from this analysis would be less than 93 feet since the minimum value of kh determined was 5 md feet. Figure B-7 shows a range of possible extrapolations of the flow capacity versus distance curves.

The following is postulated for the description of the Mesaverde Reservoir in the Rulison area. A well penetrates a major lense system of 200 to 400 feet to net pay. At some radial distance the effective net pay decreases to a minimum value of less than 150 feet. The diagram below could be a possible interpretation.



This minimum net pay at some distance is probably connected with another main lense system and acts as a feeder to the lense being produced. One could visualize this as a large tank feeding a smaller tank through a small orifice.



First the well starts depleting the smaller tank, thus giving the high initial production with the larger fracture treatments being analogous to a larger straw in the tank; thus, after depleting the small tank, the fracture does not aid production. As the small tank starts being drawn down the large tank begins feeding into the smaller system but is restricted by the orifice effect. Therefore, the withdrawal of system (1) is much faster than (2) can feed into it, thus the rate falls rapidly until equilibrium is reached between the two. When this occurs the actual rate being produced should be close to what the feeder system (1) is flowing through the orifice. Actually, in the reservoir where this occurs a constant drainage radius is felt by the well and a flow rate dependent of the minimum net pay is achieved.

Generally speaking, an average Rulison well appears to stabilize when a drainage radius of 800 to 1600 feet is reached, depending on where the well is located in the main lense system. A stabilized rate

of 60 to 150 thousand scf/ d is typical. The net pay decreases from the 400 to 200 feet near the well to less than 150 feet at the drainage boundary. Therefore, the entire field appears to be made up of these partially connected lenses with the matrix permeability being so low that each well can be considered to be in a separate system.

An independent analysis of the reservoir based upon an outcrop study follows.

SAND CONTINUITY STUDY

The problem of "sand" continuity is one of the critical facets in the evaluation of the expected reservoir behavior in the Rulison Field. In an effort to further refine data in the literature, (4) an additional field survey and laboratory data evaluation study was made.

The field portion of the study consisted of photographing relatively fresh, extensive outcrop of the Mesaverde formation using a K-20 aerial camera and Kodak Aerecon type 8403 film. The location of the photographed section and the camera location was marked on a 1/24000 topo map. The photography took a portion of three days, two days in the DeBeque Canyon-Plateau Canyon area, and one day in the Douglas Creek arch area.

The film was developed and 11 x 14 prints were made from the negatives. Prints from 15 outcrops were selected for the lab study. Prints from each outcrop were butted together to make panoramas, and either a 10 or 100-foot grid scale was plotted across each outcrop display.

Study of the photo indicated that two general classes of "sand" lense boundary could be determined --

1. Shale layers that were so continuous and thick that they were felt to be absolute barriers to fluid flow, and
2. Discontinuous shale layer or silt and muddy sandstone features that were felt to be restrictions to flow.

Figure B-8 illustrates both of these features, e. g. , continuous shale layers, and discontinuous thin shale lamellae and cross-bedded muddy sandstone. Figure B-9 illustrates the continuity of the major sandstone units.

The barriers were marked in black, and the restrictions were marked in transparent red on the photos. Each outcrop was then documented as to:

1. The orientation of the section (north, northwest, west, etc.)
2. The X, Y location of the center of the section (Using the 1000 yd grid displayed on the topo maps).
3. The average thickness and length of each major "sand" unit (bounded by the black reference marks), and
4. The average thickness and length of each minor unit (bounded by the red reference lines).

The length to thickness ratio was calculated for each bed, and a statistical evaluation was made in terms of these questions:

1. Is there a preferential orientation of the major units (i. e. , is a minimum length/thickness associated with some direction - thus indicating these outcrops cut across the channel)?
2. Is there a characteristic length/thickness ratio for all units (i. e. , can they all be considered to come from the same population)? - or
 - a. Do major units come from one population?
 - b. Do minor units come from one population?
 - c. Can minor units be assigned to separate populations based upon height?
3. Is there a characteristic length/thickness ratio for each location or some group of locations?

The evaluation was made using three techniques - factor analysis, multiple regression analysis, and an analysis of variance.

The factor analysis indicated a rather low correlation between the length/thickness ratio and the other variables, location (and/or position in the section), orientation of outcrop, or thickness.

The multiple regression analysis indicated some correlation between $\log L/h_t$ ratios and thin beds, but at a low significance level.

The analysis of variance indicated no difference at a significant probability level between the length/thickness ratios of beds at different outcrops or of different thicknesses. The critical factor in this analysis was the scatter of data, and the resulting large standard deviation. A statistical summary is presented in Tables B-VIA and B-VIB.

Although the data doesn't allow a number of powerful statements to be made at the 95% probability level, it is possible to make some interesting generalizations.

First, all the averages fell within one standard deviation of the overall average, which was >19 . Thus we can use a sand continuity ratio of ~ 20 to calculate the average continuous sand distance away from the wellbore or nuclear chimney-fractured zone.

Second, the major units have a continuity greater than the outcrop length; hence a minimum dimension in the order of 4000 feet is justified.

The outcrop analysis will be used to construct a reservoir model using the following boundary conditions.

1. Since the majority of the units are channel deposits and these "major" units are known to be elongated when viewed in plan, and since there are so many restrictions to flow within these major units that they cannot be effectively drained over long areas; the reservoir was tentatively modeled as an ellipse when viewed in plan, with a major axis twice as long as the minor axis.

In circles and ellipses of low eccentricity, the probability of a random point falling at any point on the radius or axes is approximately normally distributed with the mode falling on the radius or axis at a locus of points dividing the figure into two concentric figures with equal areas. The mode is seen to fall at a point 0.71 times the length of the radius or axes from the center, i. e., :

for an ellipse

$$\pi ab - \pi \cdot fa \cdot fb = \pi fa \cdot fb$$

$$f \cong 0.71$$

and for a circle

$$\pi r^2 - \pi f^2 r^2 = \pi f^2 r^2$$

$$f \cong 0.71$$

where:

a = minor semi-axis of ellipse

b = major semi-axis of ellipse

r = radius of circle

f = factor giving a radius or axis length that divides the figure into two concentric figures of equal area.

Hence, an eccentric well location on the concentric ellipse with the dimensions a = 0.71 x 2100 and b = 0.71 x 4200 was chosen as the most probable.

The geometry of the reservoir model in plan is presented in Figure B-10.

2. The sand (length/thickness) factor of 20 was used in conjunction with the Federal A 29-95 log to construct a permeability function. The technique used was -
 - a. To tabulate the thickness of each producing "sand" as determined from the log,
 - b. To assume an average continuous extension away from the well of 10 times the sand height (the length/thickness factor of 20 divided by 2), and to calculate the uninterrupted extension of each foot of pay away from the wellbore or end of the nuclear chimney-fracture zone, and

TABLE B-IV
REAL GAS FLOW THEORY INTEGRAL

$$\text{Calculation of } \int_{p_r}^p \frac{p}{z(p) \mu(z)} dP = M(p)$$

Pressure <u>p</u>	Gas Deviation Factor <u>z</u>	Viscosity <u>μ</u>	$\frac{z}{\mu z}$	Mean Value of $\frac{2p}{\mu z}$	<u>Δp</u>	M(p) $\frac{\text{psia}^2}{\text{cp}} \times 10^6$
200	0.9855	0.01110	36557	18278	50	0.91
250	0.9820	0.01120	45447	41002	50	2.96
300	0.9786	0.01131	54234	49840	50	5.46
350	0.9753	0.01141	62916	58575	50	8.38
400	0.9720	0.01151	71493	67204	50	11.74
450	0.9689	0.01162	79963	75728	50	15.53
500	0.9657	0.01172	88329	84146	50	19.74
550	0.9626	0.01183	96596	92462	50	24.36
600	0.9594	0.01194	104767	100682	50	29.40
650	0.9563	0.01205	112842	108805	50	34.84
700	0.9531	0.01216	120821	116831	50	40.68
750	0.9499	0.01227	128702	124762	50	46.92
800	0.9468	0.01238	136475	132589	50	53.55
850	0.9440	0.01250	144124	140299	50	60.56
900	0.9412	0.01261	151652	147888	50	67.95
950	0.9386	0.01273	159059	155355	50	75.72
1000	0.9362	0.01284	166342	162700	50	83.86
1050	0.9338	0.01296	173512	169927	50	92.35
1100	0.9314	0.01308	180586	177029	50	101.21
1150	0.9289	0.01320	187568	184077	50	110.41
1200	0.9265	0.01332	194443	191005	50	119.96
1250	0.9242	0.01344	201200	197821	50	129.85
1300	0.9220	0.01357	207842	204521	50	140.08
1350	0.9199	0.01369	214370	211106	50	150.63
1400	0.9178	0.01382	220780	217575	50	161.51
1450	0.9158	0.01394	227087	223934	50	172.71
1500	0.9137	0.01407	233318	230202	50	184.22
1550	0.9116	0.01420	239470	236394	50	196.04
1600	0.9095	0.01433	245500	242485	50	208.16
1650	0.9078	0.01446	251345	248422	50	220.58
1700	0.9064	0.01459	257031	254188	50	233.29
1750	0.9051	0.01473	262580	259805	50	246.28
1800	0.9038	0.01486	268014	265297	50	259.55

TABLE B-III

TABLE OF WELL, RESERVOIR, AND FLUID PROPERTIES
FOR FEDERAL A 29-95

Well Location: 1520 FSL and 990' FEL
Section 29, T-7-S, R-95-A
Garfield County, Colorado

Elevation: 6783.8 feet GR 6796.3 RKB

Perforations: 6596 - 6980 feet
5690 - 6424 feet
5552 - 5851.5 feet
5269 - 5394.5 feet

Depth To Where BH Pressures Were Recorded = 6900 feet

B. H. Temperature = 184 °F. (Recorded at 6900 feet)

Pressure at Base Conditions = 15.025 psia

Temperature at Base Conditions = 60 °F.

Gas Analysis:

<u>Component</u>	<u>Mole %</u>
CO ₂	1.29
N ₂	.04
C ₁	90.90
C ₂	5.14
C ₃	1.58
i - C ₄	.31
n - C ₄	.34
i - C ₅	.12
n - C ₅	.10
C ₆	.11
C ₇₊	.07
	<hr/>
	100.00%

Specific Gravity of Gas = .625

TABLE B-II

PRESSURE DRAWDOWN DATA

Federal A 29-95
Rulison Field
Mesa verde Formation

 $q_{ave} = 514.7$ thousand scf/day

 $p_d = 2400$ psi

<u>Time</u> <u>hrs.</u>	<u>Time</u> <u>days</u>	<u>ln Time</u>	<u>Pressure</u> <u>(psia)</u> <u>p_w</u>	<u>$\frac{p_d^2 - p_w^2}{q_{ave}}$</u>	<u>$\frac{M(p)}{cp}$</u> <u>(10^{+6})</u>
1.0	0.042	-3.1781	1107.4	8807.7	102.57
2.0	0.083	-2.4849	1098.0	8848.0	100.86
3.0	0.125	-2.0794	1093.4	8867.5	100.04
4.0	0.167	-1.7918	1094.8	8861.6	100.29
5.0	0.208	-1.5686	1090.2	8881.1	99.48
6.0	0.250	-1.3863	1088.7	8887.5	99.21
7.0	0.292	-1.2321	1084.0	8907.3	98.38
8.0	0.333	-1.0986	1080.9	8920.3	97.83
9.0	0.375	-0.9808	1078.3	8927.1	97.55
10.0	0.417	-0.8755	1077.3	8933.3	97.28
11.0	0.458	-0.7802	1074.7	8946.3	96.73
12.0	0.500	-0.6931	1071.5	8959.7	96.16
13.0	0.542	-0.6131	1070.0	8965.9	95.90
14.0	0.583	-0.5390	1066.9	8978.8	95.35
15.0	0.625	-0.4700	1065.3	8985.4	95.07
16.0	0.667	-0.4055	1062.2	8998.2	94.52
17.0	0.708	-0.3448	1059.1	9011.0	93.97
18.0	0.750	-0.2877	1057.5	9017.6	93.69
19.0	0.792	-0.2336	1056.0	9023.7	93.42
20.0	0.833	-0.1823	1056.0	9023.7	93.42
21.0	0.875	-0.1335	1054.4	9030.3	93.14
22.0	0.917	-0.0870	1052.8	9036.8	92.85
23.0	0.958	-0.0426	1051.3	9043.0	92.59
24.0	1.000		1049.7	9049.5	92.31
25.0	1.042	-0.0408	1049.7	9049.5	92.31
26.0	1.083	-0.0800	1049.7	9049.5	92.31
27.0	1.125	0.1178	1048.2	9055.6	92.05
28.0	1.167	0.1542	1045.1	9068.2	91.53
29.0	1.208	0.1892	1041.9	9081.2	90.98
30.0	1.250	0.2231	1040.4	9087.3	90.73
31.0	1.292	0.2559	1035.7	9106.2	89.93
32.0	1.333	0.2877	1034.1	9112.6	89.66

TABLE B-II (Cont.)

<u>Time</u> <u>hrs.</u>	<u>Time</u> <u>days</u>	<u>ln Time</u>	<u>Pressure</u> <u>(psia</u> <u>p_w</u>	<u>$\frac{p_d^2 - p_w^2}{q_{ave}}$</u>	<u>$\frac{M(p)}{psia^2}$</u> <u>cp</u> <u>(10⁺⁶)</u>
33.0	1.375	0.3185	1032.6	9118.7	89.40
34.0	1.417	0.3483	1029.5	9131.1	88.87
35.0	1.458	0.3773	1027.9	9137.5	88.60
36.0	1.500	0.4055	1026.4	9143.5	88.35
37.0	1.542	0.4329	1024.8	9149.8	88.08
38.0	1.583	0.4595	1021.7	9162.2	87.55
39.0	1.625	0.4855	1020.9	9165.3	87.41
40.0	1.667	0.5108	1018.6	9174.5	87.02
41.0	1.708	0.5355	1017.0	9180.8	86.75
42.0	1.750	0.5596	1015.4	9187.1	86.48
43.0	1.792	0.5831	1015.4	9187.1	86.48
44.0	1.833	0.6061	1013.9	9193.0	86.22
45.0	1.875	0.6286	1012.3	9199.3	85.95
46.0	1.917	0.6506	1010.8	9205.2	85.70
47.0	1.958	0.6721	1009.2	9211.5	85.42
48.0	2.000	0.6931	1009.2	9211.5	85.42

TABLE B-I

PRESSURE BUILD-UP DATA

Federal A 29-95
Rulison Field
Mesa verde Formation

Shut-In Time (hours) Δt	Wellbore Pressure (psia) p_w	$\frac{\Delta t}{t + \Delta t}$ (10^{-3})	$M(p)$ $\frac{\text{psia}^2}{\text{cp}^{+6}}$ (10^{+6})
0.500	312.7	0.194	6.20
1.000	318.8	0.389	6.56
1.500	351.6	0.583	8.49
2.000	367.1	0.777	9.54
2.500	382.8	0.971	10.59
3.000	395.2	1.165	11.42
3.500	406.1	1.359	12.21
4.000	418.6	1.553	13.16
4.500	424.8	1.747	13.62
5.000	431.1	1.940	14.10
5.500	438.9	2.134	14.69
6.000	445.1	2.328	15.16
6.500	452.9	2.521	15.78
7.000	459.1	2.714	16.30
7.500	463.8	2.908	16.69
8.000	468.4	3.101	17.08
8.500	473.8	3.294	17.54
9.000	466.3	3.487	16.91
9.500	482.5	3.680	18.27
10.000	485.6	3.873	18.53
10.500	488.7	4.066	18.79
11.000	491.8	4.259	19.05
11.500	495.0	4.452	19.32
12.000	498.1	4.644	19.58
12.500	504.3	4.837	20.14
13.000	507.4	5.029	20.43
13.500	510.5	5.222	20.71
14.000	513.6	5.414	21.00
14.500	516.8	5.607	21.29
15.000	519.8	5.799	21.57
15.500	524.6	5.991	22.02
16.000	527.7	6.183	22.30
16.500	529.2	6.375	22.44
17.000	533.9	6.567	22.88
17.500	538.6	6.759	23.31
18.000	540.2	6.950	23.46
18.500	541.7	7.142	23.60

TABLE B-I (Cont.)

Shut-In Time (hours) Δt	Wellbore Pressure (psia) p_w	$\frac{\Delta t}{t + \Delta t}$ (10^{-3})	$\frac{M(p)}{\text{psia}^2}$ $\frac{c_{p+6}}{(10^{-6})}$
19.000	543.3	7.334	23.74
19.500	547.9	7.525	24.17
20.000	549.5	7.717	24.32
20.500	551.1	7.908	24.48
20.830	552.6	8.034	24.63
22.330	555.7	8.608	24.94
22.830	557.3	8.799	25.10
23.330	558.8	8.990	25.25
23.830	560.4	9.181	25.41
24.330	563.5	9.372	25.72
24.830	565.1	9.563	25.88
25.330	568.2	9.753	26.20
25.830	569.7	9.944	26.35
26.330	572.9	10.134	26.67
26.830	574.4	10.325	26.82
27.330	576.0	10.515	26.98
27.830	579.1	10.706	27.29
28.330	580.6	10.896	27.45
28.830	583.8	11.086	27.77
29.330	586.9	11.276	28.08
29.830	588.4	11.466	28.23
30.330	591.6	11.656	28.55
30.830	593.1	11.846	28.70
31.330	594.7	12.036	28.86
31.830	597.8	12.225	29.18
32.330	599.4	12.415	29.34
32.830	602.5	12.605	29.67
33.330	604.0	12.794	29.83
33.830	605.6	12.984	30.01
34.330	607.1	13.173	30.17
34.830	608.7	13.362	30.35
35.330	610.3	13.551	30.52
35.830	611.8	13.741	30.68
36.330	613.4	13.930	30.86
36.830	616.5	14.119	31.19
37.330	618.1	14.308	31.37
37.830	621.2	14.496	31.71
38.330	622.7	14.685	31.87
38.830	624.3	14.874	32.04
39.330	625.8	15.063	32.21
39.830	627.4	15.251	32.38
40.330	629.0	15.440	32.55
40.830	630.0	15.628	32.66
41.330	633.6	15.816	33.05

TABLE B-I (Cont.)

Shut-In Time (hours) Δt	Wellbore Pressure (psia) P_w	$\frac{\Delta t}{t + \Delta t}$ 10^{-3}	$M(p)$ $\frac{\text{psia}^2}{\text{cp}}$ (10^{+6})
41.830	635.2	16.005	33.23
42.330	636.8	16.193	33.40
42.830	638.3	16.381	33.57
43.330	639.9	16.569	33.74
43.830	641.4	16.757	33.90
44.330	643.0	16.945	34.08
44.830	644.5	17.133	34.24
45.330	646.1	17.321	34.41
45.830	647.7	17.508	34.59
46.330	649.2	17.696	34.75
46.830	650.8	17.884	34.93
47.330	652.8	18.071	35.17
47.830	653.9	18.259	35.29
48.330	655.5	18.446	35.48
48.830	657.0	18.633	35.66
49.330	658.6	18.820	35.84
49.830	660.1	19.007	36.02
50.330	661.7	19.195	36.21
50.830	663.2	19.382	36.38
51.330	664.8	19.568	36.57
51.830	664.8	19.755	36.57
52.330	666.4	19.942	36.76
52.830	667.9	20.129	36.93
53.330	669.5	20.315	37.12
53.830	671.0	20.502	37.29
54.330	672.6	20.688	37.48
54.830	674.2	20.875	37.67
55.330	675.7	20.061	37.84
55.830	677.3	21.248	38.03
56.330	678.8	21.434	38.20
56.830	680.4	21.620	38.39
57.330	681.9	21.806	38.57
57.830	683.5	21.992	38.75
58.330	685.1	22.178	38.94
58.830	686.6	22.364	39.12
59.330	688.2	22.550	39.30
59.830	689.7	22.735	39.48
60.330	691.3	22.921	39.66
60.830	692.9	23.106	39.85
61.330	694.4	23.292	40.03
61.830	696.0	23.477	40.21

TABLE B-I (Cont.)

Shut-In Time (hours) Δt	Wellbore Pressure (psia) p_w	$\frac{\Delta t}{t + \Delta t}$ (10^{-3})	$\frac{M(p)}{cp}$ (10^{+6})
62.330	697.5	23.663	40.39
62.830	699.1	23.848	40.58
63.330	700.6	24.033	40.76
63.830	702.2	24.218	40.96
64.330	703.8	24.403	41.15
64.830	703.8	24.589	41.15
65.330	705.3	24.773	41.34
65.830	706.9	24.958	41.54
66.330	708.4	25.143	41.73
66.830	710.0	25.328	41.93
67.330	711.6	25.513	42.13
67.830	713.1	25.697	42.32
141.000	822.2	51.976	56.66
142.000	825.4	52.326	57.11
143.000	825.4	52.675	57.11
144.000	826.9	53.024	57.32
145.000	826.9	53.372	57.32
146.000	828.5	53.721	57.55
147.000	830.0	54.069	57.76
148.000	831.6	54.416	57.98
149.000	833.2	54.764	58.21
150.000	834.7	55.111	58.42
151.000	836.3	55.458	58.64
152.000	837.8	55.805	58.85
153.000	839.4	56.152	59.08
154.000	840.9	56.498	59.29
155.000	840.9	56.844	59.29
156.000	842.5	57.190	59.51
157.000	842.5	57.535	59.51
158.000	844.1	57.880	59.74
159.000	844.1	58.225	59.74
160.000	845.6	58.570	59.95
161.000	847.2	58.915	60.17
162.000	848.7	59.259	60.38
163.000	850.3	59.603	60.61
164.000	851.9	59.947	60.84
165.000	853.4	60.290	61.07
166.000	853.4	60.633	61.07
167.000	854.9	60.976	61.29
168.000	856.5	61.319	61.53
169.000	858.1	61.662	61.76

TABLE B-I (Cont.)

Shut-In Time (hours) Δt	Wellbore Pressure (psia) p_w	$\frac{\Delta t}{t + \Delta t}$ (10^{-3})	$M(p)$ $\frac{\text{psia}^2}{\text{cp}}$ (10^{+6})
170.000	859.6	62.004	61.98
171.000	861.2	62.346	62.22
172.000	861.2	62.688	62.22
173.000	862.7	63.029	62.44
174.000	864.3	63.370	62.68
175.000	865.8	63.711	63.90
176.000	867.4	64.052	63.14
177.000	869.0	64.392	63.37
178.000	870.5	64.733	63.60
179.000	872.1	65.073	63.83
180.000	872.1	65.412	63.83
181.000	873.6	65.752	64.05
182.000	875.2	66.091	64.29
183.000	876.7	66.430	64.51
184.000	876.7	66.769	64.51
185.000	878.3	67.108	64.75
186.000	878.3	67.446	64.75
187.000	879.9	67.784	64.99
188.000	879.9	68.122	64.99
189.000	881.4	68.459	65.21
190.000	881.4	68.797	65.21
191.000	883.0	69.134	65.44
192.000	884.5	69.470	65.67
193.000	886.1	69.807	65.90
194.000	887.7	70.143	66.14
195.000	887.7	70.479	66.14
196.000	889.2	70.815	66.36
197.000	890.8	71.151	66.60
198.000	890.8	71.486	66.60
199.000	892.3	71.821	66.82
200.000	893.9	72.156	67.06
201.000	895.4	72.491	67.28
202.000	897.1	72.825	67.53
203.000	897.1	73.159	67.53
204.000	898.6	73.493	67.75
205.000	900.1	73.827	67.97
206.000	900.1	74.160	67.97
207.000	901.7	74.493	68.22
208.000	903.2	74.826	68.46
209.000	904.8	75.159	68.70
210.000	904.8	75.492	68.70
211.000	906.4	75.824	68.95

TABLE B-I (Cont.)

Shut-In Time (hours) Δt	Wellbore Pressure (psia) p_w	$\frac{\Delta t}{t + \Delta t}$ (10^{-3})	$\frac{M(p)}{cp}$ psia^2 (10^{+6})
282.000	987.4	98.817	81.81
283.000	989.0	99.132	82.07
284.000	989.0	99.448	82.07
285.000	990.5	99.763	82.32
286.000	990.5	100.078	82.32
287.000	990.5	100.393	82.32
288.000	992.1	100.707	82.58
289.000	992.1	101.022	82.58
290.000	992.1	101.336	82.58
291.000	992.1	101.650	82.58
292.000	993.6	101.964	82.82
293.000	993.6	102.277	82.82
294.000	993.6	102.590	82.82
295.000	993.6	102.903	82.82
296.000	995.2	103.216	83.08
297.000	995.2	103.529	83.08
298.000	995.2	103.841	83.08
299.000	996.7	104.153	83.32
300.000	996.7	104.465	83.32
301.000	996.7	104.777	83.32
302.000	998.3	105.089	83.58
303.000	998.3	105.400	83.58
304.000	998.3	105.711	83.58
305.000	998.3	106.022	83.58
306.000	999.9	106.332	83.85
307.000	999.9	106.643	83.85
308.000	999.9	106.953	83.85
309.000	999.9	107.263	83.85
310.000	1001.4	107.573	84.10
311.000	1001.4	107.882	84.10
312.000	1001.4	108.192	84.10
313.000	1001.4	108.501	84.10
314.000	1003.0	108.810	84.37
315.000	1003.0	109.119	84.37
316.000	1003.0	109.427	84.37
317.000	1004.5	109.735	84.63
318.000	1004.5	110.043	84.63
319.000	1004.5	110.351	84.63
320.000	1006.1	110.659	84.90
321.000	1006.1	110.966	84.90

TABLE B-I (Cont.)

Shut-In Time (hours) Δt	Wellbore Pressure (psia) p_w	$\frac{\Delta t}{t + \Delta t}$ (10^{-3})	$\frac{M(p)}{psia^2}$ cp (10^{+6})
322.000	1006.1	111.274	84.90
323.000	1007.7	111.581	85.17
324.000	1007.7	111.887	85.17
325.000	1009.2	112.194	85.42
326.000	1009.2	112.500	85.42
327.000	1010.8	112.807	85.70
328.000	1010.8	113.112	85.70
329.000	1012.3	113.418	85.95
330.000	1012.3	113.724	85.95
331.000	1013.9	114.029	86.22
332.000	1013.9	114.334	86.22
333.000	1013.9	114.639	86.22
334.000	1015.4	114.944	86.48
335.000	1015.4	115.248	86.48
336.000	1015.4	115.553	86.48
337.000	1017.0	115.857	86.75
338.000	1017.0	116.160	86.75
339.000	1018.6	116.464	87.02
340.000	1018.6	116.768	87.02
341.000	1018.6	117.071	87.02
342.000	1020.4	117.374	87.33
343.000	1020.1	117.677	87.28
344.000	1021.7	117.979	87.55
345.000	1021.7	118.282	87.55
346.000	1023.2	118.584	87.80
347.000	1023.2	118.886	87.80
348.000	1024.8	119.188	88.08
349.000	1024.0	119.489	87.94
350.000	1026.4	119.790	88.35
351.000	1026.4	120.092	88.35
352.000	1026.4	120.393	88.35
353.000	1026.4	120.693	88.35
450.000	1070.0	148.919	95.90
456.000	1071.6	150.606	96.18
460.000	1073.1	151.727	96.45
465.000	1074.7	153.123	96.73
469.000	1076.2	154.237	97.00
474.000	1077.8	155.626	97.28
479.000	1079.3	157.010	97.55

TABLE B-I (Cont.)

Shut-In Time (hours) Δt	Wellbore Pressure (psia) p_w	$\frac{\Delta t}{t + \Delta t}$ (10^{-3})	$M(p)$ $\frac{\text{psia}^2}{\text{cp}}$ (10^{+6})
484.000	1080.9	158.389	97.83
489.000	1082.5	159.764	98.11
493.000	1084.0	160.860	98.38
496.000	1085.6	161.681	98.66
499.000	1087.1	162.500	98.93
503.000	1088.7	163.590	99.21
505.000	1090.2	164.133	99.48
508.000	1091.8	164.947	99.76
513.000	1093.4	166.301	100.04
516.000	1094.9	167.111	100.31
519.000	1094.9	167.919	100.31

- c. To calculate the percent of net pay connected to the wellbore (called the permeability function) versus the radius. This data is presented graphically as Figure B-11.

The distance at which the barriers to flow are encountered as calculated by the above technique compares favorably with that calculated kh behavior obtained from the Federal A 29-95 well test information, Figure B-7.

MATHEMATICAL MODEL CONSTRUCTIONS FOR THE NUCLEAR STIMULATED MESAVERDE GAS RESERVOIR (RULISON AREA)

From the well test and geological analyses it is obvious that the constant thickness radial gas flow model would not be descriptive of the postulated Mesaverde reservoir, lense system. Therefore, a two-dimensional, unsteady-state gas flow model was used to evaluate the future gas production of a nuclear stimulated reservoir in the Mesaverde formation of the Rulison area.

The model representing two-dimensional flow is an approximate solution of Equation (8).

$$\frac{\partial}{\partial x} \left(\frac{kh}{\mu} \frac{\partial p^2}{\partial x} \right) + \frac{\partial}{\partial x} \left(\frac{kh}{\mu} \right) = \frac{\phi H C^h}{p} \frac{\partial p^2}{\partial t} - \frac{q}{\Delta x \Delta y} \quad (8)$$

This model does not assume radial flow or constant thickness, and was more applicable for the final predictions. Also, the additional volume of the chimney can be taken into account, whereas the radial model still lacks this feature.

The first step in using this model is to superimpose a cartesian coordinate grid over an estimated isopach and flow capacity map. Data at the grid points are used in an auto-contouring program to evaluate both matrices for a certain array size. The project Rulison model required an 89 x 49 rectangular array. The basic block size was taken as a 100 foot square. The geometry of the ellipse and the well

locations are shown in Figure B-10. The general height of the blocks in the ellipse was mapped as 150 feet, with the thickness feathering to zero at the edges and rising to a height of approximately 1800 feet over the chimney.

The chimney was simulated by four blocks having the same hydrocarbon volume as that calculated for the nuclear chimney, and a permeability of 1000 md. The height and permeability were reduced in a linear semi log manner to 350 feet and 0.053 md. at the boundary of the fractured zone. The fractured zone was simulated by a 3-block wide array surrounding the chimney. The height was reduced from 350 feet, the anticipated net pay at the shot point, to 150 feet, the calculated effective matrix thickness, in a linear manner in a 7-block wide array surrounding the fractured zone. The permeability in this region of decreasing effective sand connection remained constant at 0.053 md.

The general symmetrical pattern was interrupted on one side by the approaching boundary of the ellipse. Hence, on the east the thickness varied from 350 to zero feet without encountering a 150-foot "plateau."

The geometric factors used in the model are summarized in Table B-VII.

Figure B-12 is a plot of the isopach of net pay constructed by the contouring program. A capacity map is not presented because of the large range of capacities, 7 md feet, over most of the area to 2,000,000 md feet in the chimney. Table B-VIII is a summary of the constructed model reservoir data and fluid properties.

Two cases were set up to simulate the deliverability performance of the nuclear stimulated reservoir. Case No. 1 should be considered a minimum case where the product is prorated over the 20 years. Table B-IX

is the rate schedule for case No. 1. Figure B-13 is a plot of chimney pressure decline (measured at the producing well) and average reservoir bulk volume with time. After 20 years of production 13,888 billion scf of gas was produced. The chimney pressure at this time is 695 psia. Figure B-14 is a calculated isobaric map of the reservoir after 20 years of production. Because of the eccentricity of the chimney, the northern upper half is being poorly drained, which is to be expected.

Case No. 2 was designed to exhibit the optimum deliverability potential of the well. Table B-X presents the rate schedule for this case. This simulation assumes that compressors are used when the BHF pressures fall below the pipeline back pressure, and that the chimney is drawn down to below 20 psi in 20 years. Figure B-15 is a plot of cavern pressure and reservoir bulk pressure versus time. Total production after 20 years is 16,264 billion scf of gas. This should be considered the maximum amount of gas to be produced in 20 years. Figure B-16 is another isobaric map for Case No. 2 at the end of 20 years. Again, notice the poor drainage of the upper area.

Figures B-17 and B-18 compare the rates and cumulative production in both cases with the calculated rate of a conventional Rulison well. The area between the curves in Figure B-17 represents the extra rate of production following nuclear stimulation. In Figure B-18 the area between the curves represents the extra total gas produced by nuclear stimulation. It is readily apparent that normal completion methods will not yield enough gas to make the well economically attractive. However, if the calculations hold and the nuclear explosive does as predicted, the wells will be commercial. This means that the gas reserves in the Rulison field can be made available.

APPENDIX B REFERENCES

1. Katz, D. L., Handbook of Natural Gas Engineering, pg 50, McGraw-Hill, (1959).
2. Rowan, G., and Clegg, M. W., "An Approximate Method for Transient Radial Flow," SPE Journal, V. 2, No. 3 (Sept. 1962), pg 225.
3. Al Hussainy, Ramey, H. J., "Application of Real Gas Flow Theory to Well Testing and Deliverability Forecasting," J Pet Tech (May 1966).
4. Zeito, G. A., "Interbedding of Shale Breaks and Reservoir Heterogeneities," SPE Paper 1128, Denver 1965 Meeting.

TABLE B-IV (Cont.)

Pressure <u>p</u>	Gas Deviation Factor <u>z</u>	Viscosity <u>μ</u>	<u>$\frac{2p}{\mu z}$</u>	Mean Value of <u>$\frac{2p}{\mu z}$</u>	<u>Δp</u>	M(p) <u>$\frac{\text{psia}^2}{\text{cp}} \times 10^6$</u>
1850	0.9026	0.01500	273327	270670	50	273.08
1900	0.9015	0.01513	278524	275925	50	286.88
1950	0.9005	0.01527	283609	281066	50	300.93
2000	0.8995	0.01541	288573	286091	50	315.24
2050	0.8987	0.01555	293393	290983	50	329.78
2100	0.8980	0.01569	298068	295731	50	344.57
2150	0.8975	0.01583	302605	300337	50	359.59
2200	0.8971	0.01598	307003	304804	50	374.83
2250	0.8968	0.01612	311264	309134	50	390.28
2300	0.8967	0.01627	315388	313326	50	405.95
2350	0.8967	0.01641	319375	317382	50	421.82
2400	0.8968	0.01656	323228	321302	50	437.89

TABLE B-V
LIST OF SYMBOLS USED IN EQUATIONS

	<u>Meaning</u>	<u>Dimension</u>
A	Constant $\left(\frac{1.39 \times 10^{-2} k p_i}{\phi_{HC} r^2 \bar{\mu}} \right)$	psia ² /thousand scf/day
B	Constant $\left(\frac{9.8 \times 10^{-6} k h T_{sg}}{\bar{Z} \bar{\mu} p_{sc} T} \right)$	psia ² /thousand scf/day
D	Constant $\left(\frac{2.715 \times 10^{-15} k p_{sc} M \beta}{h \bar{\mu} T_{sc} r_w} \right)$	psia ² /thousand scf /day
h	Net pay	feet
k	Effective permeability	md
kh	Capacity	md feet
M _g	Molecular weight of gas	lb/lb mole
p _i	Initial reservoir pressure	psia
p _w	Bottom hole flowing pressure	psia
p _{sc}	Pressure at standard conditions	psia
q	Flow rate	thousand scf/day
r _w	Effective wellbore radius $\left(\frac{r_{wa}}{e^s} \right)$	feet
r _{wa}	Actual wellbore radius	feet
S	Skin factor	dimensionless
T	Actual formation temperature	R
T	Temperature at standard conditions	R
z	Average gas deviation factor	dimensionless
β	Turbulence factor	feet ⁻¹
φ _{HC}	Hydrocarbon porosity	dimensionless
φ	Absolute porosity	dimensionless
μ	Average gas viscosity	cp

TABLE B-V (Cont.)

NOMENCLATURE

<u>Symbols</u>	<u>Meaning</u>	<u>Dimension</u>
β	Turbulence factor	ft ⁻¹
ϕ_{HC}	Hydrocarbon porosity	dimensionless
ϕ	Absolute porosity	dimensionless
$\bar{\mu}$	Average gas viscosity	cp

TABLE B-VI A

RULISON PROJECT
SAND CONTINUITY STUDY
EVALUATION OF LOCATION EFFECTS

Out-Crop	Sand Thickness (Feet)								Ave. L/h_t	Stand. Dev.
	5	10	15	20	30	40	50	>50		
A	>13*	>12							>13	7
B	13	>13							>13	8
C	27	17	19	18	>21	>18			>21	20
Q	16	27	14	18	24	25	>22	13	>20	16
P	25	19	33	40	19	30	37		>24	12
F		30	18	27	25	>19		20	>23	12
E	31	19	16	16	>19	>17	>16	>16	>20	15
O	27	>23	14	>21	>23	>24	>26		>18	9
N		32		>31	>27	12	17	>22	>25	14
L							>25		>25	12
Ave. L/n_t	>19	>21	>17	>21	>24	>20	>22	>17	19	
Stand. Dev.	19	16	7	8	12	10	10	5		19

* Value of L/h_t (Length/ thickness) is greater than indicated value.

TABLE B-VI B

RULISON PROJECT
SAND CONTINUITY STUDY
EVALUATION OF OUTCROP ORIENTATION EFFECTS

Outcrop Origin. AZM*	nt, Sand Thickness (Feet)								Ave. L/h _t	Stand. Dev.
	5'	10'	15'	20'	30'	40'	50'	>50'		
225°	15	17	17	16	18	17	12	14	16	14
270°	28	18	17	21	22	16		20	22	19
315°	12	22	16	11	23	26	27	13	18	15
360°	27	19	17	21	22	21	17	17	22	17
—	—	—	—	—	—	—	—	—	—	—
Ave. L/h _t	19	18	17	20	22	20	19	16	19	
—	—	—	—	—	—	—	—	—	—	—
Stand. Dev.	18	15	7	9	9	15	13	6		18

* Azimuth measured clockwise from north.

TABLE B-VII

GEOMETRIC FACTORS USED IN RESERVOIR MODEL

Reservoir Pressure at Mid Perforation	= 2400 psia
Net Pay At Well Bore	= 350 feet
Ave. Matrix Pay Connected To Well	= 150 feet
Permeability of Chimney	= 1000 md.
Permeability of Fractured Zone	= 100-1 md.
Permeability of Matrix	= 0.053 md.
Hydrocarbon Volume Created by two 50 kiloton Devices @ 7500 & 8500 feet	= 5.53×10^6 cu. feet
Maximum Length of Sand Body	= 8400 feet
Maximum Width of Sand Body	= 4200 feet

TABLE B-VIII

TABLE OF NUCLEAR STIMULATED RESERVOIR PROPERTIES

Reservoir Pore Volume	= 233.99 million cu. feet
Initial Gas-In-Place	= 34.29 billion scf
Initial Reservoir Pressure	= 2400 psia
Reservoir Temperature	= 184 °F.
Porosity	= 10%
Water Saturation	= 50%
Initial Gas Deviation Factor	= .88
Average Viscosity	= .014 cp.
Pressure At Base Conditions	= 15.025 psia
Temperature At Base Conditions	= 60 °F.

TABLE B-IX

TABLE OF FLOW RATE SCHEDULES
FOR DELIVERABILITY PREDICTIONS -
NUCLEAR STIMULATION STUDY - Case 1

Project Rulison

0	-	.878 Years	5.0 million scf/ day
.878	-	3.60 Years	2.5 million scf/ day
3.600	-	7.00 Years	1.8 million scf/ day
7.00	-	20.00 Years	1.4 million scf/ day

TABLE B-X

TABLE OF FLOW RATE SCHEDULES
FOR DELIVERABILITY PREDICTIONS -
NUCLEAR STIMULATION STUDY - Case 2

Project Rulison

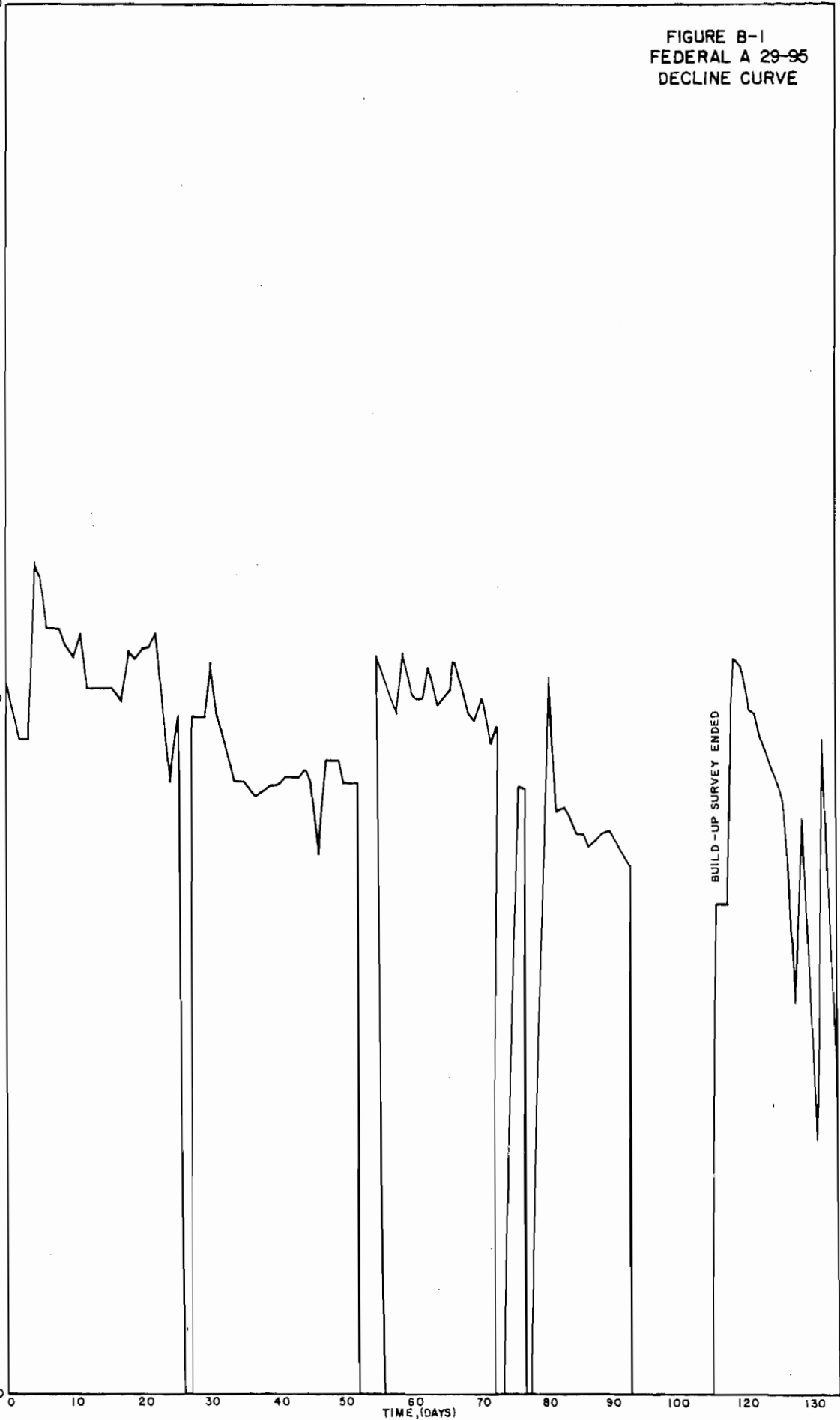
0	-	1.5 Years	5.0 million scf/ day
1.5	-	3.6 Years	3.6 million scf/ day
3.6	-	7.0 Years	2.5 million scf/ day
7.0	-	13.0 Years	1.8 million scf/ day
13.0	-	20.0 Years	1.5 million scf/ day

10,000

FIGURE B-1
FEDERAL A 29-95
DECLINE CURVE

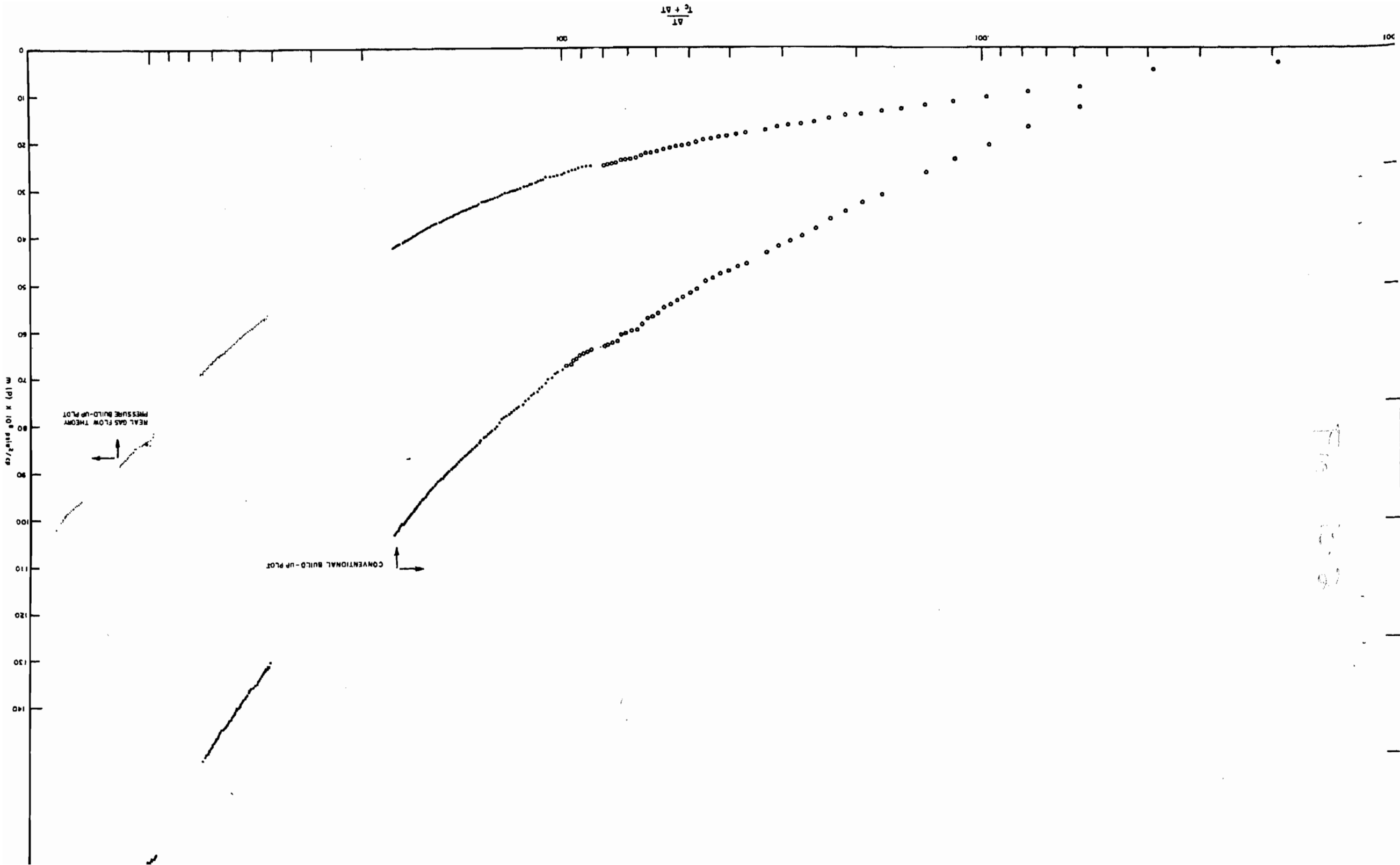
FLOW RATE (THOUSAND SCF/DAY)

100



BUILD-UP SURVEY ENDED

TIME, (DAYS)



76
10
37

FLOW DIAGRAM OF SURFACE
WELL TEST HOOK-UP
FOR FEDERAL A 29-95

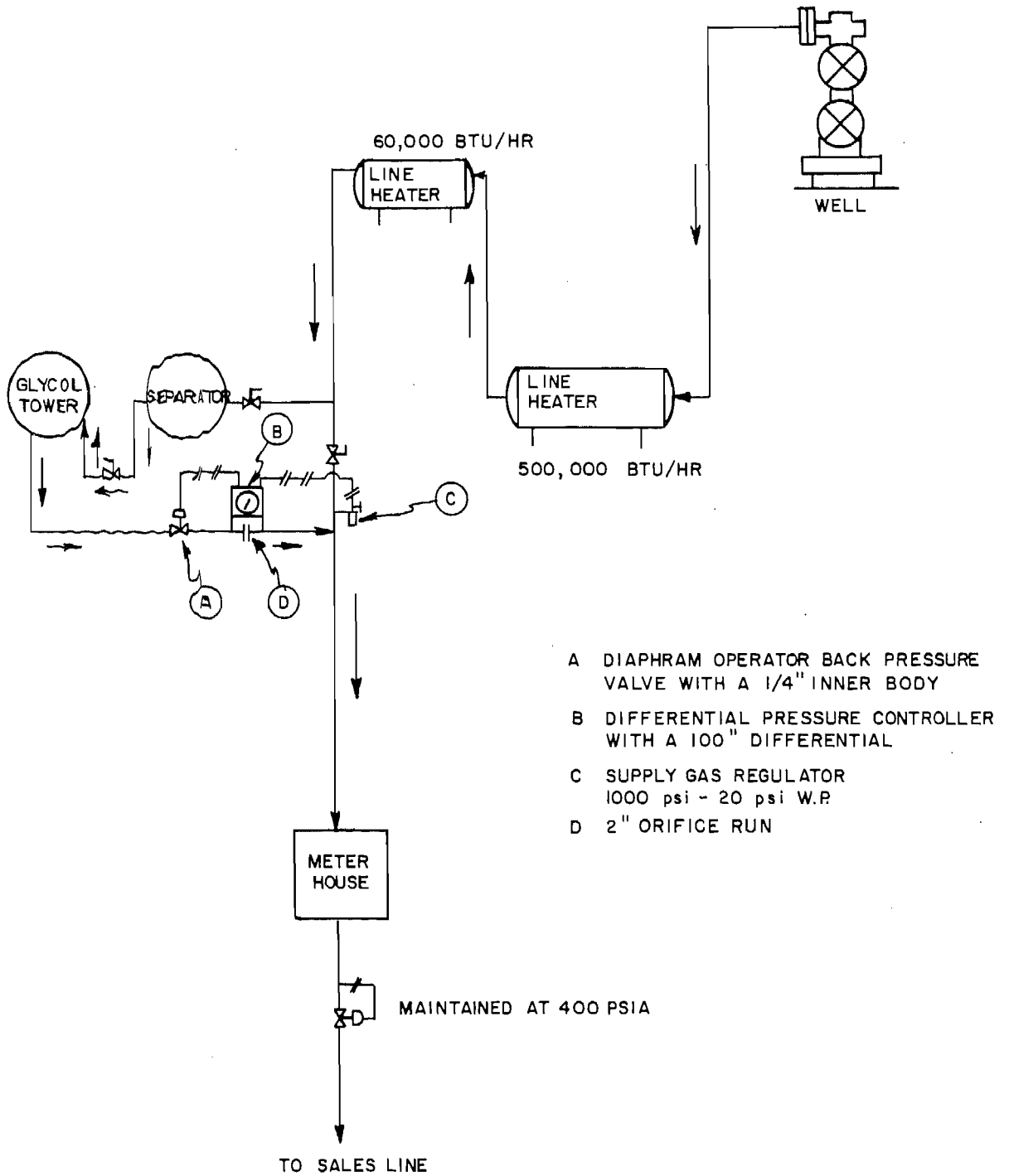
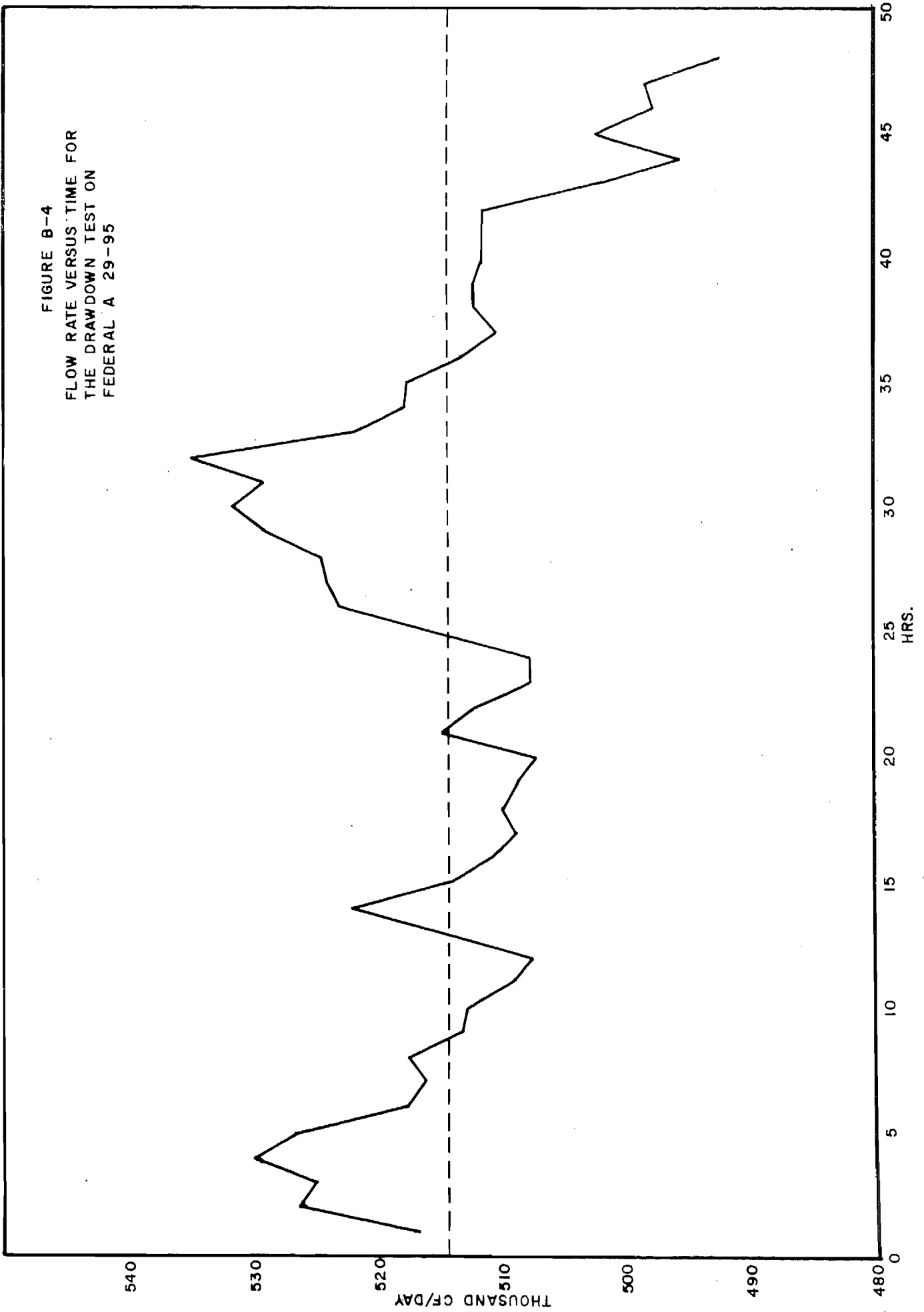
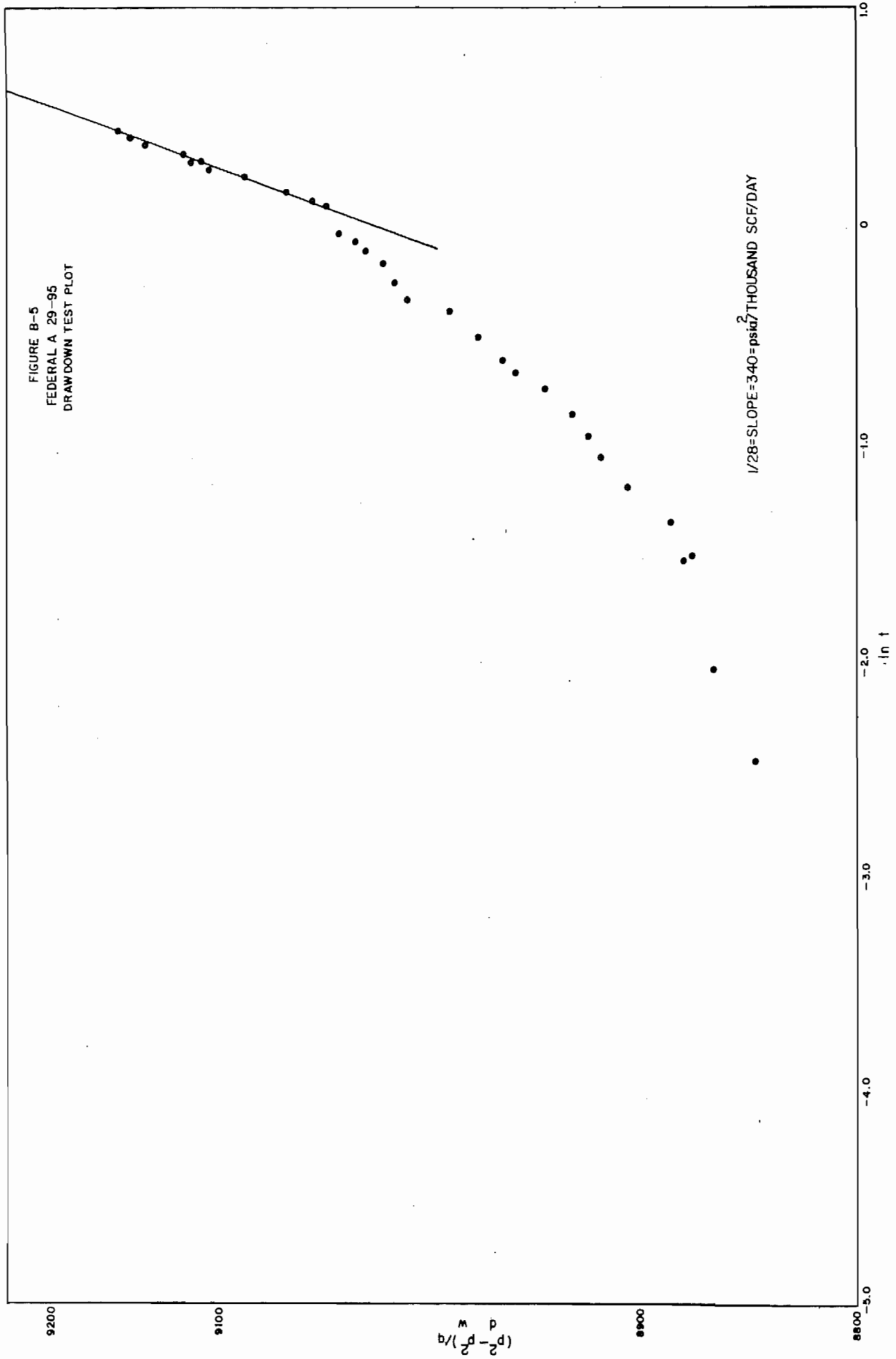


FIGURE B-3

FIGURE B-4
FLOW RATE VERSUS TIME FOR
THE DRAWDOWN TEST ON
FEDERAL A 29-95





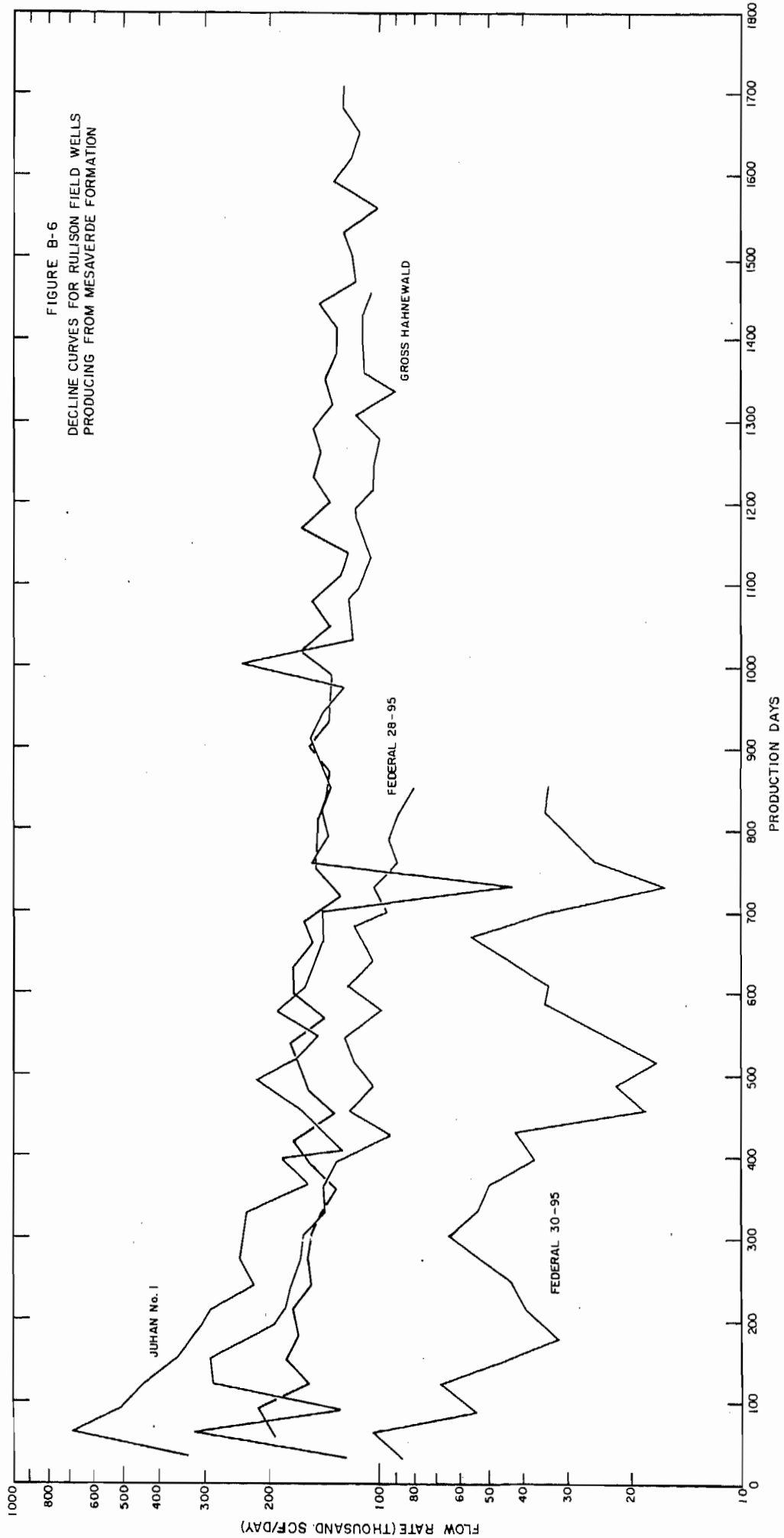


FIGURE B-6
DECLINE CURVES FOR RULISON FIELD WELLS
PRODUCING FROM MESAVERDE FORMATION

JUHON No. 1

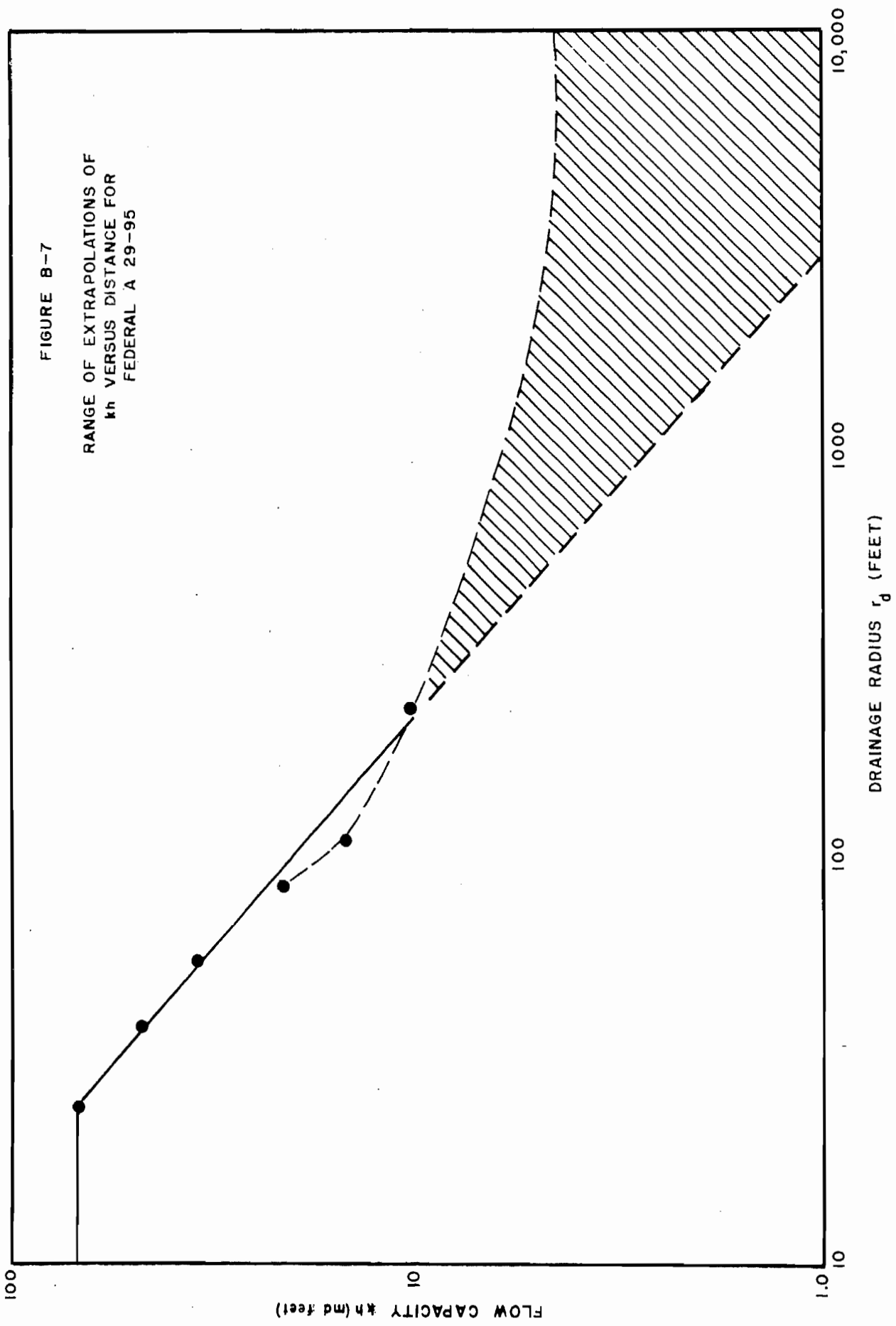
FEDERAL 28-95

FEDERAL 30-95

GROSS HAHNEWALD

FLOW RATE (THOUSAND SCF/DAY)

PRODUCTION DAYS



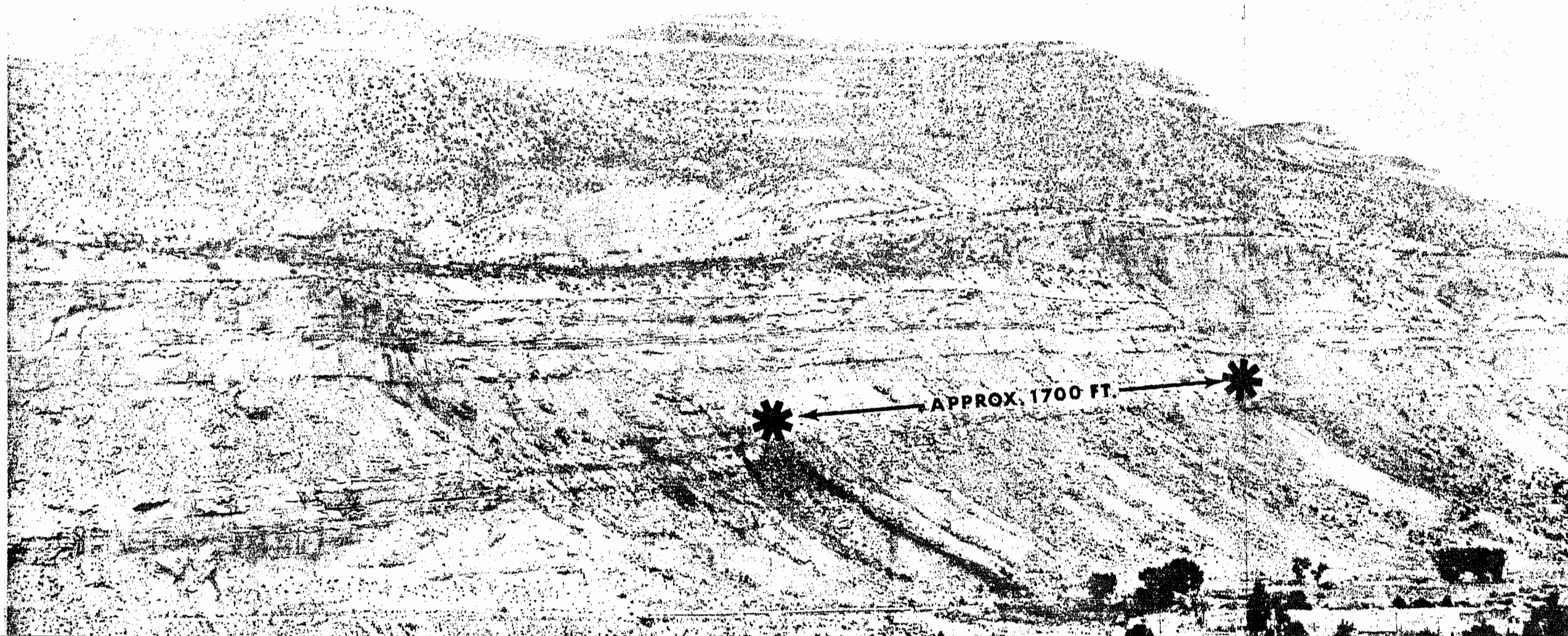
Figure

B-8



Figure

B-9



PLAN VIEW OF RESERVOIR
MODEL
RULISON FIELD , COLORADO

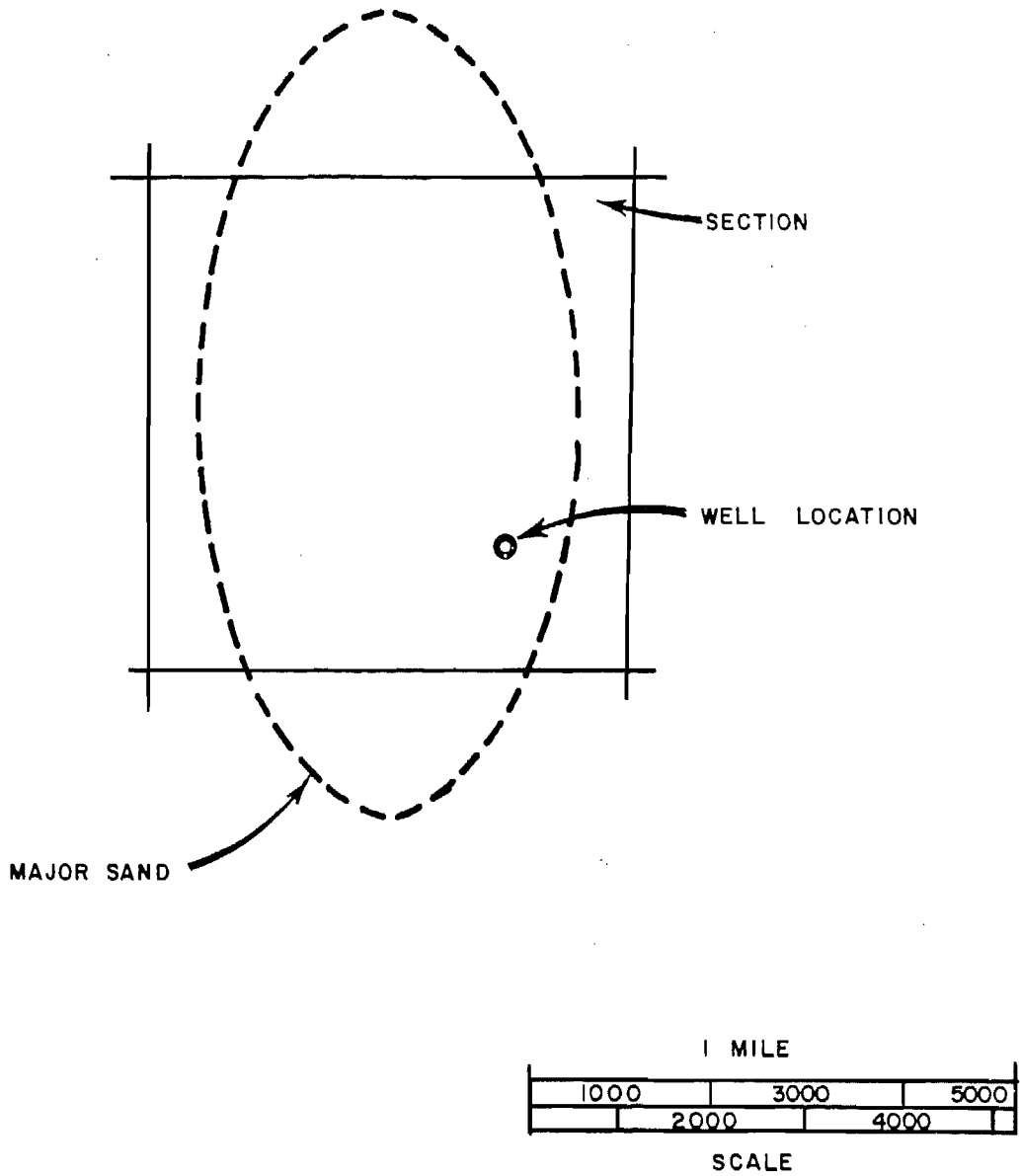


FIGURE B-10

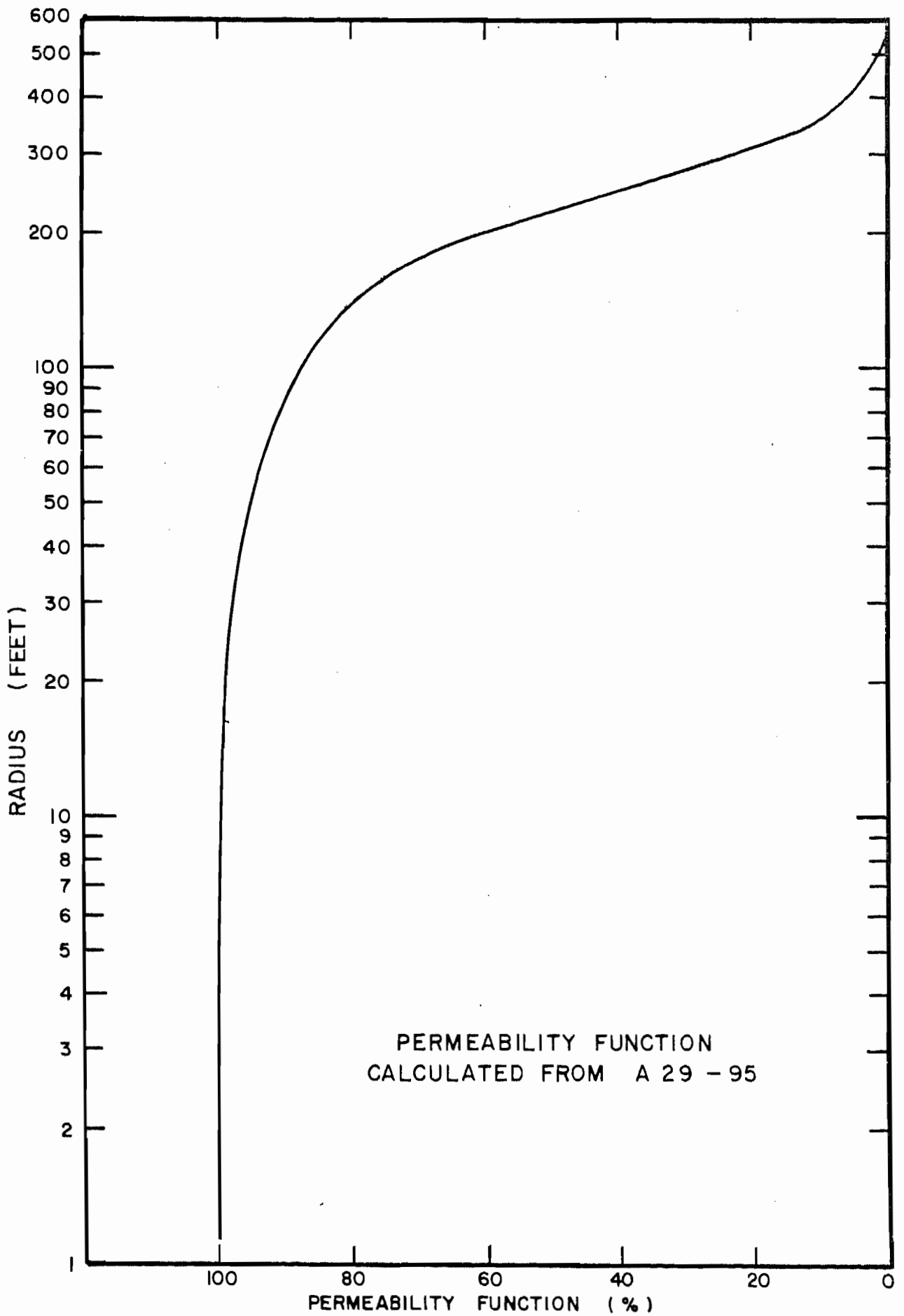


FIGURE R-11

ISOPACH MAP
MESAVERDE RESERVOIR
NUCLEAR STIMULATION MODEL
PROJECT RULISON

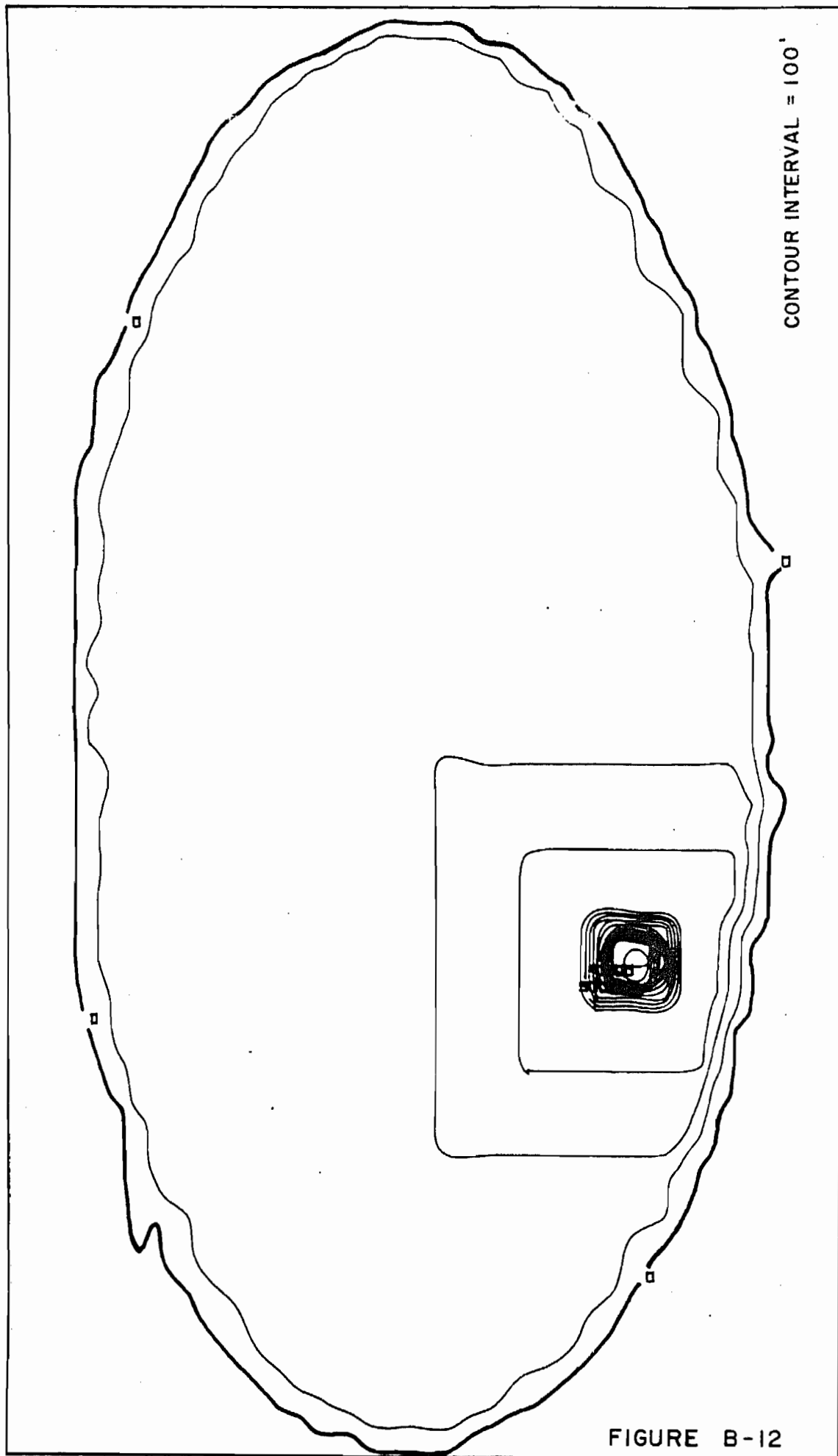
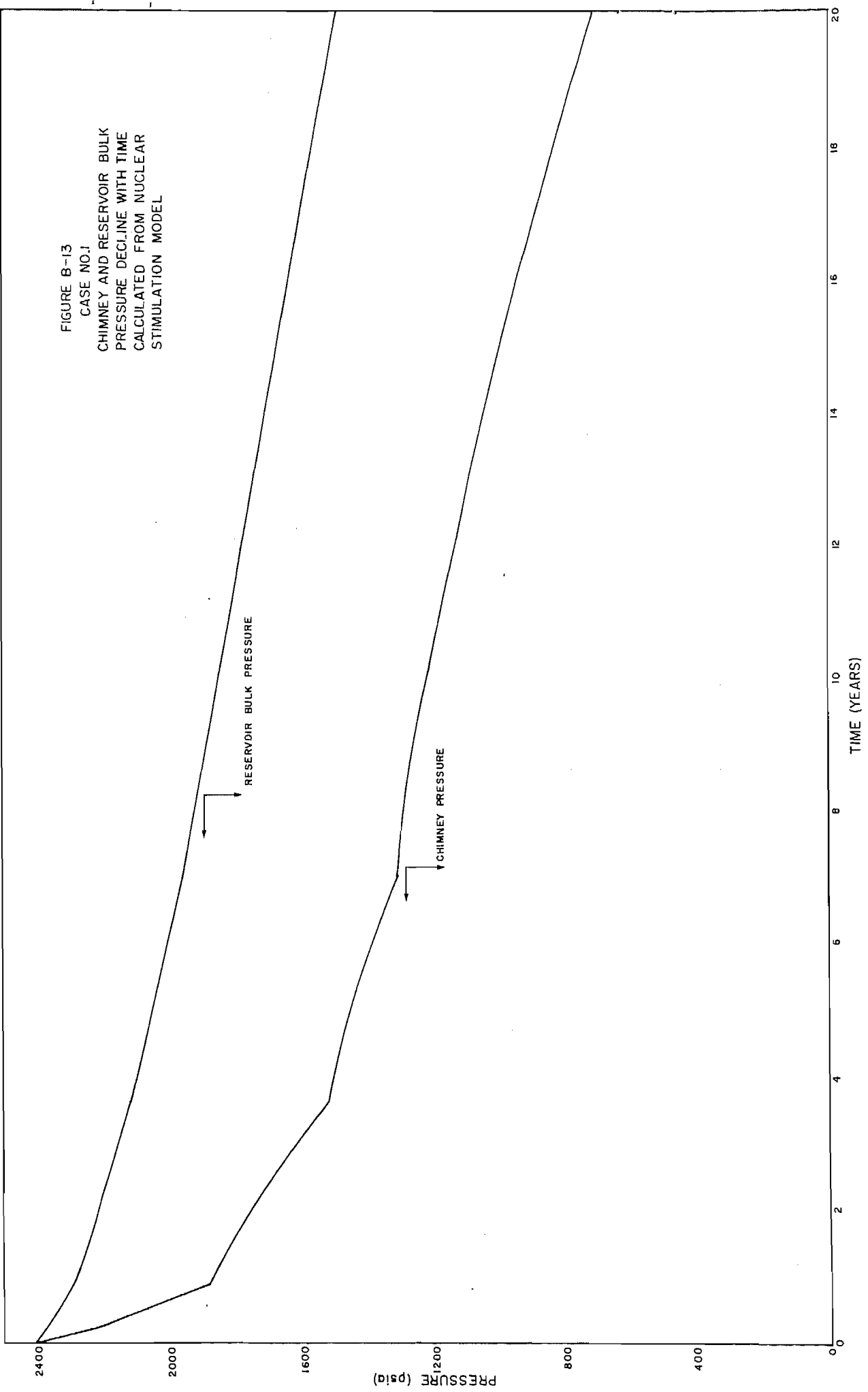


FIGURE B-12

FIGURE B-13
CASE NO. J
CHIMNEY AND RESERVOIR BULK
PRESSURE DECLINE WITH TIME
CALCULATED FROM NUCLEAR
STIMULATION MODEL



CASE No. 1
ISOBARIC MAP
AFTER 20 YEARS OF PRODUCTION
NUCLEAR STIMULATED WELL
PROJECT RULISON

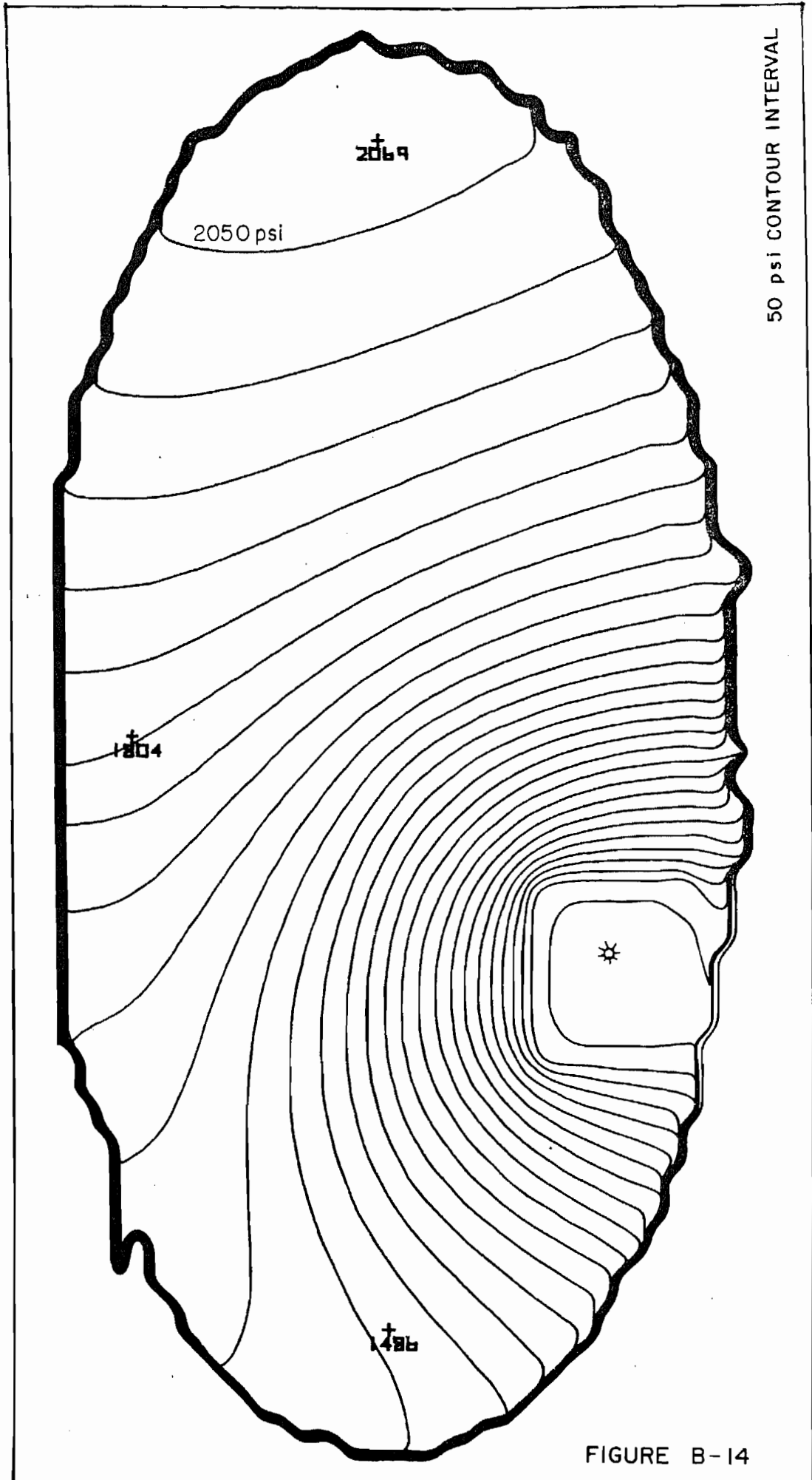
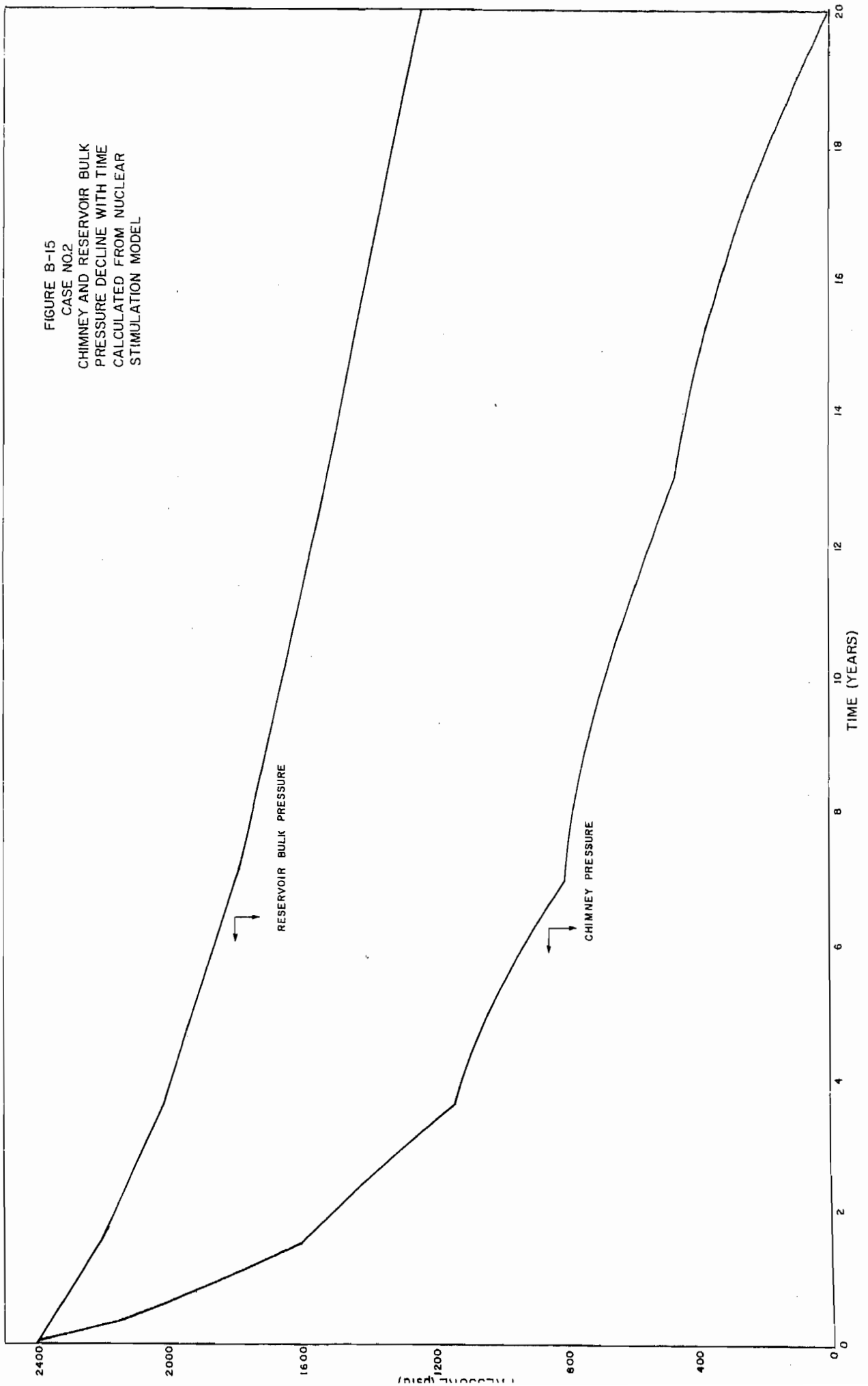


FIGURE B-14

FIGURE B-15
CASE NO.2
CHIMNEY AND RESERVOIR BULK
PRESSURE DECLINE WITH TIME
CALCULATED FROM NUCLEAR
STIMULATION MODEL



CASE No.2
ISOBARIC MAP
AFTER 20 YEARS OF PRODUCTION
NUCLEAR STIMULATED WELL
PROJECT RULISON

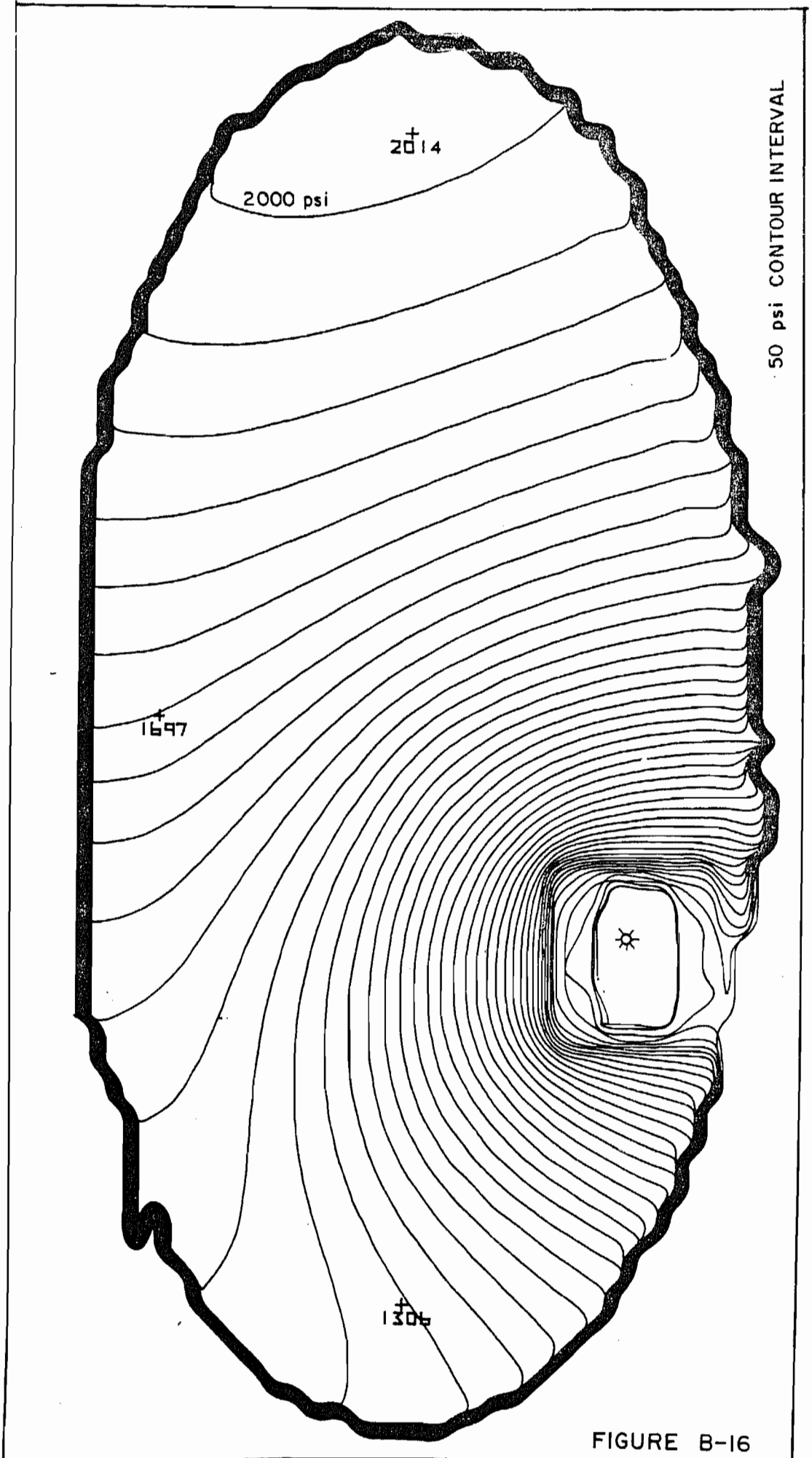
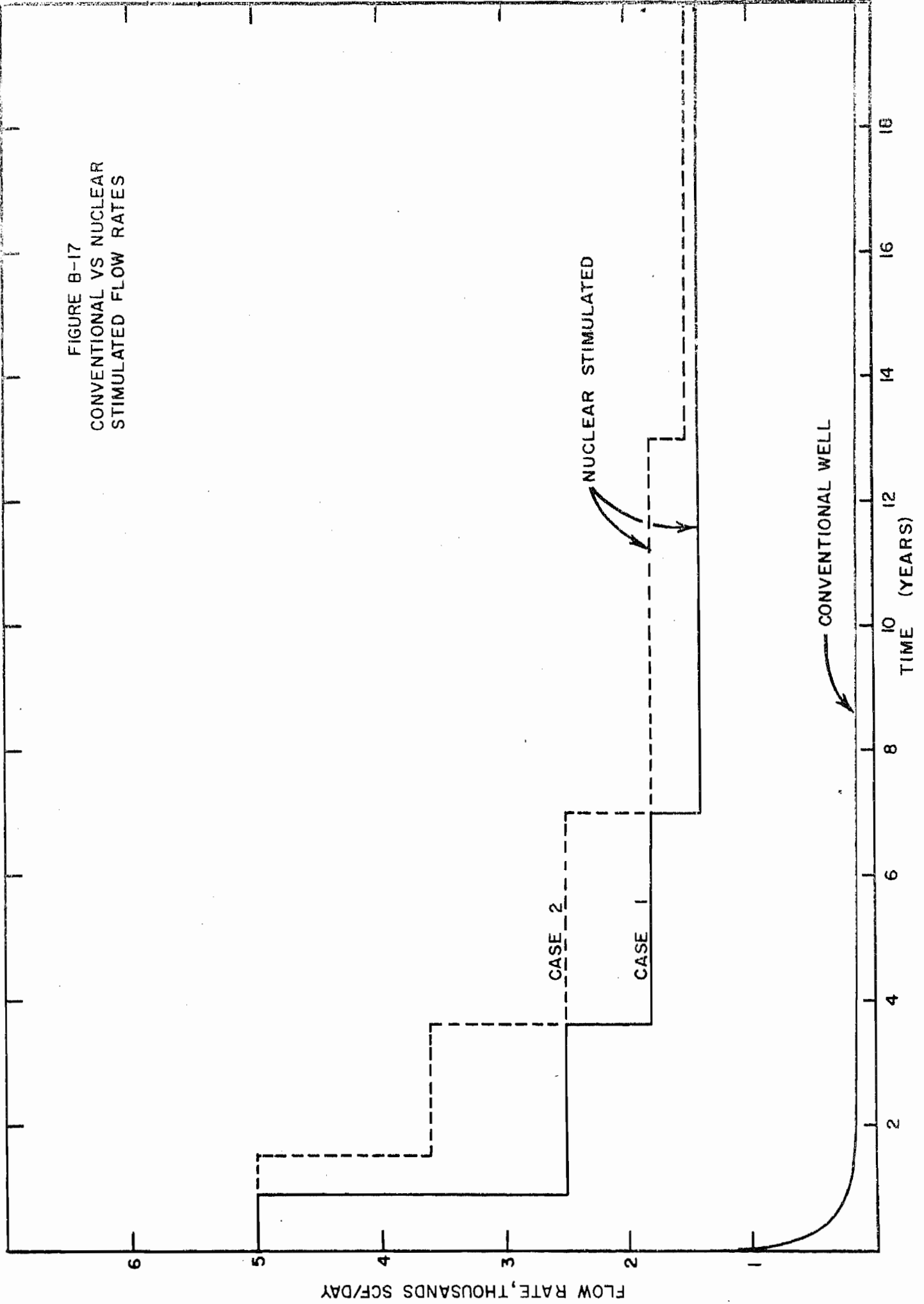


FIGURE B-16

FIGURE B-17
CONVENTIONAL VS NUCLEAR
STIMULATED FLOW RATES



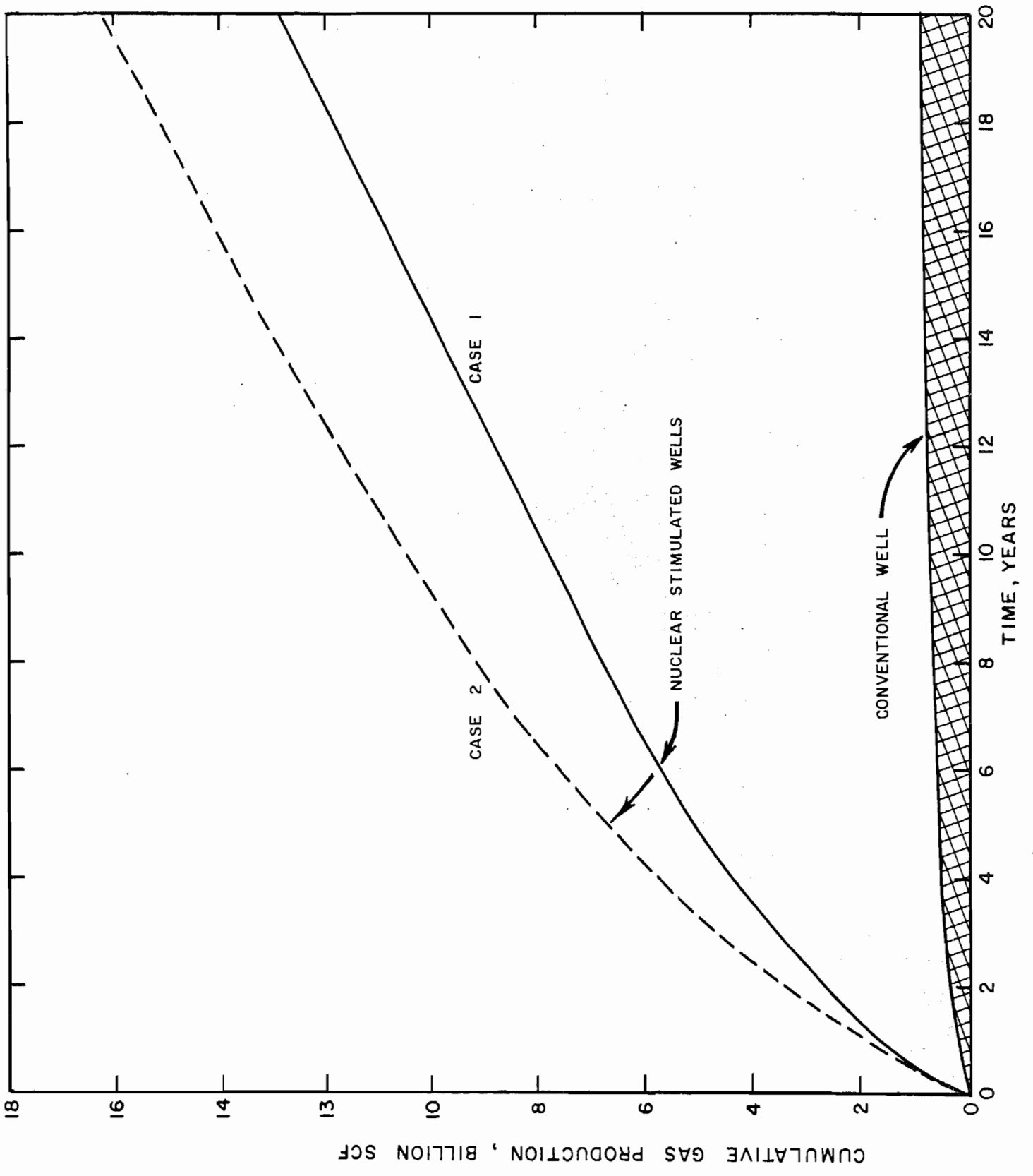


FIGURE B-18